INTEGRATING SEASONAL SPATIOTEMPORAL INTERSPECIES AND HABITAT DYNAMICS TO IDENTIFY AND HINDCAST BYCATCH HOTSPOTS OF THE YELLOWTAIL FLOUNDER FISHERY ON THE GRAND BANK

by © Alessandra Gentile

A Thesis submitted to the School of Graduate Studies in partial fulfillment of the requirements for the degree of Master of Science in Fisheries Science (Fisheries and Technology)

Fisheries and Marine Institute

School of Fisheries

Memorial University of Newfoundland

January 03, 2022

St. John's, Newfoundland and Labrador

Abstract

A long-standing problem in commercial fisheries is the incidental catch of species that are not targeted by the fishery, called bycatch. Bycatch inflicts unnecessary mortalities and potential economic loss. An economically important fishery with bycatch is the commercial yellowtail flounder bottom trawl fishery on the Grand Bank of Newfoundland. My thesis aims to mitigate bycatch in the yellowtail flounder fishery by using novel spatiotemporal models to identify dynamic bycatch hotspots. In my first chapter, I provide an overview of the yellowtail flounder fishery. In my second chapter, I run seasonal multispecies spatiotemporal models to estimate interspecies bycatch relationships using habitat variables. In my third chapter I perform short term retrospective forecasts of these models to estimate bycatch hotspots relationships. By understanding the spatiotemporal dynamics of interspecies relationships with dynamic habitat covariates, and developing a retrospective forecast model, I provide a framework for future bycatch mitigation strategies to contribute to the sustainability and economic efficiency of this fishery.

Acknowledgements

A huge thanks to my Grandma Betty. I will forever cherish the 6 months we spent living together when COVID-19 first plagued the world. I love you a whole bunch. Thank you to my mom for answering all my phone calls no matter what time I called at (as I was always forgetting the 4.5 hour time difference between us). Many extended thanks to my friends who always pushed me to be not only a better scientist, but a better person. I truly had the best support system around me throughout this whole process.

List of Tables

List of Figures

Chapter 1:
Introduction

1.1. Introduction

In this chapter, I will provide an overview of the commercial yellowtail flounder (*Limanda ferruginea* (Storer, 1839)) trawl fishery on the Grand Banks of Newfoundland in NAFO (Northwest Atlantic Fisheries Organization) Div. 3LNO (Figure 1.1) including: yellowtail flounder life history, stock management, stock history and bycatch problems within the fishery. By doing this, I will identify knowledge gaps within the yellowtail flounder fishery and provide objectives to fill these knowledge gaps in my thesis.

1.1.1.   Yellowtail Flounder Life History Traits

The yellowtail flounder has a pelagic larval stage followed by a benthic juvenile and adult phase. They are batch spawners (Murua and Saborido-Rey 2003) and aggregations of juveniles are found mixed with adults forming large oceanic nurseries (Walsh 1992). In captivity, they can produce 14 to 22 batches per season with a typical production of 550,000 eggs (Manning and Crim 1998). Eggs are small from 0.7 mm to 1.0 mm in diameter and hatch into larvae at around 65 degree days (Laurence and Howell 1981; Tilseth 1990). Pelagic larvae range from 1.0 mm to 3.5 mm and have temporary small yolk sacs (NOAA, 2019). Peak spawning occurs April to June with the greatest concentration of spawning on the southern part of the Grand Bank on the Southeast Shoal (Ollerhead et al. 2004). Coincidently, the Southeast shoal has the highest concentrations of juveniles on the Grand Bank (Ollerhead et al. 2004).

1

Males and females reach sexual maturity at age 4 or 5 (Brodie et al. 2010) and they can live up to 12 years (Pitt 1974). Mean length at maturity is 29.8cm (Robins and Ray 1986), corresponding to their recruitment to the fishery as the minimum fish size is 30 cm (Kulka 2001). Adults usually grow to a length of 38-40 cm and weight of 0.5-0.6 kg (Fisheries and Oceans Canada 2016). Fecundity increases with body length and age, as body length is an increasing function of age (Pitt 1971). Adults inhabit smooth muddy or sandy bottoms (Robins and Ray 1986), and prefer depths of 37 – 82 m with temperatures between 3-5°C (Bowering and Brodie 1991).

Adults feed mainly on small marine invertebrates such as polychaete worms, shrimps, isopods amphipods and other small crustaceans and fish (Scarratt 1996). They are preyed upon by species such as Spiny dogfish, hake, cod, monkfish and other flounder (NOAA 2019).

1.1.2. Div. 3LNO Yellowtail Flounder Stock Management

The yellowtail flounder has a distribution in the Northwest Atlantic spanning from Southern Labrador, Canada to Chesapeake Bay, USA (Fisheries and Oceans Canada 2016). There are three American stocks including the Southern New England/Mid-Atlantic stock, Cape Cod/Gulf of Maine stock and the Georges Bank Stock (NOAA 2019), and the NAFO Grand Bank stock (Northwest Atlantic Fisheries Organization 2018). The Grand Bank stock is in NAFO Div. 3LNO and is mostly found in Div. 3N where it is mainly recruited from the southeast shoal area nursery ground (Northwest Atlantic Fisheries Organization 2018). Before the mid 80s, most of the stock was located south of 45 degrees latitude (Brodie et al. 2010). The proportion of yellowtail flounder north of 45 degrees latitude has been stable since the mid 80s (Maddock Parsons 2013).

The Div. 3LNO yellowtail flounder fishery is the only stock on the Grand Banks and it is managed by NAFO as it straddles the Canadian EEZ (Exclusive Economic Zone) and the NRA (NAFO Regulatory Area) (Fisheries and Oceans Canada 2014).The Div. 3LNO stock has been under TAC regulation by NAFO since 1973 (Maddock Parsons et al. 2015). The TAC is divided into ITQs (individual transferable quotas) between countries and other parties. 97.5% of the TAC is assigned to Canada by NAFO, 2% is allocated to France (St. Pierre et Miquelon) and the last 0.5% to other NAFO parties (Fisheries and Oceans Canada 2014).

The Canadian yellowtail flounder fishery is an offshore fishery with the >100ft fleet accounting for 99.98% of the total landings in 2010 of approximately 8,000 mt, representing 11.2% of the total quantity of all species landed from NAFO Div. 3LNO (Fisheries and Oceans Canada 2014). OCI (Ocean Choice International) is an Atlantic company that owns 91.7% of the Canadian TAC (Knapman 2017). This fishery was MSC (Marine Stewardship Council) Certified in 2010 (Knapman 2017) and has industry-academic relationships with the Marine Institute (Knapman 2017).

Ocean Choice International (OCI) catches are both reported in onboard logbooks (including discards at sea) and on landing tickets (Knapman et al. 2020). Onboard observers also verify logbooks, with a minimum observer coverage of 25% (100% when fishing in the NRA) (Knapman et al. 2020). All landings are overseen by an independent dockside monitor to verify the weights of all fished products (Knapman et al. 2020). Random and planned landings inspections by enforcement officers are also conducted (Knapman et al. 2020). Satellite

monitoring data from the vessels monitoring system (VMS) is crosschecked with logbooks, observer and aerial and at-sea surveillance reports to ensure that catches are reported correctly (Knapman et al. 2020). Given the high level of monitoring with various measures (VMS, observers, log books, landings reporting and random inspections) and that there are no other Canadian vessels (other than OCI) who are engaged in this fishery, the risk of non-certified yellowtail flounder being sold as MSC certified is very low (Knapman et al. 2020).

Small fish protocols are enforced with a minimum fish size of 30 cm (Kulka 2001); therefore, yellowtail flounder less than 30 cm are not actively recruited to the fishery. They only constitute a small portion of the catch, and if incidentally caught, they are discarded at sea (Kulka 2001). Hence, surveys are needed to assess the whole population structure for stock assessment purposes. Canadian research surveys have been occurring in Div. 3LNO since 1984 for Spring surveys and 1990 for Fall surveys (Maddock Parsons et al. 2013). Yellowtail flounder are not known to have great latitudinal and longitudinal seasonal migrations (Walsh et al. 2001) so a dual season survey is sufficient to track population trends. The Engel 145' trawl was used until 1994 in the fall and 1995 in the spring, when the surveys were switched to a more efficient Campelen 1800 shrimp trawl (Maddock Parsons et al., 2013). Beginning in 1995, Spain has also conducted stratified-random surveys for groundfish in the NAFO Regulatory Area of Div. 3NO (Knapman et al. 2020). Surveys have indicated that stock abundance is highest in the 3N division (Maddock Parsons et al. 2015).

Div. 3LNO yellowtail flounder is assessed bi-yearly in the June NAFO Scientific Council Meeting (Fisheries and Oceans Canada 2014). The last official meeting report available online

was 2018 (Maddock Parsons et al. 2018). The stock is assessed using a non-equilibrium Shaefer surplus production model (Fisheries and Oceans Canada 2014; Maddock Parsons et al. 2015). It applies nominal catch data and survey biomass data while using logistic population growth (Maddock Parsons et al. 2015). 2000 - 2015 stock assessments were done using a surplus production model incorporating covariance (ASPIC) with catch and survey indices (Maddock Parsons et al. 2018). There were concerns that the ASPIC formulation was not sensitive enough, so the 2018 assessment was conducted using a surplus production model in a Bayesian Framework as it was considered to have a greater range of projection time (Maddock Parsons et al. 2018). As of 2018, the stock was healthy at 1.5 times *Bmsy* (biomass at maximum sustainable yield*) (Bmsy*=87.63 Kt) with a less than 1% risk of the stock being below *Bmsy* or *F* (fishing mortality rate) and being above *Fmsy* (maximum rate of fishing mortality at maximum sustainable yield) (Maddock Parsons et al. 2018).

1.1.3. Div. 3LNO Yellowtail Flounder Stock History

The stock has been under TAC regulation since 1973 (Maddock Parsons and Rideout 2015). TAC regulations were set in place with an initial level of 50,000 t (Maddock Parsons and Rideout 2015). During 1985 – 1993 the catches exceeded the TAC (Maddock Parsons and Rideout 2015) (Figure 1.2). In 1994 biomass had declined to 20% of the maximum sustainable yield and NAFO decided that no directed fishery would be permitted for this stock and called a moratorium in 1995 (Maddock Parsons and Rideout 2015). Pre-moratorium Div. 3LNO yellowtail flounder fishery was a mixed fishery with Atlantic cod (*Gadus morhua* (Linnaeus 1758)) and American plaice (*Hippoglossoides platessoides* (O.Fabricius,1780)) (Brodie et al. 2004). Post-moratorium, the fishery has been acting a single species fishery targeting the

yellowtail flounder (Brodie et al. 2004). Dockside monitoring has been in place post-moratorium since August 1998 when the fishery reopened (Brodie et al. 2010).

Overfishing was initially thought to cause the stock decline as before the 1984 cold water period as the biomass had reduced by half since the late 1960s (Brodie et al. 2010) which potentially could have had an effect on stock structure. Such biomass declines from overfishing may have been confounded with unfavourable environmental conditions leading to the stock collapsing on the Grand Banks (Brodie et al. 2010). Before the collapse, the Grand Banks was filled with water that was much colder than usual, and has been linked to the collapse of other stocks by increasing natural mortality (Lear and Parsons 1993). The years preceding the collapse, 1984-1993, had the longest cold water period recorded (Brodie et al. 2010) and approximately 60% of their habitat would have been in <0°C resulting in many individuals living in subzero conditions (Colbourne and Walsh 2006). Up to the early 1990s, decreasing stock size coincided with a shrinking range of preferred thermal habitat available (Walsh et al. 2004b).

In 1999 nearly 100% of the yellowtail flounder habitat bottom water temperatures rose to >0°C again (Brodie et al. 2010) and the TAC was increased to 6,000 t (Maddock Parsons et al. 2015). Even after the moratorium, during 1998 – 2001, the total catches exceeded the TAC (Maddock Parsons et al. 2015). In 2006, there was an exceptionally small catch of only 177 tons, well below the TAC of 15,000 t, because of corporate reconstruction and labour disputes preventing the Canadian fleet from fishing (Maddock Parsons et al. 2015). The decline in catch numbers for the 2009 season was due to economic conditions (Fisheries and Oceans Canada 2014). During 2011-2012 most of the catch was taken in April – June with 2012 having the lowest Canadian

catch reported since 2006 of 1795 t (Maddock Parsons et al. 2015). Since 2001, the catches have never surpassed the TAC and the stock is predicted to be in good health (Maddock Parsons et al. 2018) (Figure 1.2).

Survey data from 1996 - 2002 on the *Atlantic Lindsey*, (44m length, 665 G.R.T.,1500HP) commercial trawler revealed sex ratios vary between 46% to 53% male (Maddock Parsons et al. 2003). Maturity at size by year was estimated using Canadian spring research vessels from 1984-2012. Both males and females have been declining in size at maturity in the Spring (Maddock Parsons et al. 2018). There also seems to have been a slight downward trend in Spring female weight at length since 1996 (Maddock Parsons et al. 2018). Spring Female spawning stock biomass (SSB) also declined from 1984 to 1992, increased substantially from 1995 to 2009, and has since been sharply declining (Maddock Parsons et al. 2018). Fecundity estimates form 1993-1998 have also decreased (Rideout and Morgan 2007) since 1966-1967 (Pitt 1971). The causes of these changes in population dynamics are unknown (Maddock Parsons and Rideout 2015).

1.2. Bycatch

Bycatch, or catch of non-target organisms is among the most pervasive problems in modern day fisheries (Pérez Roda et al. 2019). Bycatch can be interspecific, and/or intraspecific if there are size restrictions. While some bycatch may be sold, retention may be illegal or undesirable, leading to the possibility of individuals being treated as discards. According to the FAO, between 2010 and 2014, discards from global marine capture fisheries between totaled 9.1 million tons (representing 10.8% of all global catches) with about 4.2 million tons (46 %) of total annual discards from bottom trawls (Pérez Roda et al. 2019). Bycatch inflicts extra mortalities affecting

ecosystem balance and potential economic loss (Pérez Roda et al. 2019). Economic deficits of bycatch are rarely published in the scientific literature. Deficits largely occur from either early closures of fisheries when bycatch limits are reached and when bycatch are discards of marketable catch (Patrick and Benaka 2013). For example, in the US. commercial fisheries, premature closures from bycatch result in losses ranging from $34.4 million to $453.0 million per year and bycatch discards result in losses of $427.0 million in ex-vessel revenue and as much as $4.2 billion in seafood sales, $1.5 billion in income and 64,000 jobs (Patrick and Benaka 2013).

Hall et al. (2000) indicated that in the past, bycatch was often ignored by most fisheries scientist and managers because it was not visible, most likely on a smaller magnitude, and/or thought to be less significant for stock assessment. Thus, leading to interferences between fisheries and ecosystems not being prioritized. It is known that stocks with lower levels of biomass have been found to be the least responsive to fisheries management measures and are the most vulnerable to changes in their environment (Vert-pre et al. 2013). Therefore, even with no-directed fishery for stocks in moratorium, sometimes they are caught as bycatch having an impact on population recovery and can create conservation problems when catches surpass sustainable harvest rates.

Mitigating unwanted catch is not straightforward. In addition to increasing gear selectivity, targeted spatiotemporal planning for multiple species simultaneously using ecosystem based management strategies has been proposed via a decision tree (Dunn et al. 2011). For example, static spatial management strategies restrict fishing access to a specific area and can potentially limit bycatch species when fishing gear cannot be modified. However, many demersal fish are

not static and move to remain in optimal environments to suite their physical and feeding conditions causing their distribution to vary with ocean dynamics at various life stages (Perry et al. 2005; Nye et al. 2009; Pinsky et al. 2013; Asch 2015), and therefore static time-area closures can be ineffective for dynamic processes like bycatch avoidance (Hobday and Hartmann 2006; Howell et al. 2008, 2015; Hobday et al. 2011). Thus, it is important to investigate the spatiotemporal dynamics of both the target and bycatch species simultaneously to ensure the sustainability of the ecosystem.

1.2.1. *Bycatch in the Div. 3LNO Yellowtail Flounder Fishery*

The Div. 3LNO yellowtail flounder fishery is purely commercial; there is no recreational or Aboriginal association (Fisheries and Oceans Canada 2014). The most common gear used is the otter trawl and catches by other types of gear have been less that 10 t annually since 2002 (Maddock Parsons et al. 2013). There are gear restrictions in place to mitigate bycatch. Otter trawls consist of a funnel-shaped net that is towed by a boat at a speed of 2 - 4 knots across the seafloor (Gordon et al. 2008). In 1977 NAFO regulated areas were set to have a minimum codend mesh size of 130mm, and in 1998 Fisheries and Oceans Canada set the minimum codend mesh size to be 145 mm in the Canadian EEZ for Canadian fleets (Maddock Parsons et al. 2013). All OCI vessels use the Golden Top trawl 165 mm inside mesh size for the trawl and 150– 155 mm for the cod end, with a headline height of 2.75 m (Knapman et al. 2020). OCI uses otter trawls only with flying doors and elevated sweeps since 2013 and comprehensive monitor and surveillance system like fishing sensors (Scanmar and marport) (Knapman et al. 2020). Vessel trips last approximately 30 days (Knapman et al. 2020).

Due to the gear used and the high overlap of niches with other groundfish species, the yellowtail flounder fishery is susceptible to bycatch, including species with lower levels of stock biomass. Under MSC definitions, the target species in this fishery is the yellowtail flounder. Bycatch is classified as either, main primary species, minor primary species, minor secondary species or endangered, threatened or protected (Knapman et al. 2020). Primary species have management tools in place to help achieve stock management objectives as either limit or target reference points (Knapman et al. 2020). Secondary species are species that do not meet the primary species definition and are not endangered, threatened or protected. A 'main' designation is given if it compromises 5% or more of the biomass (or 2% if the species is less resilient) of the total catch of all the species (Knapman et al. 2020). This designation can be challenged. See Table 1.1 for a list of the top 10 species caught in the yellowtail flounder fishery from 2013-2018.

The fishery is currently subjected to a wide variety of measures to limit bycatch specific to its primary bycatch species. These include that effort is limited through licensing and the application of quota or bycatch limits for managed species, and the fishery is required to use a cod end mesh of no less than 145 mm (Knapman et al. 2020). The yellowtail flounder fishery also has extensive experience operating within bycatch limits, and considerable efforts are made to increase selectivity for yellowtail flounder (Blyth-Skyrme et al. 2015). The fishery is currently limited to a bycatch cap of 15% of American plaice, and whichever is the greater of 5% or 1,240 kg for 3NO witch flounder (*Glyptocephalus cynoglossides* (Linnaeus, 1758)) and 4% or 1,000 kg for of 3NO Atlantic cod (Knapman et al. 2020). According to the OCI report in 2017, they conducted 14 total fishing trips with 1010 total number of hauls (Knapman 2017).

They caught 4,737,781 kg of yellowtail flounder, 45,591 kg (<1%) cod bycatch and 167,268 kg (3.5%) American plaice bycatch (Knapman 2017).

If the bycatch limits are exceeded in any one haul, the vessel is required to move a minimum of 10 nautical miles from any position in the previous tow before continuing fishing, and leave the Division and not return for at least 60 hours if the bycatch limit is also exceeded on the subsequent tow (Knapman et al. 2020). After 60 hours, vessels may return but an initial trial tow of less than 3 hours is required to be undertaken (Knapman et al. 2020). Minimum fish sizes also apply, if the number of undersized fish in a single haul exceeds 10% of the total catch the vessel is required to move at least 5 nautical miles from the previous tow before fishing again (Northwest Atlantic Fisheries Organization 2019). Vessels are also subject to a target rate of 25% observer coverage (Fisheries and Oceans Canada 2019). Small fish protocols are enforced with a minimum fish size of 30 cm (Kulka 2001). Areas are closed for 10 days when the number of undersized fish caught in one haul reaches 15% of the total catch (Kulka 2001). The minimum codend mesh size in NAFO regulated areas is 130mm since 1977 (Maddock Parsons et al. 2013).

There are also some static fishing spatial restrictions in place. Static spatial management strategies restrict fishing access to a specific area and can potentially limit bycatch species when fishing gear cannot be modified. VMEs (vulnerable marine ecosystems) have been defined by the FAO on The Grand Bank; however, all exceed the depth range of the yellowtail flounder fishery (>200m) therefore the fishery does not come in contact with VMEs (Knapman et al. 2020). Even if there were static VMEs within the yellowtail flounder depth range, static time-area closures can be ineffective for dynamic processes like bycatch avoidance (Hobday and

Hartmann 2006; Howell et al. 2008, 2015; Hobday et al. 2011) as fish are not static and move to remain in optimal environments to suite their physical and feeding conditions causing their distribution and phenology's to vary with ocean dynamics at various ontological stages (Perry et al. 2005; Nye et al. 2009; Pinsky et al. 2013; Asch 2015). OCI also participates in a voluntary temporal spawning closure for six weeks mid-June to early-August to avoid product quality issues associated with fish spawning (this is not regulated) (Knapman et al. 2020).

Although there is no longer a directed fishery on species in moratoria, sometimes they are caught as bycatch having an impact on population recovery and can create conservation problems when levels of harvest are not sustainable for the bycatch species. Stocks with lower levels of biomass (such as ones in moratoria) can be the least responsive to fisheries management measures and are the most vulnerable to changes in their environment (Vert-pre et al. 2013). Therefore, not only is it important to examine the direct effects of bycatch removal on stock biomass, but also it is important to investigate the indirect effects of environmental variability, especially for stocks with lower biomass levels like ones in moratoria. In the yellowtail flounder fishery, main primary bycatch species American plaice (Div. 3LNO) and minor primary bycatch species witch flounder (Div. 3NO* moratorium lifted in 2015, Div. 2J3KL), and Atlantic cod (Div. 3NO, Div. 3L) are currently in moratorium (Knapman et al. 2020). I will focus on the relationships between these three bycatch species in moratorium in the yellowtail flounder fishery for my thesis.

1.2.2. Bycatch Species of Focus: Atlantic Cod

The Div. 3LNO yellowtail flounder fishery intersects two Atlantic cod stocks; both Div. 2J3KL and Div. 3NO Atlantic cod have been in moratoria since 1994 (Fisheries and Oceans Canada

2019). Atlantic cod has peak spawning in May, and has limited spawning throughout the year (Ollerhead et al. 2004).

The Div. 2J3KL stock is highly migratory as they overwinter near the edge of the continental shelf and spend spring and summers in shallow waters along the coast onto the plateau of the Grand Banks (Fisheries and Oceans Canada 2019). The offshore biomass of cod has increased in most stock areas in the past decade except in southern Div. 3L (Fisheries and Oceans Canada 2019). The greatest number of spawning females is found in Div. 3L (Ollerhead et al. 2004).

The Div. 3NO stock stays in the shallower parts of the banks in summer (mostly the SE shoal in 3N), and the slopes of the Grand Bank in the Winter when cooling occurs (Rideout et al. 2015). The stock biomass is widely distributed in the Fall (Fisheries and Oceans Canada 2019). Spring biomass is low in both Div. 3N and 3O from 1994 to 2006 and the biomass has been increasing in Div. 3N since 2011 (Fisheries and Oceans Canada 2019). 95% of the total Canadian catch of Div.3NO Atlantic cod was taken by the Div.3LNO yellowtail flounder fishery in 2013-2014 as bycatch (Rideout et al. 2015).

1.2.3. Bycatch Species of Focus: American plaice

The Div. 3LNO yellowtail flounder fishery overlaps with the Div. 3LNO American plaice stock which has been in moratorium since 1994 (Fisheries and Oceans Canada 2019). American plaice spawns from February to September with peak spawning in May (Ollerhead et al. 2004). Before 1998 American plaice was primarily distributed in 3L, but since then they have been distributed mainly in 3N (Ollerhead et al. 2004). Analysis of 1985-1989 surveys delimited two major areas

of juvenile American plaice, The Northern Slope and The Southern Edge of the Grand Bank (Walsh 1991). The Southern Edge of the Grand Bank straddles the 200 nm jurisdictional limit; juveniles are discarded inside the 200 nm limit and targeted outside the 200 nm limit (Walsh 1991). American plaice is a relatively more shallow water species preferring colder water predominant at depths of 90-250m and bottom temperatures of -0.5 °C to 2.5 °C (Bowering and Brodie 1991). A tagging study revealed that American plaice is rather sedentary, with little migration between bank areas associated with spawning, feeding and prevailing environmental conditions (Pitt 1969). American plaice spawn ubiquitously across the Grand Banks and no large spawning migrations occur (Pitt 1969).

1.2.4. Bycatch Species of Focus: Witch Flounder

The Div. 3LNO yellowtail flounder fishery intersects with both the Div. 2JK3L and Div. 3NO witch flounder stocks. Div. 2J3KL witch flounder have been in moratoria since 1994 while the 3NO witch flounder moratorium was lifted in 2015 (Fisheries and Oceans Canada 2019). On the Grand Banks, witch flounder is a deep water species dominant at depths of 184-366 m and temperatures of 2.0-6.0 °C (Bowering and Brodie 1991). Peak spawning occurs April through July with the largest concentration of spawning females found on the southern Grand Bank in Div. 3O in the beginning of the summer, and later in the summer on the Northern Grand bank in Div 3L and 3N (Ollerhead et al. 2004).

Div. 2J and 3L biomass indices have been showing an overall increase since 2004 and reached a high in 2015 (Wheeland et al. 2019). Div 3K generally accounts for the majority of the biomass for this stock with an average of 51% being located in this division from 1983-2017 (Wheeland

et al. 2019). By the early 1990's the stocks distribution was limited to very small catches along the continental shelf slope, and more to the southern area of the stock boundary (Wheeland et al. 2019). As the biomass indices have increased over the last several years, a redistribution of the stock has been observed, with biomass once again spread across portions of the shelf and deeper channels primarily in 3K, in addition to the slope waters (Wheeland et al. 2019). The distribution of Div. 2J3KL biomass by depth favours deep waters towards the northern extent of the stock area (Wheeland et al. 2019).

Spring Div. 3NO stock indices are variable and primarily driven by the overall higher abundance and biomass in Div. 3O (Wheeland et al. 2019). It is likely that some witch flounder may be distributed at a depth below the survey range, particularly in the spring, following spawning in deeper waters, contributing to variability in survey estimates (Wheeland et al. 2019). Fall 3NO stock indices are less variable with a generally increasing trend in biomass and abundance from 1997-2004 and have increased or remained stable since 2016 (Brodie 2019). Div. 3O also dominates the majority of the biomass estimates in the fall surveys (83% on average) (Brodie 2019).

1.3. Knowledge Gaps

Throughout this text, I have touched upon some of the complexities of how the Div. 3LNO yellowtail flounder fishery is managed. To summarize, measurements in place to avoid bycatch in the yellowtail flounder fishery already include: voluntary spawning closure, bycatch limits and gear restrictions (Fisheries and Oceans Canada 2019). However, the dynamic seasonal spatiotemporal relationship between habitat covariates and interspecies relationships of the

bycatch species I summarized have not been investigated. This information could lead to more accurate stock assessment models by increasing efficacy and decreasing variance. Thus, having the potential to increase bycatch forecast ability, and more precise and efficient fishing efforts.

1.3.1. Identifying Dynamic Spatiotemporal Relationships Informed by Habitat Covariates and Species Correlations

There are links in the literature between habitat covariates and variation in recruitment, distribution, and abundance in the yellowtail flounder fishery. For example, yellowtail flounder can survive wide fluctuations in salinity and temperature (Walsh 1992; Perry and Smith 1994) and exhibit diel and seasonal variations in depth and temperature (Walsh and Morgan 2004). Density and depth were also found to be the most influential in affecting spatial variation of juveniles in the nursery area on the Southeast shoal when compared to temperature, sediment type, location and salinity (Walsh et al. 2004b). Temporal changes in salinity, but not temperature, was negatively significantly correlated with recruitment variability (Walsh et al. 2004b).

During periods of low abundance, the adult population was found to be spatially contracted and aggregated in the southern Grand Bank from 1975-2001, and environmental covariates (temperature, depth, sediment type) had less influence on spatial variation (Simpson and Walsh 2004). Conversely, during periods of high abundance, the population expanded into the Northern Grand Bank and the environmental covariates had more influence on spatial variation; with depth having the greatest influence (38%) on spatial variation, followed by temperature (19%) and then sediment type (2%) (Simpson and Walsh 2004). Analysis of near-bottom temperatures

on the Grand Bank from 1990-2005 relative to the distribution and abundance of yellowtail flounder revealed a shift in thermal habitat from the cold sub-zero °C conditions during the first half of the 1990s to a relatively warm environment during the latter half of the 1990s and early 2000s coinciding with bottom temperatures to >0°C for almost 100% of the traditional bottom habitat (Colbourne and Walsh 2006). A strong linear association was found between bottom temperatures and mean catches rates on the southern Grand Bank with catch rates increasing with temperatures (Colbourne and Walsh 2006). This thermal shift observed in the latter half of 1990s and early 2000s, matched the population increase in abundance and expansion into the northern Grand Bank found by Simpson and Walsh (2004).

Using spatial and temporal patterns of the 2004 Canadian fleet, catches were in shallower depths and localized to the SE shoal in the winter compared to deeper waters and more widespread distributions in other seasons; also greater catches were taken in warmer waters than in colder waters (Walsh and Brodie 2006). From 1969-2006, biomass and surplus production also vary in response to environmental conditions; biomass, but not surplus production, was influenced by the negative phase of the North Atlantic Oscillation (associated with warmer bottom temperatures on the Grand Bank); regional scale warmer temperatures were found to increase both biomass and surplus production (Colbourne and Walsh 2006).

Many studies only focus on just temporal or spatial correlation between habitat covariates and yellowtail flounder and are lacking integration of spatiotemporal variation. Not only are dynamic spatiotemporal habitat relationships needed in species distribution models, but dynamic interspecies relationships also need to be connected, especially for bycatch mitigation purposes.

Using a multispecies spatiotemporal approach to mitigate bycatch is a relatively novel idea. Recently, there has been development in the spatial planning of fisheries in the Mediterranean sea to negate the negative effects of undersized fish discards by using scientific surveys to identify aggregations of juveniles (intraspecies) to identify bycatch density hotspots using ArcMap (Milisenda et al. 2021). Dynamic seasonal spatiotemporal bycatch hotspots have not been identified for the yellowtail flounder fishery, with or without habitat covariates.

1.3.2. Forecasting Dynamic Bycatch Hotspots

There is a recent interest in forecasting species distribution shifts, especially as many ecosystems worldwide are shifting in response to rapid changes in environmental conditions. Ecosystem resource management requires forecasting species distributions over various short- and long-term timescales to ensure the most sustainable level of management. In fisheries, long-term forecasts can be used to make industry decisions such as long-term capitalization of profit and develop strategies for long-term sustainability of the respective fishery (Tommasi et al. 2017). Short-term seasonal forecasts can be used to modify fleet behaviour to ensure the most effective and efficient fishing strategies such as bycatch reduction (Tommasi et al. 2017).

In the most recent NAFO report, a medium-term projection to 2022 of yellowtail flounder relative biomass and fishing mortality using a Schaefer (Schaefer 1954) surplus production model in a Bayesian framework was provided under four scenarios: fishing at status quo, 85% F_{MSY} (Fishing mortality at maximum sustainable yield), 2/3 F_{MSY}, and F_{MSY} (Maddock Parsons et al. 2018). The risk of the total biomass being below B_{lim} at the end of all projection periods is less than 1% (Maddock Parsons et al. 2018). These projections were only for the total stock and

did not represent any spatiotemporal change. They also did not test the significance of any habitat covariates, interspecies relationships that could possibly strengthen their model predictions. Nor was there any bycatch forecasting.

Stock assessment models generally lack dynamic spatial structure as explained above, and therefore have no capability to forecast changes in stock distribution as habitat conditions shift the distribution of the stock even when the spatial distribution of many marine species has been shown to be particularly sensitive to changing climate over multi-annual to decadal scales (Nye et al. 2009; Pinsky et al. 2013; Poloczanska et al. 2013; Bell et al. 2015; Thorson et al. 2016b). Integration of nowcasting (real-time) (Hobday and Hartmann 2006; Howell et al. 2008, 2015) and short-term seasonal forecasts incorporating oceanic conditions into habitat preference models have recently been pursued to forecast spatial distributions of species and to set dynamic time-area closures to decrease bycatch (Hobday et al. 2011; Dunn et al. 2016). Incorporating dynamic habitat covariates and interspecies relationships into forecasting models will strengthen the ability to predict short term bycatch hotspots. However, before forecast models can be used, hindcast models need to be tested to assess the predictability of these models.

1.4. Objectives

Using Div. 3LNO yellowtail flounder fishery as a case study, the overarching goal of this thesis is to incorporate interspecific bycatch species dynamics and habitat variables to identify and hindcast dynamic seasonal spatiotemporal bycatch hotspots.

In chapter two, I will use interspecies relationships and habitat variables to identify interspecies distribution patterns for the yellowtail flounder and three of its bycatch species: American plaice, Atlantic cod and witch flounder, using a multispecies VAST (vector-autoregressive spatiotemporal) model. As noted in Section 1.3.1, dynamic spatiotemporal habitat relationships, or dynamic bycatch relationships have not been identified for this fishery.

In chapter three, I will use the model developed in chapter two to perform retrospective forecast model testing to evaluate the forecast ability of my model. As noted in Section 1.3.2, there is a lack of spatiotemporal forecasts for the yellowtail flounder fishery as there is currently only a Shaefer surplus production model which only takes into consideration temporal effects of the whole stock. This current model could be missing finer details that a spatiotemporal model incorporating bycatch interspecies relationships and habitat covariates would include. This novel work will provide the fishery with a novel dynamic framework to forecast bycatch hotspots thus leading to a more efficient and sustainable fishing practices.

1.5. Tables

Table 1.1: Estimated bycatch (t) in the yellowtail flounder fishery of the top 10 bycatch species from 2013-2018 identified by MSC. Target species, main primary species, minor primary species, minor secondary species are identified by MSC. Table adapted from Knapman et al. (2020) table 11.

Rank	Species Name	Mean Annual Observed Total Catch (t)	Catch as % of Mean Annual Observed Total	Estimated Total Annual Catch Scaled to YTF Observer Data
1	***Yellowtail flounder**	**2899.072**	**87.453**	**7178.600**
2	***American plaice**	**210.584**	**6.352**	**521.400**
3	Thorny skate	52.116	1.572	129.000
4	***Atlantic cod**	**44.878**	**1.354**	**111.100**
5	Skate (NS)	29.156	0.880	72.200
6	Atlantic wolffish	26.888	0.811	66.600
7	Sea cucumber (NS)	13.188	0.398	32.700
8	Atlantic halibut	8.052	0.257	19.900
9	***Witch flounder**	**8.524**	**0.243**	**21.100**
10	Sculpins	4.354	0.131	10.800
11	Sculpins (NS)	3.794	0.114	9.400
12	Sea raven	2.922	0.088	7.200
13	Sand lances (NS)	2.684	0.081	6.600
14	Toad crab (NS)	2.354	0.071	5.800
15	Haddock	1.376	0.042	3.400
16	Greenland Halibut	0.998	0.030	2.500
17	Round skate	0.960	0.029	2.400
18	Starfish (NS)	0.510	0.015	1.300
19	Porbeagle shark	0.446	0.013	1.100
20	Lancetfishes (NS)	0.284	0.009	0.700

key:
Target species
Main Primary Species
Minor Primary Species
Minor Secondary Species
Endangered, threatened, and protected species
*species included in our model

1.6. Figures
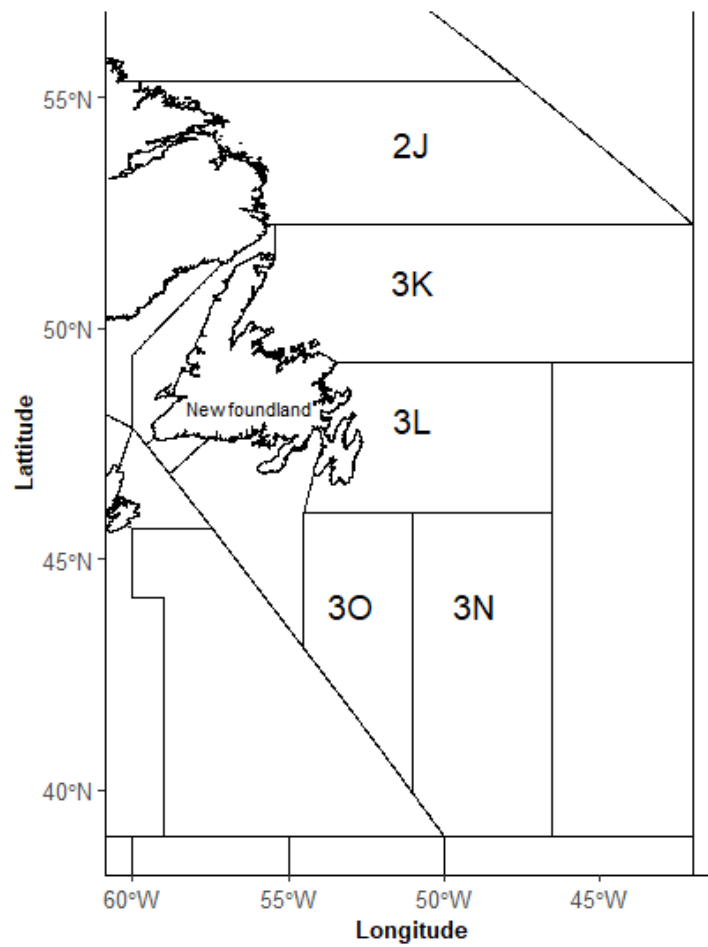
Figure 1.1 Map of NAFO Div. 2J3KLNO in The Northwest Atlantic.
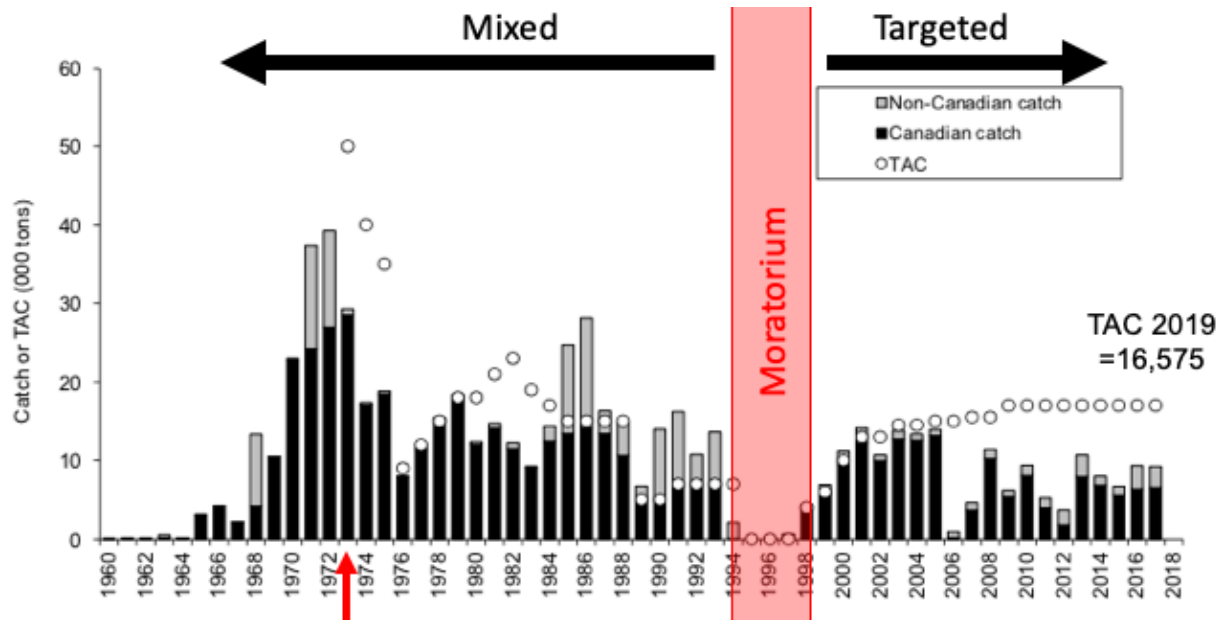
Figure 1.2 Catch history of the Div. 3LNO yellowtail flounder fishery from 1960-2018 including Canadian catch, non-Canadian catch and TAC. Red arrow indicates 1973; the year in which the TAC was first allotted. The red rectangle indicates the years the fishery was in moratorium 1995-1998. The Canadian TAC in 2019 was set to 16,575 kg (Northwest Atlantic Fisheries Organization 2019). Figure was adapted from Maddock Parsons (2018) Figure 1.

1.7. Bibliography

Asch, R.G. 2015. Climate change and decadal shifts in the phenology of larval fishes in the California Current ecosystem. Proc Natl Acad Sci USA **112**(30): E4065–E4074. doi:10.1073/pnas.1421946112.

Atkinson, D., Rose, G.A., Murphy, E., and Bishop, C.A. 1997. Distribution changes and abundance of northern cod (*Gadus morhua*). Canadian Journal of Fisheries and Aquatic Sciences **54**: 132–138. doi:10.1139/f96-158.

Bell, R.J., Richardson, D.E., Hare, J.A., Lynch, P.D., and Fratantoni, P.S. 2015. Disentangling the effects of climate, abundance, and size on the distribution of marine fish: an example based on four stocks from the Northeast US shelf. ICES J Mar Sci **72**(5): 1311–1322. Oxford Academic. doi:10.1093/icesjms/fsu217.

Bi, H., Peterson, W.T., and Strub, P.T. 2011. Transport and coastal zooplankton communities in the northern California Current system. Geophysical Research Letters **38**(12). doi:10.1029/2011GL047927.

Bigelow, H.B., and Schroeder, W.C. 1953. Fishes of the Gulf of Maine. U.S. Fish Wildl. Serv., Fish. Bull. 53(74), 1-577.

Blyth-Skyrme, R., Atkinson, B., and Angel, J. 2015. MSC Sustainable Fishereies Certification: OCI Grand Bank Yellowtail Flounder Trawl Fishery. Public Certification Report, OCI.

Boudreau, S.A., Anderson, S.C., and Worm, B. 2015. Top-down and bottom-up forces interact at thermal range extremes on American lobster. Journal of Animal Ecology **84**(3): 840–850. doi:10.1111/1365-2656.12322.

Bowering, W.R., and Brodie, W.B. 1991. Distribution of commercial flatfishes in the Newfoundland-Labrador region of the Canadian Northwest Atlantic and changes in certain biological parameters since exploitation. Neth. J. Sea Res. **27**(3/4): 407–422.

Breivik, O.N., Storvik, G., and Nedreaas, K. 2016. Latent Gaussian models to decide on spatial closures for bycatch management in the Barents Sea shrimp fishery. Canadian Journal of Fisheries and Aquatic Sciences. NRC Research Press. doi:10.1139/cjfas-2015-0322.

Brodie, W. 2019. An assessment of the witch flounder resource in NAFO Divisions 3NO. : 35.

Brodie, W.B., Kulka, D.W., and Power, D. 2004. The Canadian Fishery from Yellowtail Flounder in NAFO Divisions 3LNO in 2002 and 2003. NAFO SCR Doc. 04/41, Serial No. N4992. St. John's, NL.

Brodie, W.B., Walsh, S.J., and Atkinson, D.B. 1998. The effect of stock abundance on range contraction of yellowtail flounder (*Pleuronectes ferruginea*) on the Grand Bank of Newfoundland in the Northwest Atlantic from 1975 to 1995. Journal of Sea Research **39**(1): 139–152. doi:10.1016/S1385-1101(97)00056-7.

Brodie, W.B., Walsh, S.J., and Maddock Parsons, D. 2010. An evaluation of the collapse and recovery of the yellowtail flounder *(Limanda ferruginea)* stock on the Grand Bank. ICES Journal of Marine Science **67**(9): 1887–1895. doi:10.1093/icesjms/fsq121.

Colbourne, E.B., and Walsh, S.J. 2006. The distribution and abundance of yellowtail flounder (*Limanda ferruginea*) in relation to bottom temperatures in NAFO Divisions 3LNO based on multi-species surveys from 1990–2005. NAFO SCR Document 06/ 23.

Combes, V., Chenillat, F., Di Lorenzo, E., Rivière, P., Ohman, M.D., and Bograd, S.J. 2013. Cross-shore transport variability in the California Current: Ekman upwelling vs. eddy dynamics. Progress in Oceanography **109**: 78–89. doi:10.1016/j.pocean.2012.10.001.

Copeman, L.A. 2001. Lipid Nutrition during early development of Yellowtail flounder (*Limanda ferruginea*). Memorial University of Newfoundland, St. John's, NL.

Cosandey-GodinAurelie, Teixeira, K., WormBoris, and Mills, F. 2014. Applying Bayesian spatiotemporal models to fisheries bycatch in the Canadian Arctic. Canadian Journal of Fisheries and Aquatic Sciences. NRC Research Press. doi:10.1139/cjfas-2014-0159.

Currie, J.C., Thorson, J.T., Sink, K.J., Atkinson, L.J., Fairweather, T.P., and Winker, H. 2019. A novel approach to assess distribution trends from fisheries survey data. Fisheries Research **214**: 98–109. doi:10.1016/j.fishres.2019.02.004.

Daufresne, M., Lengfellner, K., and Sommer, U. 2009. Global warming benefits the small in aquatic ecosystems. Proceedings of the National Academy of Sciences **106**(31): 12788–12793. doi:10.1073/pnas.0902080106.

DFO. 2000. Yellowtail Flounder on Georges Bank. DFO Sci. Stock Status Rep. A3- 15.

Dunn, D.C., Boustany, A.M., and Halpin, P.N. 2011. Spatio-temporal management of fisheries to reduce by-catch and increase fishing selectivity. Fish and Fisheries **12**(1): 110–119. doi:10.1111/j.1467-2979.2010.00388.x.

Dunn, D.C., Maxwell, S.M., Boustany, A.M., and Halpin, P.N. 2016. Dynamic ocean management increases the efficiency and efficacy of fisheries management. PNAS **113**(3): 668–673. National Academy of Sciences. doi:10.1073/pnas.1513626113.

Fisheries and Oceans Canada. 2014. Yellowtail Flounder (*Limanda ferruginea*) - NAFO Divisions 3LNO - As of December 2012. Available from https://www.dfo-mpo.gc.ca/fisheries-peches/ifmp-gmp/groundfish-poisson-fond/yellowtail-limande-div3LNO-eng.html [accessed 30 September 2019].

Fisheries and Oceans Canada. 2016. Yellowtail Flounder. Available from https://dfo-mpo.gc.ca/species-especes/profiles-profils/yellowtail-flounder-limande-queue-jaune-eng.html [accessed 2 October 2019].

Fisheries and Oceans Canada. 2019. Integrated Fisheries Management Plan: Groundfish Newfoundland and Labrador Region NAFO Subarea 2 + Divisions 3KLMNO.

Gao, J., Thorson, J.T., Szuwalski, C., and Wang, H.-Y. 2020. Historical dynamics of the demersal fish community in the East and South China Seas. Mar. Freshwater Res. **71**(9): 1073. doi:10.1071/MF18472.

Gordon, D.C., Kenchington, E.L.R., Gilkinson, K.D., Fader, B.J., Bourbonnais-Boyce, C., MacIsaac, K.G., Henry, L., and Vass, W.P. 2008. Summary of the Western Bank oteer trawling experiment (1997-1999) effects on benthic habitat and communities. Canadian Technical Report of Fisheries and Aquatic Sciences 2822, Fisheries and Oceans Canada, Dartmouth, Nova Scotia.

Hall, M.A., Alverson, D.L., and Metuzals, K.I. 2000. By-Catch: Problems and Solutions. Marine Pollution Bulletin **41**(1–6): 204–219. doi:10.1016/S0025-326X(00)00111-9.

Hobday, A.J., and Hartmann, K. 2006. Near real-time spatial management based on habitat predictions for a longline bycatch species. Fisheries Management and Ecology **13**(6): 365–380. doi:10.1111/j.1365-2400.2006.00515.x.

Hobday, A.J., Hartog, J.R., Spillman, C.M., and Alvesc, O. 2011. Seasonal forecasting of tuna habitat for dynamic spatial management. Canadian Journal of Fisheries and Aquatic Sciences **68**(5): 898–911. doi:https://doi.org/10.1139/f2011-031.

Howell, E.A., Hoover, A., Benson, S.R., Bailey, H., Polovina, J.J., Seminoff, J.A., and Dutton, P.H. 2015. Enhancing the TurtleWatch product for leatherback sea turtles, a dynamic habitat model for ecosystem-based management. Fisheries Oceanography **24**(1): 57–68. doi:10.1111/fog.12092.

Howell, E.A., Kobayashi, D.R., Parker, D.M., Balazs, G.H., and Polovina, J.J. 2008. TurtleWatch: a tool to aid in the bycatch reduction of loggerhead turtles Caretta caretta in the Hawaii-based pelagic longline fishery. Endangered Species Research **5**(2–3): 267–278. doi:10.3354/esr00096.

Keister, J.E., Lorenzo, E.D., Morgan, C.A., Combes, V., and Peterson, W.T. 2011. Zooplankton species composition is linked to ocean transport in the Northern California Current. Global Change Biology **17**(7): 2498–2511. doi:10.1111/j.1365-2486.2010.02383.x.

Knapman, P. 2017. MSC Sustainable Fisheries Certification. Report for the OCI Grand Bank Yellowtail Flounder Trawl Fishery. 2nd Surveillance- 'Review of Information". Acoura Marine Ltd.

Knapman, P., Cook, R., and Blyth-Skyrme, R. 2020. OCI Grand Bank Yellowtail Flounder Trawl: Public Comment Draft Report June 2020. : 180.

Kristensen, K., Nielsen, A., Berg, C.W., Skaug, H., and Bell, B.M. 2016. TMB: Automatic Differentiation and Laplace Approximation. Journal of Statistical Software **70**(1): 1–21. doi:10.18637/jss.v070.i05.

Kulka, D.W. 2001. Description of the Yellowtail Flounder Fishery on the Grand Banks with Comparison to Past Years. NAFO SCR Doc 02/73, Ser. No. N4686.

Latimer, A.M., Banerjee, S., Sang Jr, H., Mosher, E.S., and Silander Jr, J.A. 2009. Hierarchical models facilitate spatial analysis of large data sets: a case study on invasive plant species in the northeastern United States. Ecology Letters **12**(2): 144–154. doi:10.1111/j.1461-0248.2008.01270.x.

Laurence, G.C., and Howell, W.H. 1981. Embryology and influence oftemperature and salinity on early development and survival of Yellowtail flounder *Limanda ferruginea*. Marine Ecology Progress Series **6**: 11–18.

Lear, W.H., and Parsons, L.S. 1993. History and management of the fishery for northern cod in NAFO Divisions 2J, 3K and 3L. Canadian Bulletin of Fisheries and Aquatic Science **226**: 55–89.

Lindgren, F. 2012. Continuous Domain Spatial Models in. The ISBA Bulletin 19, 14–20.: 8.

Lindgren, F., Rue, H., and Lindström, J. 2011. An explicit link between Gaussian fields and Gaussian Markov random fields: the stochastic partial differential equation approach. Journal of the Royal Statistical Society: Series B (Statistical Methodology) **73**(4): 423–498. doi:10.1111/j.1467-9868.2011.00777.x.

MacCall, A. 1990. Dynamic geography of marine fish populations. Washington University Press, Washington.

Maddock Parsons, D. 2013. Divisions 3LNO Yellowtail Flounder (*Limanda ferruginea*) in the 2011 and 2012 Canadian Stratified Bottom Trawl Surveys. NAFO SCR Doc.

Maddock Parsons, D., Brodie, W.B., and Dwyer, K. 2003. Update on Cooperative Surveys of Yellowtail Flounder in NAFO Divisions 3LNO, 1996-2002. NAFO SCR Doc. 03/18, Serial No N4825.

Maddock Parsons, D., Morgan, J., Brodie, B., and Power, D. 2013. Assessment of NAFO Div. 3LNO Yellowtail Flounder, NAFO SCR Doc. 13/37, Serial No. N6192.

Maddock Parsons, D., Morgan, J., Power, D., and Healey, B. 2015. Assessment of NAFO Div. 3LNO Yellowtail Flounder. NAFO SCR Doc. 15/029, Serial N. N6453.

Maddock Parsons, D., Morgan, M.J., and Rogers, R. 2018. Assessment of Yellowtail Flounder in NAFO Divisions 3LNO using a new Stock Production Model in Bayesian Framework. NAFO SCR Doc. 18/038, Serial No.N6828.

Maddock Parsons, D., and Rideout, R. 2015. Divisions 3LNO Yellowtail Flounder (*Limanda ferruginea*) in the 2013 and 2014 Canadian Stratified Bottom Trawl Surveys. NAFO SCR Doc. 09/32, Serial No. N6450.

Manning, A.J., and Crim, L.W. 1998. Maternal and inter-annual comparison of the ovulatory periodicity, egg production and egg quality of the batch-spawning yellowtail flounder. journal of Fish Biology **53**: 954–972.

Martin, T.G., Wintle, B.A., Rhodes, J.R., Kuhnert, P.M., Field, S.A., Low-Choy, S.J., Tyre, A.J., and Possingham, H.P. 2005. Zero tolerance ecology: Improving ecological inference by modelling the source of zero observations. Ecology letters **8**(11): 1235–1246. Wiley-Blackwell. doi:10.1111/j.1461-0248.2005.00826.x.

Maunder, M.N., and Punt, A.E. 2013. A review of integrated analysis in fisheries stock assessment. Fisheries Research **142**: 61–74. doi:10.1016/j.fishres.2012.07.025.

Milisenda, G., Garofalo, G., Fiorentino, F., Colloca, F., Maynou, F., Ligas, A., Musumeci, C., Bentes, L., Gonçalves, J.M.S., Erzini, K., Russo, T., D'Andrea, L., and Vitale, S. 2021. Identifying Persistent Hot Spot Areas of Undersized Fish and Crustaceans in Southern European Waters: Implication for Fishery Management Under the Discard Ban Regulation. Front. Mar. Sci. **8**. Frontiers. doi:10.3389/fmars.2021.610241.

Murua, H., and Saborido-Rey, F. 2003. Female reproductive strategies of marine fish species of the North Atlantic. J. Northwest Atl. Fish. Sci. **33**: 23–31.

NOAA. 2019. Yellowtail Flounder | NOAA Fisheries. Available from https://www.fisheries.noaa.gov/species/yellowtail-flounder [accessed 10 October 2019].

Northwest Atlantic Fisheries Organization. 2018. Yellowtail Flounder *(Limanda ferruginea)* in Divisions 3L, 3N and 3O. NAFO SCS Doc. 18-19, Serial No. N6849. Halifax, Nova Scotia.

Northwest Atlantic Fisheries Organization. 2019. Conservation and Enforcement Measures.

Nye, J.A., Link, J.S., Hare, J.A., and Overholtz, W.J. 2009. Changing spatial distribution of fish stocks in relation to climate and population size on the Northeast United States continental shelf. Marine Ecology Progress Series **393**: 111–129. doi:10.3354/meps08220.

Ollerhead, L.M.N., Morgan, M.J., Scruton, D.A., and Marie, B. 2004. Mapping Spawning Times and Locations for Ten Commercially Important Fish Species Found on the Grand Banks of Newfoundland. Science Branch Fisheries and Oceans Canada P.O. Box 5667 St.John's, NL, Canada A1C 5X1.

Ovaskainen, O., Hottola, J., and Siitonen, J. 2010. Modeling species co-occurrence by multivariate logistic regression generates new hypotheses on fungal interactions. Ecology **91**(9): 2514–2521. doi:10.1890/10-0173.1.

Patrick, W.S., and Benaka, L.R. 2013. Estimating the economic impacts of bycatch in U.S. commercial fisheries. Marine Policy **38**: 470–475. doi:10.1016/j.marpol.2012.07.007.

Pérez Roda, M.A., Gilman, E., Huntington, T., Kennelly, S.J., Suuronen, P., Chaloupka, M., Medley, P.A.H., and Food and Agriculture Organization of the United Nations. 2019. A third assessment of global marine fisheries discards. FAO Fisheries and Aquaculture Technical Paper No. 633. Rome, FAO. 78 pp.

Perry, A.L., Low, P.J., Ellis, J.R., and Reynolds, J.D. 2005. Climate Change and Distribution Shifts in Marine Fishes. Science **308**(5730): 1912–1915. American Association for the Advancement of Science. doi:10.1126/science.1111322.

Perry, R.I., and Smith, S.J. 1994. Identifying habitat associations of marine fishes using survey data: an application to the Northwest Atlantic. Canadian Journal of Fisheries and Aquatic Sciences **51**: 589–602.

Pinsky, M.L., Worm, B., Fogarty, M.J., Sarmiento, J.L., and Levin, S.A. 2013. Marine Taxa Track Local Climate Velocities. Science **341**(6151): 1239–1242. American Association for the Advancement of Science. doi:10.1126/science.1239352.

Pitt, T.K. 1969. Migrations of American Plaice on the Grand Bank and in St. Mary's Bay, 1954, 1959, and 1961. Journal of the Fisheries Board of Canada. NRC Research Press Ottawa, Canada. doi:10.1139/f69-115.

Pitt, T.K. 1971. Fecundity of the Yellowtail Flounder (*Limanda ferruginea*) from the Grand Bank, Newfoundland. J. Fish. Res. Bd. Can. **28**(3): 456–457. doi:10.1139/f71-061.

Pitt, T.K. 1974. Age composition and growth of yellowtail flounder *(Limanda ferruginea*) from the Grand Bank. J. Fish. Res. Board. Can. **31**: 1800–1802.

Poloczanska, E.S., Brown, C.J., Sydeman, W.J., Kiessling, W., Schoeman, D.S., Moore, P.J., Brander, K., Bruno, J.F., Buckley, L.B., Burrows, M.T., Duarte, C.M., Halpern, B.S., Holding, J., Kappel, C.V., O'Connor, M.I., Pandolfi, J.M., Parmesan, C., Schwing, F., Thompson, S.A., and Richardson, A.J. 2013. Global imprint of climate change on marine life. Nature Climate Change **3**(10): 919–925. Nature Publishing Group. doi:10.1038/nclimate1958.

Rideout, R.M., Ings, D.W., Brattey, J., and Dwyer, K. 2015. An Assessment of the Cod Stock in NAFO Divisions 3NO. : 51.

Rideout, R.M., and Morgan, M.J. 2007. Major changes in fecundity and the effect on population egg production for three species of north-west Atlantic flatfishes. Journal of Fish Biology **70**(6): 1759–1779. doi:https://doi.org/10.1111/j.1095-8649.2007.01448.x.

Roberts, S.M., Boustany, A.M., and Halpin, P.N. 2020. Substrate-dependent fish have shifted less in distribution under climate change. Communications Biology **3**(1): 1–7. Nature Publishing Group. doi:10.1038/s42003-020-01325-1.

Robertson, M.D., Gao, J., Regular, P.M., Morgan, M.J., and Zhang, F. 2021. Lagged recovery of fish spatial distributions following a cold-water perturbation. Scientific Reports **11**(1): 9513. Nature Publishing Group. doi:10.1038/s41598-021-89066-x.

Robins, C.R., and Ray, G.C. 1986. A field guide to Atlantic coast fishes of North America. Houghton Mifflin Company, Boston, U.S.A.

Rogers, L.A., Griffin, R., Young, T., Fuller, E., Martin, K.S., and Pinsky, M.L. 2019. Shifting habitats expose fishing communities to risk under climate change. Nature Climate Change **9**(7): 512–516. Nature Publishing Group. doi:10.1038/s41558-019-0503-z.

Scarratt, D.J. 1996. Atlantic Mariculture: Flounders. Communications Branch, Department of Fisheries and Oceans. Scotia-Fundy Region, Halifax, Canada.

Schaefer, M.B. 1954. Some aspects of the dynamics of populations important to the management of commercial marine fisheries. Bull. Int.-Am. Trop. Tuna Com. 1: 25-56.

Selden, R.L., Thorson, J.T., Samhouri, J.F., Bograd, S.J., Brodie, S., Carroll, G., Haltuch, M.A., Hazen, E.L., Holsman, K.K., Pinsky, M.L., Tolimieri, N., and Willis-Norton, E. 2020. Coupled changes in biomass and distribution drive trends in availability of fish stocks to US West Coast ports. ICES J Mar Sci **77**(1): 188–199. Oxford Academic. doi:10.1093/icesjms/fsz211.

Simpson, M.R., and Walsh, S.J. 2004. Changes in the spatial structure of Grand Bank yellowtail flounder: testing MacCall's basin hypothesis. Journal of Sea Research: 12.

Sunday, J.M., Bates, A.E., and Dulvy, N.K. 2012. Thermal tolerance and the global redistribution of animals. Nature Clim Change **2**(9): 686–690. doi:10.1038/nclimate1539.

Swain, D.P., and Wade, E.J. 1993. Density-Dependent Geographic Distribution of Atlantic Cod (*Gadus morhua*) in the Southern Gulf of St. Lawrence. Canadian Journal of Fisheries and Aquatic Sciences **50**(4): 725–733.

Thorson, J. 2017. Three problems with the conventional delta-model for biomass sampling data, and a computationally efficient alternative. Canadian Journal of Fisheries and Aquatic Sciences **75**. doi:10.1139/cjfas-2017-0266.

Thorson, J.T. 2018. Forecast skill for predicting distribution shifts: A retrospective experiment for marine fishes in the Eastern Bering Sea. Fish and Fisheries **20**(1): 159–173. doi:10.1111/faf.12330.

Thorson, J.T. 2019a. Forecast skill for predicting distribution shifts: A retrospective experiment for marine fishes in the Eastern Bering Sea. Fish and Fisheries **20**(1): 159–173. doi:10.1111/faf.12330.

Thorson, J.T. 2019b. Guidance for decisions using the Vector Autoregressive Spatio-Temporal (VAST) package in stock, ecosystem, habitat and climate assessments. Fisheries Research **210**: 143–161. doi:10.1016/j.fishres.2018.10.013.

Thorson, J.T., Adams, C.F., Brooks, E.N., Eisner, L.B., Kimmel, D.G., Legault, C.M., Rogers, L.A., and Yasumiishi, E.M. 2020. Seasonal and interannual variation in spatio-temporal models for index standardization and phenology studies. ICES Journal of Marine Science **77**(5): 1879–1892. doi:10.1093/icesjms/fsaa074.

Thorson, J.T., and Barnett, L.A.K. 2017. Comparing estimates of abundance trends and distribution shifts using single- and multispecies models of fishes and biogenic habitat. ICES Journal of Marine Science **74**(5): 1311–1321. doi:10.1093/icesjms/fsw193.

Thorson, J.T., Ianelli, J.N., Larsen, E.A., Ries, L., Scheuerell, M.D., Szuwalski, C., and Zipkin, E.F. 2016a. Joint dynamic species distribution models: a tool for community ordination and spatio-temporal monitoring. Global Ecology and Biogeography **25**(9): 1144–1158. doi:10.1111/geb.12464.

Thorson, J.T., Pinsky, M.L., and Ward, E.J. 2016b. Model-based inference for estimating shifts in species distribution, area occupied and centre of gravity. Methods in Ecology and Evolution **7**(8): 990–1002. doi:10.1111/2041-210X.12567.

Thorson, J.T., Rindorf, A., Gao, J., Hanselman, D.H., and Winker, H. 2016c. Density-dependent changes in effective area occupied for sea-bottom-associated marine fishes. Proc. R. Soc. B **283**(1840): 20161853. doi:10.1098/rspb.2016.1853.

Thorson, J.T., Scheuerell, M.D., Shelton, A.O., See, K.E., Skaug, H.J., and Kristensen, K. 2015a. Spatial factor analysis: a new tool for estimating joint species distributions and correlations in species range. Methods in Ecology and Evolution **6**(6): 627–637. doi:10.1111/2041-210X.12359.

Thorson, J.T., Skaug, H., Kristensen, K., Shelton, A.O., Ward, E.J., Harms, J.H., and Benante, J.A. 2015b. The importance of spatial models for estimating the strength of density dependence. Ecology 96, 1202–1212. doi:doi:10.1890/14-0739.1.

Tilseth, S. 1990. New marine fish species for cold-water farming. Aquaculture **85**(1–4): 235–245.

Tommasi, D., Stock, C.A., Hobday, A.J., Methot, R., Kaplan, I.C., Eveson, J.P., Holsman, K., Miller, T.J., Gaichas, S., Gehlen, M., Pershing, A., Vecchi, G.A., Msadek, R., Delworth, T., Eakin, C.M., Haltuch, M.A., Séférian, R., Spillman, C.M., Hartog, J.R., Siedlecki, S.,

Samhouri, J.F., Muhling, B., Asch, R.G., Pinsky, M.L., Saba, V.S., Kapnick, S.B., Gaitan, C.F., Rykaczewski, R.R., Alexander, M.A., Xue, Y., Pegion, K.V., Lynch, P., Payne, M.R., Kristiansen, T., Lehodey, P., and Werner, F.E. 2017. Managing living marine resources in a dynamic environment: The role of seasonal to decadal climate forecasts. Progress in Oceanography **152**: 15–49. doi:10.1016/j.pocean.2016.12.011.

Vert-pre, K.A., Amoroso, R.O., Jensen, O.P., and Hilborn, R. 2013. Frequency and intensity of productivity regime shifts in marine fish stocks. Proceedings of the National Academy of Sciences **110**(5): 1779–1784. doi:10.1073/pnas.1214879110.

Walsh, S.J. 1991. Commercial fishing practices on offshore juvenile flatfish nursery grounds on the Grand Banks of Newfoundland. Netherlands Journal of Sea Research **27**(3): 423–432. doi:10.1016/0077-7579(91)90043-Z.

Walsh, S.J. 1992. Factors influencing distribution of juvenile yellowtail flounder (Limanda ferruginea) on the Grand Bank of Newfoundland. Netherlands Journal of Sea Research **29**: 193–203.

Walsh, S.J., and Brodie, W.B. 2006. Exploring relationships between bottom temperatures and spatial and temporal patterns in the Canadian fishery for yellowtail flounder on the Grand Bank. NAFO SCR Doc 06/26, Serial No. N5245.

Walsh, S.J., and Morgan, M.J. 2004. Observations of natural behaviour of Yellowtail flounder derived from data storage tags. ICES Journal of Marine Science **61**(7): 1151–1156. doi:10.1016/j.icesjms.2004.07.005.

Walsh, S.J., Simpson, M., and Morgan, M.J. 2004a. Continental shelf nurseries and recruitment variability in American plaice and yellowtail flounder on the Grand Bank: insights into stock resiliency. Journal of Sea Research **51**(3–4): 271–286. doi:10.1016/j.seares.2003.10.003.

Walsh, S.J., Simpson, M.R., Morgan, J., Dwyer, K., and Stansbury, D. 2001. Distribution of juvenile yellowtail flounder, American plaice and Atlantic cod on the southern Grand Bank: a discussion of nursery areas and marine protected areas. NAFO SCR Doc. 01/78, Serial No. N4457.

Walsh, S.J., Simpson, M.R., and Morgan, M.J. 2004b. Continental shelf nurseries and recruitment variability in American plaice and yellowtail flounder on the Grand Bank: insights into stock resiliency. J Sea Res **51**: 271–286.

Warren, W., Brodie, W.B., Stansbury, S., Walsh, S.J., Morgan, J., and Orr, D. 1997. Analysis of the 1996 Comparative Fishing Trial between the Alfred Needier with the Engel 145 trawl and the Wilfred Templeman, with the Campelen 1800 trawl.

Warren, W.G. 1996. Report on the Comparative Fishing Trial Between the Gadus Atlantica and Teleost.

Warton, D.I., Blanchet, F.G., O'Hara, R.B., Ovaskainen, O., Taskinen, S., Walker, S.C., and Hui, F.K.C. 2015. So Many Variables: Joint Modeling in Community Ecology. Trends in Ecology & Evolution **30**(12): 766–779. doi:10.1016/j.tree.2015.09.007.

Wheeland, L., Rogers, B., Rideout, R., and Maddock Parsons, D. 2019. Assessment of Witch Flounder (*Glyptocephalus cynoglossus*) NAFO Divisions 2J3KL. Canadian Science Advisory Secretariat(CSAS) Research Document 2019/066, St. John's NL.

Wilderbuer, T., Stockhausen, W., and Bond, N. 2013. Updated analysis of flatfish recruitment response to climate variability and ocean conditions in the Eastern Bering Sea. Deep Sea Research Part II: Topical Studies in Oceanography **94**: 157–164. doi:10.1016/j.dsr2.2013.03.021.

Chapter 2:
Identifying Seasonal Spatiotemporal Distribution Changes and Interspecies Correlations of the Grand Banks Yellowtail Flounder Fishery and its Bycatch Species

2.1. Introduction

Bycatch, or catch of non-target organisms is among the most pervasive problems in modern day fisheries (Pérez Roda et al. 2019). Hall et al. (2000) indicated that in the past, bycatch was often ignored by most fisheries scientist and managers because it was not visible, most likely on a smaller magnitude, and/or thought to be less significant for stock assessment; leading to interferences between fisheries and ecosystems not being prioritized. However, stocks with lower levels of biomass have been found to be the least responsive to fisheries management measures and are the most vulnerable to changes in their environment (Vert-pre et al. 2013). Stocks in moratoria whom biomass has been depleted to a low level that there is no longer a directed fishery, can still be caught as bycatch; having an impact on population recovery and can create conservation problems when catches surpass sustainable harvest rates.

Climate affects species abundance and distribution via complex ways and changes in both abiotic and biotic factors work together to influence species distribution (Perry et al. 2005). Benthic species like groundfish, whose distribution is primarily determined by static physiographic conditions, have shifted significantly less than pelagic species, who's distributions are primarily associated with dynamic oceanographic conditions over the past 30 years (Roberts et al. 2020). That being said, dynamic oceanographic conditions like temperature should still be considered for groundfish management to gain better understanding of small and large-scale processes affecting the spatial and spatiotemporal demographic processes. Marine ectotherms, such as

demersal fish, typically fully occupy the extent of latitudes within their thermal tolerance limits, and are consequently predicted to expand at their poleward range boundaries and contract at their equatorward boundaries directly with climate warming (Sunday et al. 2012). Climate change can also effect depth of demersal fish species as they move to deeper colder water to escape warming shallower waters. Dulvy et al. found coherent deepening of 28 demersal fish assemblages of 3-6 m per decade form 1980-2004 in the North Sea in response to climate change (2008). Climate can also indirectly impact fish via bottom up ecosystem shifts impacting species distribution shifts through: variation in prey fields and energy transfer in response to fluctuations in alongshore and cross-shelf transport (Bi et al. 2011; Keister et al. 2011; Combes et al. 2013; Wilderbuer et al. 2013), climate related changes in the abundance of predators, competitors, and parasites (Boudreau et al. 2015), and climate-driven changes in primary productivity structure and dynamics (Daufresne et al. 2009).

The effects of habitat quality covariates on fish abundances are sometimes difficult to measure for many marine species, including demersal marine fishes. Instead, differences in habitat effects may be inferred from spatial variation of the density of species with similar habitat requirements. For example, a Bayesian hierarchal statistical approach in a multispecies analysis of four invasive plant species in the northeastern USA were used to infer abundance of a single invasive plant species (Latimer et al. 2009). Multivariate logistic regression has also been used on 22 species of wood-decaying fungus to reveal similar habitat requirements (Ovaskainen et al. 2010). Joint dynamic species distribution models (JDSDMs) can estimate abundance trends for butterfly species that are infrequently encountered but have similar spatiotemporal dynamics among other related and more common butterfly species (Thorson et al. 2016a). JDSDMs have also been used

to explore the relationships between fishes and species associated with specific habitats using a vector auto-regressive spatiotemporal model (VAST) (Thorson and Barnett 2017).

VAST (ie. Thorson and Barnett 2017; Thorson 2019b) has been used to study the spatiotemporal abundance and distribution shifts among multiple species (Thorson 2019a). In fact, multispecies VAST models were found to be more parsimonious, had better predictive performance and estimated fine-scale variation in density for species with relatively few encounters compared to fitting single species models with similar precision for estimates of abundance and distribution shifts (Thorson and Barnett 2017). This was concluded by fitting eight species of US Pacific Coast rockfish (*Sebastes spp.*), thornyheads (*Sebastolobus spp.*), and structure-forming invertebrates (SFIs) to a multispecies VAST model (Thorson and Barnett 2017). Multispecies VAST models have also been used to estimate covariation in multispecies catch rates across four seasons, attributed to spatial habitat preferences and environmental response in the East and South China seas of nine major commercial species (Gao et al. 2020).

On the Grand Banks off Newfoundland, the commercial fisheries for yellowtail flounder, American plaice, Atlantic cod and witch flounder entered moratoria in the early 1990s because their respective stocks had collapsed. The Div. 3LNO yellowtail flounder fishery re-opened in 1998 and catches numerous species as bycatch (Table 1.1). However, bycatch species such as American plaice (Div. 3LNO), witch flounder (Div. 2J3KL, Div. 3NO moratorium lifted in 2015), and Atlantic cod (Div. 2J3KL, Div. 3NO) are currently still in moratoria (Knapman et al. 2020). The Div. 3LNO yellowtail flounder fishery hauls are limited to a bycatch cap of 15% of American plaice, and whichever is the greater of 5% or 1,250 kg for Div.3NO witch flounder, and 4%, or 1,000 kg for Div. 3NO Atlantic cod (Knapman et al. 2020). Measurements in place

to avoid bycatch in the yellowtail flounder fishery already include voluntary spawning closure, and gear restrictions (Fisheries and Oceans Canada 2019). Although the yellowtail flounder fishery has extensive experience of operating within bycatch limits (Knapman et al. 2020) and considerable efforts have been made to increase selectivity (Blyth-Skyrme et al. 2015), intuitive spatiotemporal distribution maps would be very useful to identify and avoid bycatch hotspots for more efficient fishing practices.

Therefore, in chapter two, I implement a multi-species VAST model to estimate the spatiotemporal distribution changes for yellowtail flounder and three of its common bycatch species in moratoria; American plaice, witch flounder and Atlantic cod. I integrate dynamic and static habitat covariates to improve the model fit. I estimate each species biomass, density, center of gravity, effective area occupied, correlation between species and effects of habitat covariates for both DFO Fall and Spring bottom trawl surveys to further understand the interspecies relationship dynamics. This is the first application of VAST in the Northwest Atlantic ecosystem, in which environmental effects and interspecies relationships are modelled together.

2.2. Materials and Methods

2.2.1   Data Collection

I examined annual stratified random bottom trawl surveys conducted in the Spring (April- June, number of tows = 41 796) and Fall (September – December, number of tows =38 480) (Table 2.1) by the Canadian Department of Fisheries and Oceans (DFO), on the Grand Bank of Newfoundland in NAFO Div. 3LNO (Figure 1.1), from 1984 – 2018 and with depths <950m

(after 1984 spring surveys conducted in 3LNO, 1983-1989 only 3L was surveyed in the Fall) (Figure 2.1 & 2.2) (Paul Regular, Department of Fisheries and Oceans, Newfoundland, unpubl. Data). Only tows that had bottom temperature recorded were included in our models (Spring number of tows= 41 364, Fall number of tows = 38 044). The *Engel 145*' trawl was used until 1994, when the surveys were switched to a more efficient *Campelen 1800* shrimp trawl in 1995 (Maddock Parsons et al. 2013). The *Campelen 1800* shrimp trawl is more efficient at catching smaller fish than the The *Engel 145*' trawl therefore they have different catch rates (Warren 1996; Warren et al. 1997). In this study, I used the converted data set for the *Engel 145*' years and raw values for *Campelen 1800* years to maintain continuity of our time-series. This conversion was done by multiplying the biomass caught by the conversion factor estimated by comparative fishing efforts (Warren 1996; Warren et al. 1997). Industry catch data was not used because of privacy constraints; therefore, I only used the DFO bottom trawl survey data.

Ocean Choice International (Atlantic company that owns 91.7% of the Canadian yellowtail flounder TAC (Knapman 2017)) lists American plaice and thorny skate as the main primary bycatch species (Knapman et al. 2020). They also list Atlantic cod, Atlantic halibut, witch flounder and Greenland halibut as minor primary bycatch species (Knapman et al. 2020) in the yellowtail flounder fishery. However, thorny skate, Atlantic halibut and Greenland halibut catches using the Engel gear were not converted to Campelen trawl equivalents; therefore, these species are not included in the Div. 3LNO converted multi-species bottom trawl survey dataset. Even though thorny skate, Atlantic halibut and Greenland halibut catches using the Campelen surveys since 1995 (Fall) or 1996 Spring) are available but not used in this thesis because of the shorter time-series. Therefore, data was only extracted for yellowtail flounder, Atlantic cod,

witch flounder and American plaice using the Rstrap database from DFO collaborators (Table 2.1). Total catch in weight of male, female and unidentified gendered fish were included.

Bottom depth (mean depth of tow) and bottom temperature were measured at each tow location and used as habitat variables in our model. Bottom depth was rescaled and natural log transformed to reduce variation to a reasonable range (Thorson 2021). Bottom substrate data has been routinely collected of the Grand Bank from 1994-2004 using the ROXANN acoustic seabed classification system; seabed roughness and hardness indices from the echo sounder were classified as: mud, sand, sand/shell, gravel, small rock, and boulders/bedrock (Elaine Hynick, Department of Fisheries and Oceans, Newfoundland, unpubl. Data). Categorical substrate data was extracted to each tow using nearest neighbor (k=5) using the class package in R (https://www.rdocumentation.org/packages/DMwR/versions/0.4.1/topics/kNN).

2.2.2. Model Components

Conventional delta models composed of two GLMs, one for the positive catch rates and one for the encounter-probability; they are commonly used in fisheries science to estimate biomass indices (e.g. Martin et al. 2005; Maunder and Punt 2013), and as a joint dynamic species distribution model for zero-inflated survey data (Thorson and Barnett 2017).

I will use a modified delta model (See Table 2.2 for a description of all symbols in the model). that specifies a probability distribution for biomass sampled at each survey tow b for four species: yellowtail flounder, American plaice, witch flounder and Atlantic cod to incorporate information on interspecies relationships community dynamics. The parameterization used

involves a delta model to separately model encounter probability $p(c, s, t)$ (described below) and biomass density via positive catch rates $r(c, s, t)$ (described below) with B being the probability distribution for catches. Where s is tow location, c is species and t is year.

$$(2.1) \Pr(b = B) = \begin{cases} 1 - p(c, s, t) & if\ B = 0 \\ p(c, s, t) \times \text{Gamma}\{B|\log{(r(c, s, t))}, \sigma_b{}^2\} & if\ B > 0 \end{cases}.$$

Usually, conventional delta models have a logit-link that keeps encounter probability and positive catch rates separate; however, this has difficulties in interpreting covariates by assuming independence between the two delta model components, and biologically implausible forms when removing covariates (Thorson 2017). A Poisson-link delta model (Thorson 2017) solves these problems by capturing the correlation between encounter probability and positive catch rates therefore; decreasing residual spatial variation, improving fit and ensuring the effect of changing habitat covariates is additive between components of the delta model (Thorson 2017) (see Appendix B). I used the Poisson-link delta model for each Fall and Spring survey separately from 1984-2018.

Encounter probability $p(s, c, t)$ is defined in the Poisson-link delta model given the assumption that individuals are randomly distributed in the geographic sampling area, such that the probability of encountering at least one fish is:

$$(2.2)\ p(c, s, t) = 1 - \exp\left(-\alpha \times n(c, s, t)\right),$$

Where α is the constant area swept (Table 2.2) (see Appendix A) by each operation of a bottom

trawl sample and $n(c, s, t)$ is predicted number-density as described below. Positive catch rates

$r(c, s, t)$ is:

$$(2.3)\ r(c, s, t) = \frac{\alpha \times n(c, s, t)}{p(c, s, t)} \times w(c, s, t),$$

where $w(c, s, t)$ is predicted biomass per species encountered as described below.

The two GLMs for the model are: (Eq. 2.4) predicted number-density $n(c, s, t)$ for each species c

at each tow location s at year t; and (Eq 2.5) predicted biomass per group of individuals

encountered $w(c, s, t)$.

(2.4)

$$\log\left(n(c, s, t)\right) = \beta_n(c) + \sum_{f=1}^{f_{\beta_n}} L_{\beta_n}(c, f)\beta_n(t, f) + \sum_{f=1}^{f_{\omega_n}} L_{\omega_n}(c, f)\omega_n(s, f)$$

$$+ \sum_{f=1}^{f_{\varepsilon_n}} L_{\varepsilon_n}(c, f)\varepsilon_n(s, f, t)\ +\ \gamma_{n1}(c, t, p_1)X_{n1}(s, t, p_1) + \gamma_{n2}(c, t, p_2)X_{n2}(s, t, p_2)$$

$$+ \gamma_{n3}(c, p_3)X_{n3}(s, p_3)\ +\ \gamma_{n4}(c, p_4)X_{n4}(s, p_4) + \gamma_{n5}(c, p_5)X_{n5}(s, p_5)$$

$$+ \gamma_{n6}(c, p_6)X_{n6}(s, p_6) + \gamma_{n7}(c, p_7)X_{n7}(s, p_7),$$

(2.5)

$$\log(w(c,s,t) = \beta_w(c) + \sum_{f=1}^{n_{\beta w}} L_{\beta_w}(c,f)\beta_w(t,f) + \sum_{f=1}^{n_{\omega w}} L_{\omega_w}(c,f)\omega_w(s,f)$$

$$+ \sum_{f=1}^{n_{\varepsilon w}} L_{\varepsilon_w}(c,f)\varepsilon_w(s,f,t) + \gamma_{w1}(c,t,p_1)X_{w1}(s,t,p_1) + \gamma_{w2}(c,t,p_2)X_{w2}(s,t,p_2)$$

$$+ \gamma_{w3}(c,p_3)X_{w3}(s,p_3) + \gamma_{w4}(c,p_4)X_{w4}(s,p_4) + \gamma_{w5}(c,p_5)X_{w5}(s,p_5)$$

$$+ \gamma_{w6}(c,p_6)X_{w6}(s,p_6) + \gamma_{w7}(c,p_7)X_{w7}(s,p_7).$$

I set the number of factors equal to the total number of species ($c= 4, f=4$). It is possible that a lower number of factors would be parsimonious, but I chose the largest possible number as it was still computationally manageable. The structure of the two linear predictors $n(c,s,t)$ and $w(c,s,t)$ is identical; with a fixed temporal intercept $\beta(c)$, a random temporal component $\beta(t,f)$, a random spatial component $\omega(s,f)$, and a random spatiotemporal component $\varepsilon(s,f,t)$. Each respective component has 4 factors ($f = 4$); temporal f_β, spatial f_ω, and spatiotemporal f_ε. L represents the loading matrices that generate temporal covariation L_β, spatial covariation L_ω, and spatiotemporal covariation L_ε respectively. Similar to the loadings in spatial factor analysis, the loading matrix represents the liner relationship between latent and random fields and the log $n(c,s,t)$ and $\log w(c,s,t)$.

I included a separate effect of each habitat covariate p for each species c. $\gamma(c,t,p)$ is the fixed effect of the respective density covariate $X(s,t,p)$ for species c that changes over the years t (X is a three-dimensional array for bottom temperature as a dynamic covariate that changes over

time, and two-dimensional array for depth and substrate as static covariates).

$\gamma_{n1}(c,t,p_1)$ represents the linear effect of temperature (°C), while $\gamma_{n2}(c,t,p_2)$ represents the quadratic effect of temperature for year t, and species c. $\gamma_{n3}(c,p_3), \gamma_{n4}(c,p_4), \gamma_{n5}(c,p_5)$, and $\gamma_{n6}(c,p_6)$ represent the 1st, 2nd, 3rd, and 4th order b spline basis functions for the log of depth (m) for each species c. $\gamma_{n7}(c,p_7)$ represents the estimated linear effect of substrate type (6 categories mentioned in 2.2.1). Models were run separately for Spring and Fall surveys. Significant habitat coefficients were evaluated via model selection (section 2.2.3).

K-means algorithm was used to identify the location of 100 knots (largest number computationally manageable) to minimize the total distance between the location of the tow to the nearest knot. We define all spatial and spatiotemporal variation using 100 knots distributed. The spatial and spatiotemporal variances are approximated by Gaussian Markov random fields (Thorson et al. 2015c). The correlation matrix is based on a vector of distance between any pair of locations; Matern correlation is the sparse approximation to inverse of covariance (Lindgren et al. 2011) and is used to estimate a separate decorrelation rate for each linear predictor respectively. This approximation for Matern correlation function has been used in spatiotemporal models (ie. Thorson and Barnett 2017). I used the Matern correlation is because the computation for VAST is large and the sparse matrix speeds up the process.

2.2.3. Model Fit

I compared multiple models with various settings for the temporal structure of random effects for both Fall and Spring surveys. Specifically, I compared different combinations of independent,

random-walk and autoregressive (AR1) processes for temporal intercepts (β_n and β_w) and spatiotemporal (ε_n and ε_w) vectors. I confirmed that the models converged (maximum gradient < 10^{-6}) with a Newton Optimizer with two extra steps to find the likelihood estimates. Then I confirmed that the parameters are estimable by confirming that the hessian matrix is positive definite at the maximum likelihood estimates.

To select the best model parameters, I performed an AIC comparison as suggested by (Thorson 2019b). Once I determined the best model settings for both seasons, I applied the same model selection process on habitat covariates for both Fall and Spring surveys. Once the best model was selected, habitat coefficients confidence intervals were also assessed for significance. Model fit was also explored by examining the spatial quantile residuals to ensure there was no clustering (Figure 2.3 & 2.4).

Models were fit using the VAST package (ver. 3.6.1, https://github. com/James-Thorson/VAST, accessed 16 February 2020) for spatial, temporal and spatiotemporal covariances and abundance indices in the R statistical environment (R Core Team 3.5.2). The association between tows and knots is accomplished by using a triangulated mesh with 100 knots via bilinear interpolation following standard practices in the software R-INLA (ver. 20.03.17, http://www.r-inla.org/, accessed 16 February 2020;(Lindgren 2012)). Model parameters are estimated using Template Model Builder (TMB) to implement the Laplace approximation to the marginal likelihood of fixed effects (ver. 1.7.18, see https:// github.com/kaskr/adcomp/wiki, accessed 16 February 2020; accessed 16 February 2020 ,Kristensen et al. 2016), and a gradient based non-linear

optimizer to identify the values of parameters that maximizes the marginal likelihood. Bias

correction was not used due to computing time restraints.

2.2.4. Estimating Correlation

After fitting the model, I calculated model covariance among species V. I used factor-analysis

decomposition (Thorson et al. 2015a, 2016a), to estimate interspecies correlation:

$$(2.7)\ V_{\omega n} = L_{\omega n} L_{\omega n}{}^{T}\ ,$$

Where $L_{\omega n}$ is a 4×4 matrix defining the first 4 columns of the Cholesky decomposition of

covariance matrix $V_{\omega n}$. $L_{\omega n}{}^{T}$ is the matrix-transpose of $L_{\omega n}$. $V_{\omega n}$ represents spatial covariance

for numbers density. $V_{\omega n}$ has identical set up to $V_{\omega w}, V_{\varepsilon n}\ and\ V_{\varepsilon w}$ for there respective spatial and

spatiotemporal processes (Warton et al. 2015; Thorson et al. 2016a, 2016b). The covariation

among species ($V_{\omega n}$, $V_{\omega w}, V_{\varepsilon n}\ and\ V_{\varepsilon w}$) are treated as a fixed effect. Correlation matrices were

derived from the covariance matrices (cor(x,y) = cov(x,y)/sd(x)sd(y)).

2.2.5. Density

Predicted biomass density $d(c, s, t)$ (kg/ km^2) for each location for each species c, every year t

and location s was calculated from the model,

$$(2.8)\ d(c, s, t) = p(c, s, t) * r(c, s, t).$$

I use $d(c, s, t)$ to plot spatiotemporal species density distributions.

2.2.6. Biomass

Predicted biomass density $d(c, s, t)$ are used to predict total biomass $I(c, t)$ for the entire domain

for each species c in each year t to estimate temporal trends in biomass (Thorson et al. 2015b):

$$(2.9)\ I(c,t) = \sum_{s=1}^{n_s} a(s) \times d(c,s,t) .$$

Where n_s is the number of fine-scale predictions at each modelled location s and $a(s)$ is the area

associated with model location s ; $d(c, s, t)$ is the predicted biomass-density for each species c,

location s and year, t.

2.2.7. Centre of Gravity

The centre of gravity $Z(c, t, m)$, known as the spatiotemporal centroid of each species

distribution (Thorson et al. 2016b), was calculated to estimate distribution shifts North-South and

East-West:

$$(2.9)\ Z(c,t,m) = \sum_{s=1}^{n_s} \frac{z(m) \times a(s) \times d(c,s,t)}{I(c,t)} .$$

Where z(m) is a matrix representing the location for each prediction; the location in eastings and

northings of each centre of gravity thus representing movement North-South and East-West.

2.2.8. *Effective Area*

Estimated effective-area occupied is defined as the area occupied assuming equal density over the entire area; it can be used to monitor or predict range expansion or contraction or density-dependent range expansion (Thorson et al. 2016c). To estimate effective-area occupied, first the biomass-weighted average density $D(c,t)$ was calculated:

$$(2.10) \; D(c,t) = \sum_{s=1}^{n_s} \frac{a(s) \times d(c,s,t)}{I(c,t)} d(c,s,t) \, ,$$

Effective area occupied $A(c,t)$, was calculated by dividing the total biomass by the biomass-weighted average density to get the area containing the population at the specific biomass-weighted average density.

$$(2.11) \; A(c,t) = \frac{I(c,t)}{D(c,t)} \, .$$

2.3. Results

2.3.1. *Model selection*

To select the best model structure, I ran an AIC comparison (Table 2.3). The model structure with the best fit was a random walk for the temporal intercept and independent for the spatiotemporal intercept (Fall AIC = 170228.7, Spring AIC = 191621.6). To select the best habitat covariates, I ran an AIC comparison (Table 2.4). The best model with the lowest AIC value for both seasons included a basis-spline with four degrees of freedom to model the nonlinear effect of log-transformed bottom depth, bottom temperature was modeled as a linear

effect with quadratic order effect, and substrate was modeled as a linear effect (Fall AIC = 164050.1, Spring AIC = 182707.1). The spatial quantile residuals were evenly distributed, and no clustering was observed for both the Fall and Spring (Figure 2.3 & 2.4). There was seasonal differences between habitat covariates parameter estimates for all species (Table 2.5 & 2.6). I attempted to detangle the habitat covariate effects, but it was difficult to interpret as the two linear predictors were kept separate. Therefore, I did not include a habitat covariate breakdown in this thesis.

2.3.2. *Correlation Among Species*

I will focus on the correlation between yellowtail flounder and the respective bycatch species. For both Fall and Spring, spatial biomass had the largest effect on species correlation compared to spatial numbers density, spatiotemporal biomass and spatiotemporal numbers density (Figure 2.5 & 2.6). In the Fall, spatial correlation in numbers density was weakest between yellowtail flounder and Atlantic cod (0.4) and strongest between yellowtail flounder and witch flounder (0.7) (Figure 2.5). Spatial correlation in biomass was strong for all three species relative to yellowtail flounder (>0.6) (Figure 2.5). Spatiotemporal correlation in numbers density relationship was weak for all species relative to yellowtail flounder (<0.4) (Figure 2.5). Spatiotemporal correlation in biomass was weakest for witch flounder relative to yellowtail flounder (0.1) while American plaice and yellowtail flounder had the strongest relationship (0.8) (Figure 2.5). In the spring, the correlation in the spatial effect of numbers density was relatively weak for all species relative to yellowtail (<0.4) (Figure 2.6). Inversely, spatial correlation in biomass was strong for all bycatch species relative to yellowtail flounder (>0.7) (Figure 2.6). Spatiotemporal correlation in numbers density for to yellowtail flounder was strong for

American plaice (0.7) and weak for Atlantic cod (0.4) and witch flounder (0.4) (Figure 2.6).

Spatiotemporal correlation in biomass for yellowtail flounder was strong with American plaice

(0.8) and weak with Atlantic cod (0.2) and witch flounder (0.3) (Figure 2.6).

2.3.3. Estimated Density

Yellowtail flounder is concentrated mainly in Div. 3N and Div. 3O in the south-eastern shoal

nursery area (Figure 2.7 & 2.8). Witch flounder is mainly concentrated along the edges of the

Grand bank in deeper water (Figure 2.11 & 2.12). American plaice is the most ubiquitous of the

four species having higher concentrations on the southern tip of 3N (Figure 2.13 & 2.14).

Atlantic cod has a higher concentration on the Southeastern shoal and northern 3L (Figure 2.9 &

2.10).

2.3.4. Estimated Biomass

Overall biomass trends for all four species in both Spring and Fall (Figure 2.15) reached

relatively low levels around the ground fish moratoria of 1995. Yellowtail flounder biomass

recovered since then and surpassed biomass values prior to 1995, while the other three species

did not. This represents the stocks still in moratoria: Div. 3LNO American plaice, Div. 3NO +

Div. 2J3KL Atlantic cod and Div. 3NO (moratorium lifted in 2014) + Div. 2J3KL witch

flounder.

2.3.5. Estimated Centre of Gravity

Centre of gravity east in the Fall for all four species is relatively stable (Figure 2.16). Centre of

gravity east in the Spring has shifted eastward for all four species, and the shift is greatest for

Atlantic cod, from a low of 355.76 UTM E in 1994 to a high of 614.83 UTM E in 2017 (Figure 2.16). Atlantic cod and witch flounder displayed the greatest degree of variability of centre of gravity east in the Spring between all four species (Figure 2.16). Centre of gravity north in the Fall moved southward for all four species, with the biggest shifts for Atlantic cod, American plaice and witch flounder during the moratoria. The centre of gravity have been shifting more northward since then, with Atlantic cod surpassing its pre-moratorium northward distribution in the Fall (Figure 2.17) (see Appendix C & D). Pre-moratorium Atlantic cod had a centre of gravity north high of 5168.95 UTM N, with a low during the moratorium in 1994 of 4997.10 UTM N, and a most recent northward distribution in 2018 surpassing the pre-moratorium high of 5302.50 UTM N (Figure 2.17). Centre of gravity north in the Spring dropped southward for all four species, mainly Atlantic cod, American plaice and witch flounder during the moratoria and has been relatively stable since then (Figure 2.17).

2.3.6. *Estimated Effective Area*

Effective area for yellowtail flounder, witch flounder and Atlantic cod dropped slightly during the Fall and more drastically during the Spring at the beginning of the moratoria and recovered early in the 2000s (Figure 2.18). Effective area for American plaice slowly dropped during the moratorium and recovered during the Fall, while it still remains low in the Spring (Figure 2.18). Atlantic cod during the spring showed the most variation between years of the four species (Figure 2.18).

2.4. Discussion

Our case study focused on estimating interspecies interannual and seasonal changes in distribution with habitat covariates for a commercially important stock, Div. 3LNO yellowtail flounder and three of its common bycatch species in moratoria: American plaice, witch flounder and Atlantic cod. I estimated interannual and seasonal trends between species and habitat covariates to estimate biomass, distribution, and range expansion trends.

Generally, I found high spatial correlation in biomass between yellowtail flounder and all three of the bycatch species in question for both Fall and Spring (Figure 2.5 & 2.6). American plaice had the strongest spatiotemporal correlation with yellowtail flounder for both numbers density and biomass for both Fall and Spring (Figures 2.5 & 2.6). This coincides with the reported bycatch from the OCI yellowtail flounder fishery as American plaice is the most commonly caught bycatch species (Table 1.1). The strong interspecies correlation (Figure 2.5 & 2.6) hints that the species may be occupying similar habitats (see Appendix E); however, relating habitat covariates to trends in species distribution was not the goal of my thesis and this warrants further research.

I compared interannual abundance-weighted average density between seasons as a measure of seasonal timing for all four species to provide a basis for comparison of species distribution shifts as demonstrated in past studies (ie. Thorson et al. 2020). There appears to be slight seasonal variation between all species. Yellowtail flounder concentrated in mainly Div. 3N and Div. 3O in the southeastern shoal nursery area for both Spring and Fall with lower density in Div. 3L in the Spring than the Fall in more recent years (Figure 2.7 & 2.8). Witch flounder is

mainly concentrated along the edges of the Grand bank in deeper water for both Fall and Spring (Figure 2.11 & 2.12). American plaice is the most ubiquitous of the four species having higher concentrations on the southern tip of Div. 3N in Fall and Spring and more dispersed density in Div. 3L during the Spring (Figure 2.13 & 2.14). Atlantic cod has a higher concentration on the Southeast shoal in Fall and Spring and north Div. 3L in Spring (Figure 2.9 & 2.10). Highest overlap of all four species occurs on the south-eastern shoal during the Spring - coincidently overlapping with the highest concentration of yellowtail flounder (Figure 2.8). Trends in recent years seem to be similar within species. The largest interannual variation of density distribution was observed before, during and after the moratoria.

During the moratoria in the early 1990s, all four species centre of gravity shifted southward in the Fall and have been shifting norward towards their pre-moratoria distribution since the recovery (Figure 2.17). This shift northward was stronger in the Fall than the Spring for all four species (Figure 2.17). During the moratoria, center of gravity east dropped west for Atlantic cod and witch flounder, while yellowtail flounder and American plaice have been steadily climbing east over the observed time period (Figure 2.16). As I did not dissect the relationships between habitat variables and distribution shifts, I cannot determine the effect of the habitat variables on distribution shifts - I can only hypothesize. The observed seasonal differences suggests there may be some seasonal effects; possibly due to habitat spawning restrictions in the Spring. The rate of climate driven shifts in species distribution is often measured by using the centre of gravity; the centroid of the distribution can be measured as longitude and latitude (Pinsky et al. 2013; Thorson et al. 2016b; Currie et al. 2019). Centre of gravity is a useful proxy for large scale climate-driven distribution shifts across regions but does not capture specifics about the

density available to individual microhabitats (Rogers et al. 2019; Selden et al. 2020). The moratoria corresponded with a period of cold water on the Grand Banks and yellowtail flounder and American plaice shifted southward during this regime shift, while yellowtail flounder has redistributed northwards and American plaice has not when warmer water returned during the Spring (Robertson et al. 2021); This was congruent with our findings, therefore temperature may be a potential driver in these distribution shifts (Figure 2.17). However, future research should investigate how the habitat variables (temperature, depth and substrate) in our model interacted with species distribution shifts. Even fishing pressure and population structure can have an effect on species distributions.

The proportion of yellowtail flounder north of 45 degrees latitude has been stable since the mid 80s (Maddock Parsons 2013). Before that, most of the stock was located south of 45 degrees latitude (Brodie et al. 2010). Corresponding with our results, an increase in stock abundance coincides with a northward expansion from 1995 to 2005 correlating to increase in water bottom temperatures (Walsh and Brodie 2006) (Figure 2.15 & 2.17). Centre of gravity shifts northward and eastward in the fall for Atlantic cod and witch flounder are influenced by two stock dynamics (Figures 2.16 & 2.17). Both have a Div. 2J3KL stock and a Div. 3NO stock; with the Div. 3NO stocks are both still in moratoria respectively. The centre of gravity shifts northward observed in Div. 3LNO for Atlantic cod and witch flounder may be because the Div. 2J3KL stocks are recovering at a faster rate than the Div. 3NO stocks (see Appendix C & D). It could also be residual noise from intersecting stocks as I did not account for movement between stocks in my model. The observed pattern is a combination of real stock shifts and asynchronies of multiple stocks warranting further investigation.

For both yellowtail flounder and American plaice, the observed range contraction at low population levels correlates with increased selection for preferred habitats, whereas during periods of stock recovery and increases in population levels, the range expands into less favourable habitats (Simpson and Walsh 2004) (Figure 2.15 & 2.18).   These are examples of a commonly known phenom called an abundance occupancy relationship; increase in abundance also leads to an increase in occupancy (Gaston et al. 20000). Abundance occupancy relationships have also been used to described the collapse of the Atlantic cod (Swain and Wade 1993; Atkinson et al. 1997) and yellowtail flounder (Brodie et al. 1998). Interestingly, the quantity of nursery area utilized by American plaice is positively related to population size but no relationship was found between yellowtail flounder population size as yellowtail flounder has more specific nursery habitat requirements (Walsh et al. 2004). American plaice is slower to respond to over exploitation than yellowtail flounder as density dependency appears to be stronger in yellowtail flounder contributing to a more stable stock (Walsh et al. 2004). This corresponds to our findings that American plaice had delayed effective area recovery during the moratoria compared to yellowtail flounder which is most prominent in the spring (Figure 2.18).

There are over a dozen hypothesis that have been proposed to try to explain abundance occupancy relationships, some are compounding and work cohesively together (Borregaard and Rahbek 2010). One hypothesis is MacCall's basin model - geographic range of marine fish is related to population density as a function of habitat selection (MacCall 1990); which also was found to explain a small but important portion of the spatial dynamics for bottom fish in the Eastern Bearing sea (Thorson et al. 2016). MacCall's basin model may be an appropriate

hypothesis for these two scenarios as for both yellowtail flounder and American plaice, their range contraction was also correlated to decreased water temperatures on the Grand banks leading to unfavourable habitat conditions and increased habitat selectivity (Robertson et al. 2021).

Bottom temperature, depth and substrate type had significant effects on my model (Table 2.4). Though these covariates may or may not directly influence biomass and/or numbers density, they are assumed as proxies for unobtainable or not yet fully understood mechanisms that govern the interactions between species of interest and their surrounding environment. For example, depth, which is relatively easy and inexpensive to measure, may be a highly significant covariate in a model. Realistically, even if depth is highly significant in a model, it probably is not the main mechanism that governs species distribution as it may represent less easily quantifiable parameters such as food supply, predator limitations, pressure limits, preferred light levels, salinity and/or thermal tolerance. These relationships can be difficult to detangle and identify down to a single mechanism – even if a single mechanism even exists.

Influence of oceanographic conditions on species distribution varies by functional group. Roberts, Boustany and Haplin (2020) concluded that benthic species are more associated with substrate and less with temperature like pelagic species and therefore may shift less under future climate change. Not only can oceanographic conditions effect distributions, but fishing pressures can as well. On the Grand banks, our species in question were subject to the effects of overfishing resulting in moratoria which affected their species distribution. This could be the main driver of the shifts southward toward the southeast shoal (i.e. when population numbers are

low) and expanding northward (ie. when population numbers are high) that I am seeing in the

model results and could be artifacts of abundancy occupancy relationships. However, it is hard to

separate these effects without further research into multi-covariate spatiotemporal models.

2.5. Tables

Table 2.1 List of species involved in the models with the number of tows from 1984-2018 for each species (* indicates NAFO managed stock, red indicates NAFO zone in our model).

Common Name	Number of Tows >0 kg Fall	Number of Tows >0 kg Spring	Directed Fishery	Moratorium
Yellowtail flounder	2649	3674	**3LNO***	
Atlantic cod	5758	6258		2J3KL/ 3NO*
Witch flounder	3316	3029	**3NO***	2J3KL
American plaice	8599	9671		**3LNO***

Table 2.2 List of symbols describing the VAST model. Fixed effects and Random effects only described for Predicted numbers density $n(c, s, t)$, but are the same for predicted biomass $w(c, s, t)$ with a subscript w instead of n.

	GLM	Dimension
$n(c, s, t)$	Predicted Numbers Density	c, s, t
$w(c, s, t)$	Predicted Biomass	c, s, t
	Fixed Effects in $n(c, s, t)$	
$\beta_n(c)$	Temporal Intercept	c
$\gamma_{n1}(c, t, p_1)$	Variation in Linear Bottom Temperature	c, t, p_1
$\gamma_{n2}(c, t, p_2)$	Variation in Quadratic Bottom Temperature	c, t, p_2
$\gamma_{n3}(c, p_3)$	Variation in bs (deg=1) log Bottom Depth	c, p_3
$\gamma_{n4}(c, p_4)$	Variation in bs (deg=2) log Bottom Depth	c, p_4
$\gamma_{n5}(c, p_5)$	Variation in bs (deg=3) log Bottom Depth	c, p_5
$\gamma_{n6}(c, p_6)$	Variation in bs (deg=4) log Bottom Depth	c, p_6
$\gamma_{n7}(c, p_7)$	Variation in Linear substrate	c, p_7
$L_{\beta n}(c, f)$	Loading Matrix for Temporal Variation	c, f
$L_{\omega n}(c, f)$	Loading Matrix for Spatial Variation	c, f
$L_{\varepsilon n}(c, f)$	Loading Matrix for Spatiotemporal Variation	c, f
k_n	Decorrelation distance in $\varepsilon_n(c, s, t)$	s
k_v	Decorrelation distance in matern	s
H	Rotation matrix for Geometric Anisotropy	2,2

Random Effects in $n(c,s,t)$		
$\beta_n(c,t)$	Temporal variation	c,t
$\varepsilon_n(c,s,t)$	Spatiotemporal variation	c,s,t
$\omega_n(c,s)$	Spatial variation	c,s
Derived Quantities		
$p(c,s,t)$	Encounter Probability	c,s,t
$r(c,s,t)$	Encounter Rate	c,s,t
$d(c,s,t)$	Local Predicted biomass density	c,s,t
$I(c,t)$	Predicted Total Biomass	c,t
$Z(c,t,m)$	Centre of Gravity	c,s,m
$D(c,t)$	Biomass-Weighted Average Density	c,t
$A(c,t)$	Effective Area Occupied	c,t
$V_{\omega n}$	Correlation Among Species in $\omega_n(c,s)$	c,c
$V_{\varepsilon n}$	Correlation Among Species in $\varepsilon_n(c,s,t)$	c,c
$V_{\omega w}$	Correlation Among Species in $\omega_w(c,s)$	c,c
$V_{\varepsilon w}$	Correlation Among Species in $\varepsilon_w(c,s,t)$	c,c
Index		
t	Year	
s	Location for each survey tow	
c	Species	
f	factor	
b	Biomass per survey tow	
m	Matrix of UTM E and UTM N	
p_1	Linear Bottom Temperature	
p_2	Quadratic Bottom Temperature	
p_3	bs (deg=1) log Bottom Depth	
p_4	bs (deg=2) log Bottom Depth	
p_5	bs (deg=3) log Bottom Depth	
p_6	bs (deg=4) log Bottom Depth	
p_7	Substrate Type	
Data		
$X_{n1}(s,t,p_1)$	Linear Bottom Temperature Covariate Matrix	s,t,p_1
$X_{n2}(s,t,p_2)$	Quadratic Bottom Temperature Covariate Matrix	s,t,p_2
$X_{n3}(s,p_3)$	bs (deg=1) log Bottom Depth Covariate Matrix	s,p_3
$X_{n4}(s,p_4)$	bs (deg=2) log Bottom Depth Covariate Matrix	s,p_4
$X_{n5}(s,p_5)$	bs (deg=3) log Bottom Depth Covariate Matrix	s,p_5
$X_{n6}(s,p_6)$	bs (deg=4) log Bottom Depth Covariate Matrix	s,p_6
$X_{n7}(s,p_7)$	Substrate Type Covariate Matrix	s,p_7
Constants		
v	Matern Smoothness Constant	1

a	Area Swept per tow	0.02
f_{β_n}	Number of Factors in Temporal Variation	4
f_{ω_n}	Number of Factors in Spatial Variation	4
f_{ε_n}	Number of Factors in Spatiotemporal Variation	4

Table 2.3 Model selection AIC results for spatial and spatiotemporal intercepts for models that converged (maximum gradient $< 10^{-6}$) for Fall and Spring VAST.

Temporal	Spatiotemporal	Fall AIC	Fall ΔAIC	Spring AIC	Spring ΔAIC
Constant	Independent	170545.8	317.1	191926.7	305.1
Independent	Independent	170504.4	275.7	191858.1	236.5
Random Walk	Independent	170228.7	0	191621.6	0

Table 2.4 Covariate selection AIC for depth, substrate type and bottom temperature for models that converged (maximum gradient $< 10^{-6}$) for Fall and Spring VAST.

Depth	Substrate	Bottom Temperature	Fall AIC	Fall ΔAIC	Spring AIC	Spring ΔAIC
X	X	X	170228.8	6178.7	191621.6	8914.5
X	X	Linear	169335.2	5285.1	190697.1	7990
X	X	quadratic	169335.2	5285.1	190697.1	7990
X	X	linear + Quadratic	169335.2	5285.1	190697.1	7990
X	X	Linear + I(Quadratic)	168775.3	4725.2	189687.4	6980.3
Linear	X	X	166980.5	2930.4	189274.6	6567.5
quadratic	X	X	166980.5	2930.4	189274.6	6567.5
bs(deg=2)	X	X	166263.1	2213	188072.6	5365.5
bs(log,deg=2)	X	X	166559.5	2509.4	188550.5	5843.4
bs(deg=3)	X	X	166016.4	1966.3	187931.6	5224.5
bs(log,deg=3)	X	X	165850.2	1800.1	187909.8	5202.7
bs(deg=4)	X	X	165806.6	1756.5	187808.7	5101.6
bs(log,deg=4)	X	X	165254.6	1204.5	187457	4749.9
X	Linear	X	169914.8	5864.7	191380.4	8673.3
bs(log,deg=4)	Linear	Linear+ I (Quadratic)	164050.1	0	182707.1	0

Table 2.5 Estimated habitat covariate response of bottom temperature, depth and substrate for Fall 1984-2018 for numbers density and biomass on all four species (YT= yellowtail flounder, AC= Atlantic cod, WF=witch flounder and AP= American plaice).

	Covariate	Formula	Species	Estimate	SE	Significance
Numbers Density	Depth	b-spline (deg=1)	AP	4.95	2.65	TRUE
			AC	2.41	2.66	FALSE
			WF	31.85	4.69	TRUE
			YT	5.95	5.15	TRUE
		b-spline (deg=2)	AP	3.58	1.47	TRUE
			AC	-1.44	1.78	FALSE

			WF	4.72	1.69	TRUE
			YT	-5.90	4.87	TRUE
		b-spline (deg=3)	AP	1.57	1.84	FALSE
			AC	6.67	2.81	TRUE
			WF	22.59	3.11	TRUE
			YT	-2.86	8.65	FALSE
		b-spline (deg=4)	AP	0.63	1.08	FALSE
			AC	-9.49	1.44	TRUE
			WF	17.30	2.25	TRUE
			YT	-8.58	7.18	TRUE
	Bottom Temperature	Linear	AP	-0.12	0.09	TRUE
			AC	0.35	0.07	TRUE
			WF	0.37	0.09	TRUE
			YT	0.24	0.11	TRUE
		Quadratic	AP	0.00	0.01	FALSE
			AC	-0.04	0.01	TRUE
			WF	-0.04	0.01	TRUE
			YT	-0.02	0.02	TRUE
	Substrate	Linear	AP	-0.01	0.04	FALSE
			AC	0.07	0.03	TRUE
			WF	-0.08	0.03	TRUE
			YT	-0.06	0.05	TRUE
Biomass	Depth	b-spline (deg=1)	AP	-1.75	2.72	FALSE
			AC	4.26	2.95	TRUE
			WF	9.92	3.57	TRUE
			YT	-0.64	6.77	FALSE
		b-spline (deg=2)	AP	1.55	1.53	TRUE
			AC	-2.33	1.88	TRUE
			WF	1.10	1.56	FALSE
			YT	1.79	7.55	FALSE
		b-spline (deg=3)	AP	-3.74	1.94	TRUE
			AC	4.86	2.94	TRUE
			WF	3.15	2.37	TRUE
			YT	-11.98	14.93	FALSE
		b-spline (deg=4)	AP	1.95	1.09	TRUE
			AC	-1.44	1.41	TRUE
			WF	5.25	1.51	TRUE
			YT	9.39	13.97	FALSE
	Bottom Temperature	Linear	AP	0.04	0.09	FALSE
			AC	0.14	0.07	TRUE

Covariate	Formula	Species	Estimate	SE	Significance
		WF	0.01	0.10	FALSE
		YT	-0.11	0.11	FALSE
	Quadratic	AP	-0.01	0.01	TRUE
		AC	-0.01	0.01	FALSE
		WF	0.00	0.01	FALSE
		YT	0.00	0.02	FALSE
Substrate	Linear	AP	-0.11	0.04	TRUE
		AC	0.01	0.03	FALSE
		WF	-0.01	0.03	FALSE
		YT	-0.05	0.06	FALSE

Table 2.6 Estimated habitat covariate response bottom temperature, depth and substrate for Spring 1984-2018 for numbers density and biomass on all four species (YT= yellowtail flounder, AC= Atlantic cod, WF=witch flounder and AP= American plaice).

	Covariate	Formula	Species	Estimate	SE	Significance
Numbers Density	Depth	b-spline (deg=1)	AP	3.89	2.57	TRUE
			AC	5.69	2.31	TRUE
			WF	26.63	5.46	TRUE
			YT	-0.66	4.31	FALSE
		b-spline (deg=2)	AP	4.49	1.68	TRUE
			AC	-1.94	1.41	TRUE
			WF	5.21	1.99	TRUE
			YT	0.83	3.23	FALSE
		b-spline (deg=3)	AP	-0.99	1.88	FALSE
			AC	10.98	2.12	TRUE
			WF	17.94	3.80	TRUE
			YT	-11.25	5.12	TRUE
		b-spline (deg=4)	AP	0.26	1.00	FALSE
			AC	-5.17	1.04	TRUE
			WF	15.05	2.56	TRUE
			YT	-3.19	2.34	TRUE
	Bottom Temperature	Linear	AP	0.03	0.11	FALSE
			AC	0.53	0.07	TRUE
			WF	0.61	0.09	TRUE
			YT	0.26	0.10	TRUE
		Quadratic	AP	-0.01	0.01	FALSE
			AC	-0.06	0.01	TRUE

			WF	-0.05	0.01	TRUE
			YT	-0.04	0.01	TRUE
	Substrate	Linear	AP	-0.01	0.04	FALSE
			AC	0.06	0.03	TRUE
			WF	-0.05	0.03	TRUE
			YT	-0.02	0.05	FALSE
Biomass	Depth	b-spline (deg=1)	AP	0.45	2.62	FALSE
			AC	1.65	2.66	FALSE
			WF	7.19	4.27	TRUE
			YT	0.90	4.35	FALSE
		b-spline (deg=2)	AP	-1.99	1.71	TRUE
			AC	-1.04	1.82	FALSE
			WF	2.32	1.50	TRUE
			YT	-1.70	3.43	FALSE
		b-spline (deg=3)	AP	1.95	1.95	TRUE
			AC	1.89	2.61	FALSE
			WF	2.02	3.00	FALSE
			YT	-3.87	5.62	FALSE
		b-spline (deg=4)	AP	1.16	1.00	TRUE
			AC	0.30	1.29	FALSE
			WF	3.56	1.67	TRUE
			YT	1.92	2.92	FALSE
	Bottom Temperature	Linear	AP	0.08	0.11	FALSE
			AC	0.23	0.08	TRUE
			WF	0.19	0.09	TRUE
			YT	0.10	0.11	FALSE
		Quadratic	AP	-0.01	0.01	TRUE
			AC	-0.02	0.01	TRUE
			WF	-0.02	0.01	TRUE
			YT	-0.02	0.01	TRUE
	Substrate	Linear	AP	-0.05	0.04	TRUE
			AC	-0.01	0.03	FALSE
			WF	-0.01	0.03	FALSE
			YT	-0.06	0.05	TRUE

2.6. Figures
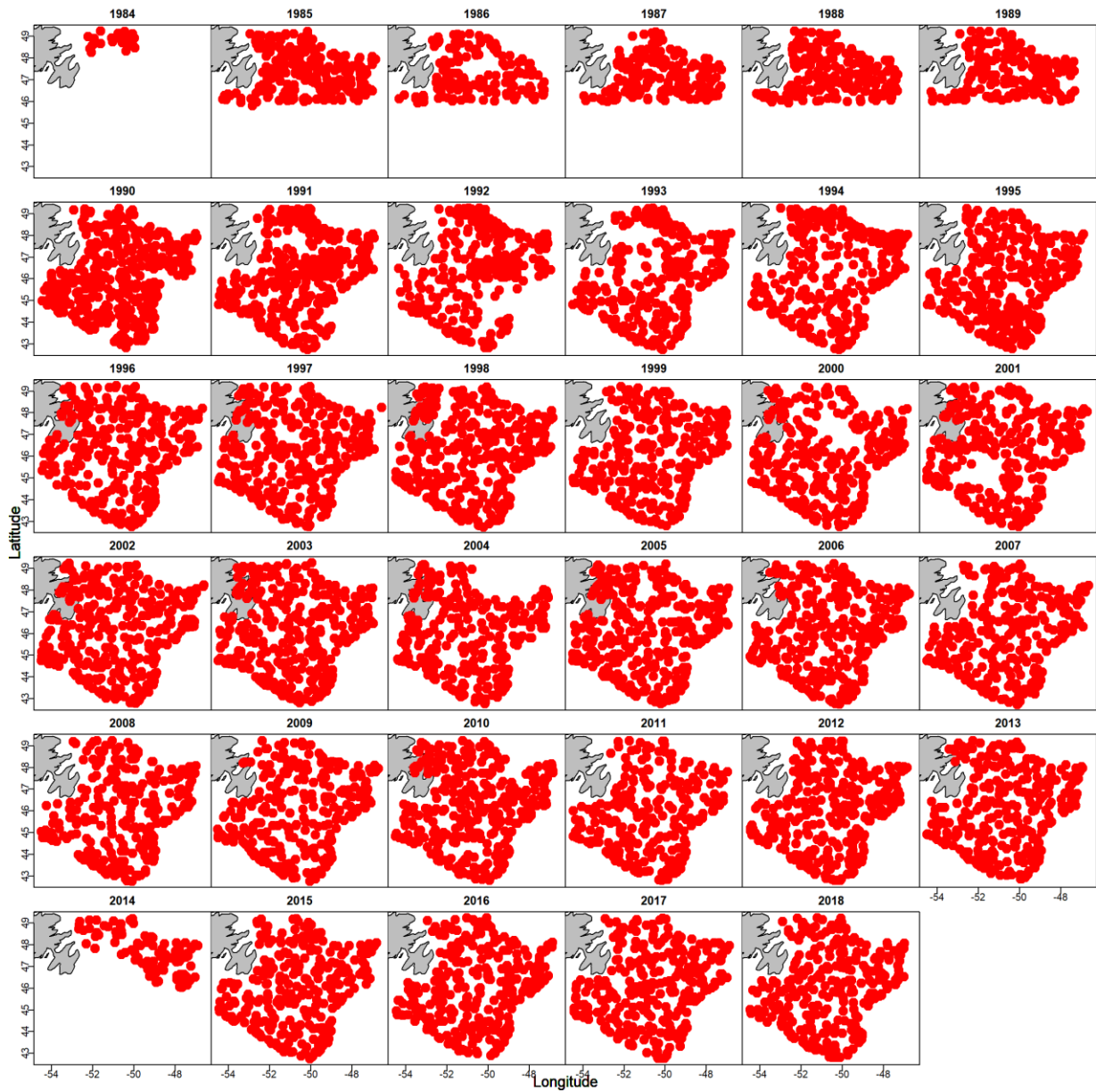
Figure 2.1 Map of DFO survey coverage from 1984-2018 for Fall. Red indicates survey coverage, and white indicates areas that were not covered by the survey.
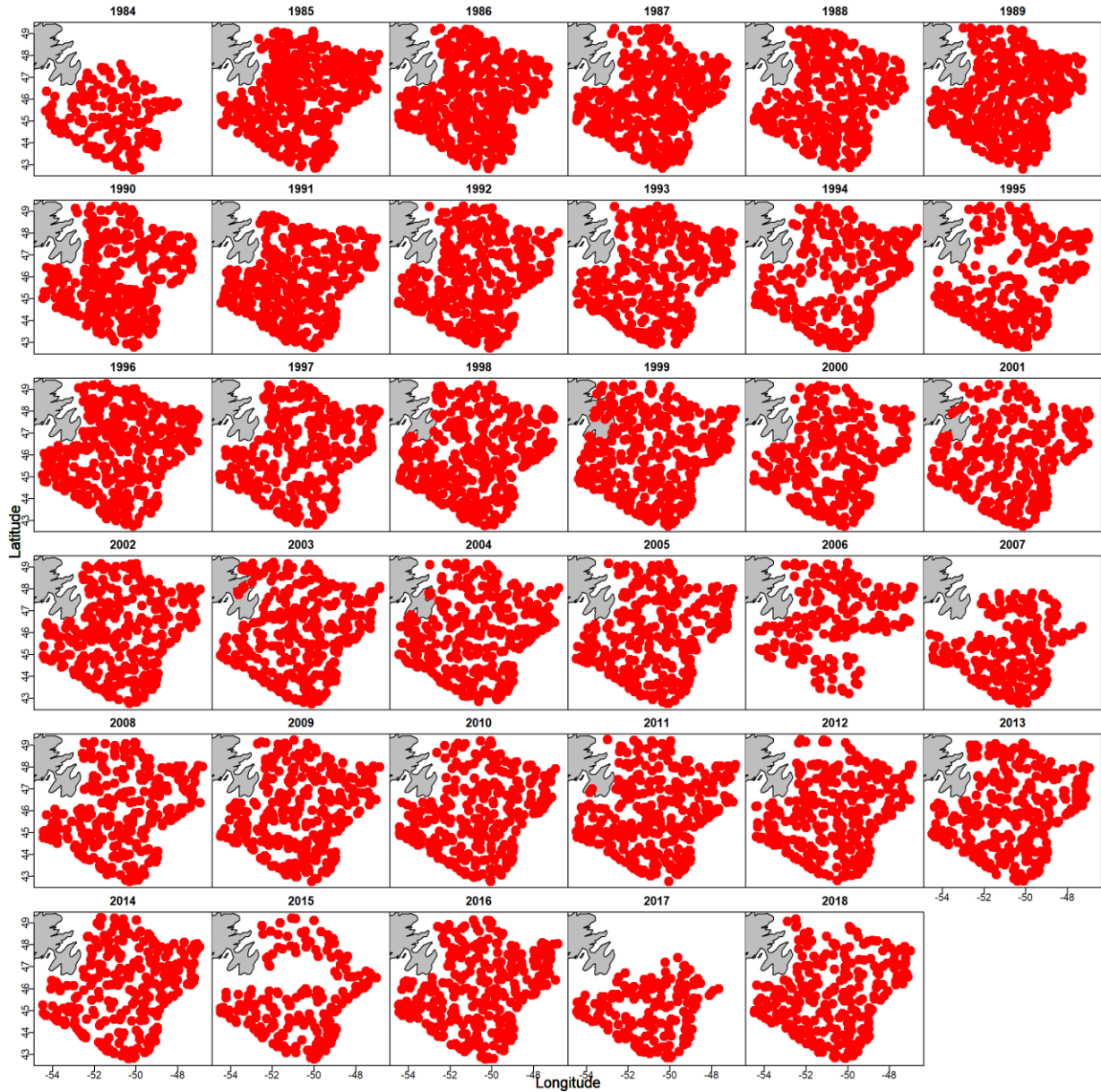
Figure 2.2 Map of DFO survey coverage from 1984-2018 for Spring. Red indicates survey coverage, and white indicates areas that were not covered by the survey.
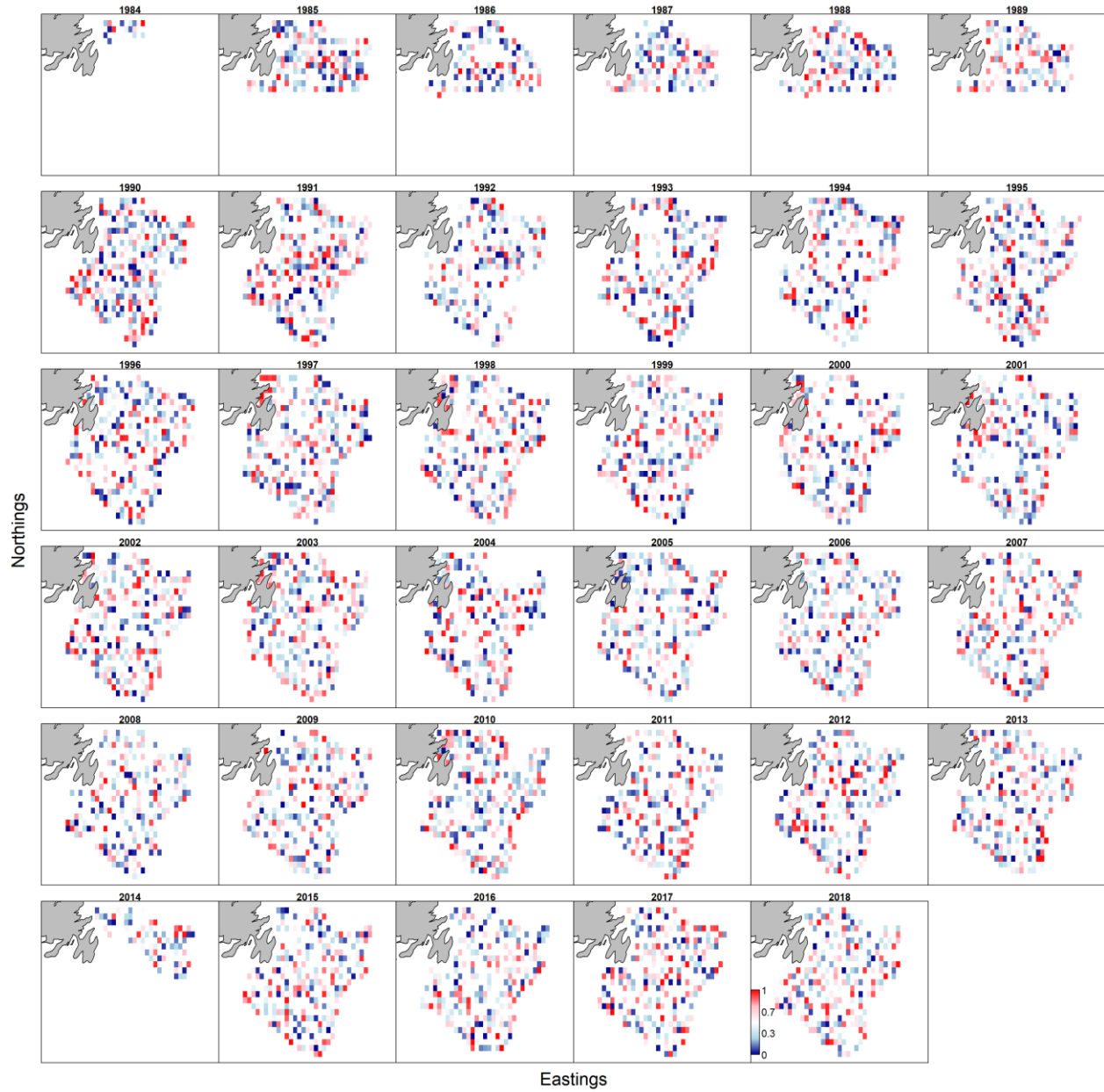
Figure 2.3 Spatial quantile residuals for the VAST model applied to the Fall survey data. Residuals range from 1 (red) to 0 (blue) for each tow and white indicates areas with no tows.

Figure 2.4 Spatial quantile residuals for the VAST model applied to the Spring survey data. Residuals range from 1 (red) to 0 (blue) for each tow and white indicates areas with no tows.
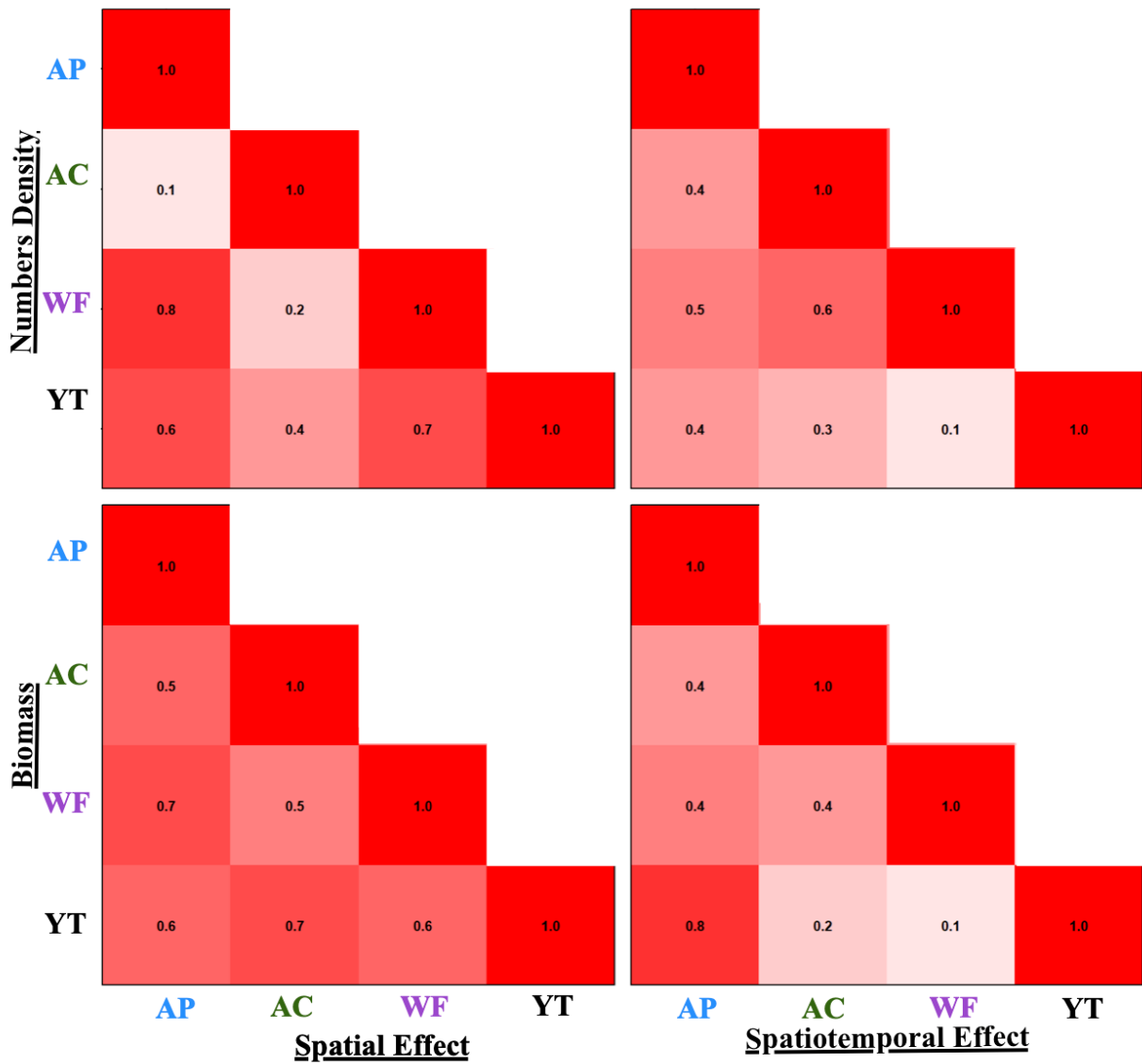
Figure 2.5 Estimated spatial and spatiotemporal correlation among four species for numbers density and biomass for Fall. (YT= yellowtail flounder, AC= Atlantic cod, WF=witch flounder and AP= American plaice).
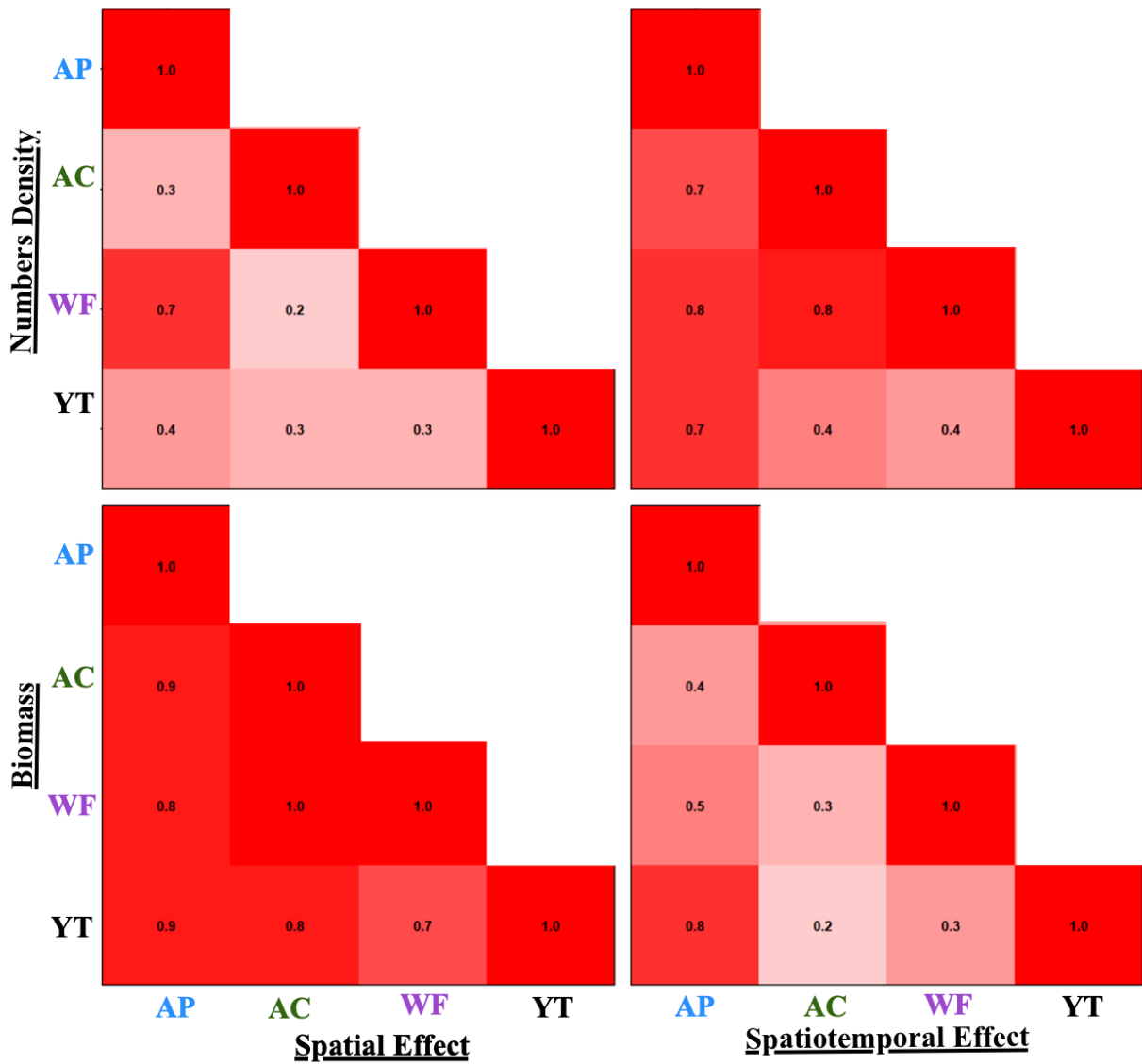
Figure 2.6 Estimated spatial and spatiotemporal correlation among four species for numbers density and biomass for Spring. (YT= yellowtail flounder, AC= Atlantic cod, WF=witch flounder and AP= American plaice).
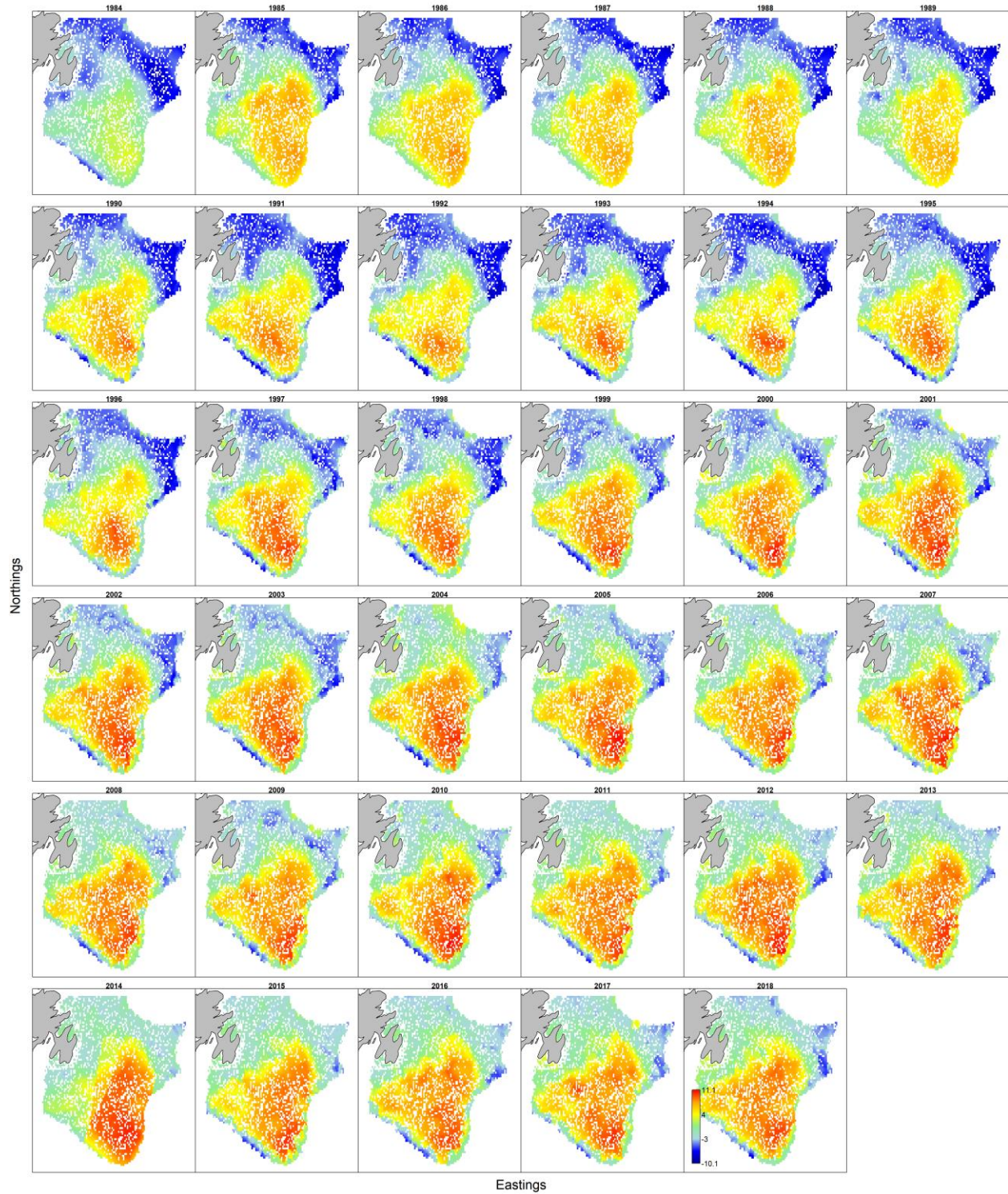
Figure 2.7 Natural log density distribution (kg/25 km^2) plot for yellowtail flounder NAFO Div. 3LNO Fall 1984-2018 from VAST. White cells indicate areas where no tows were done over the time series.
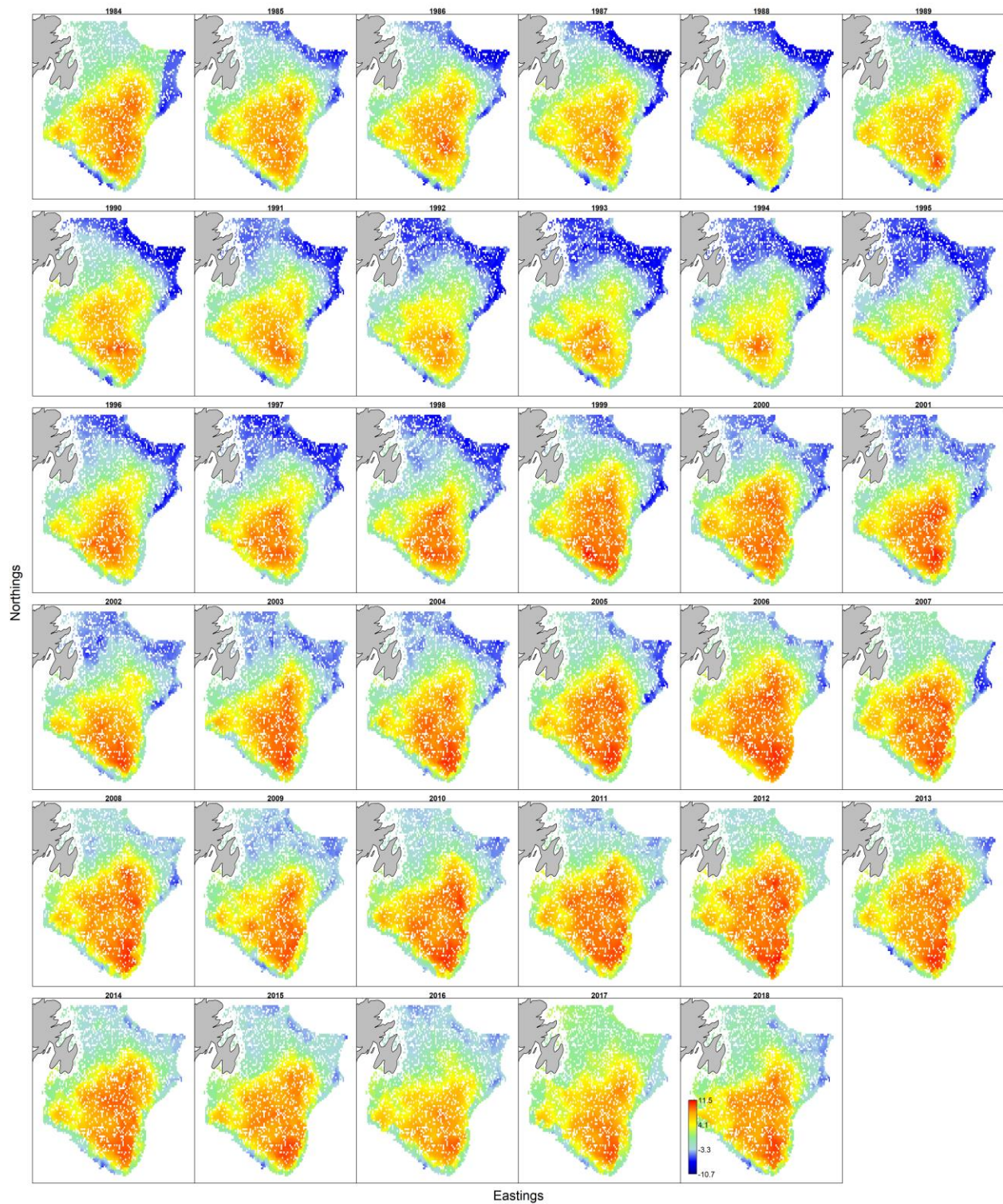
Figure 2.8 Natural log density distribution (standardized to kg/25 km^2) plot for yellowtail flounder NAFO Div. 3LNO Spring 1984-2018 from VAST. White cells indicate areas where no tows were done over the time series.
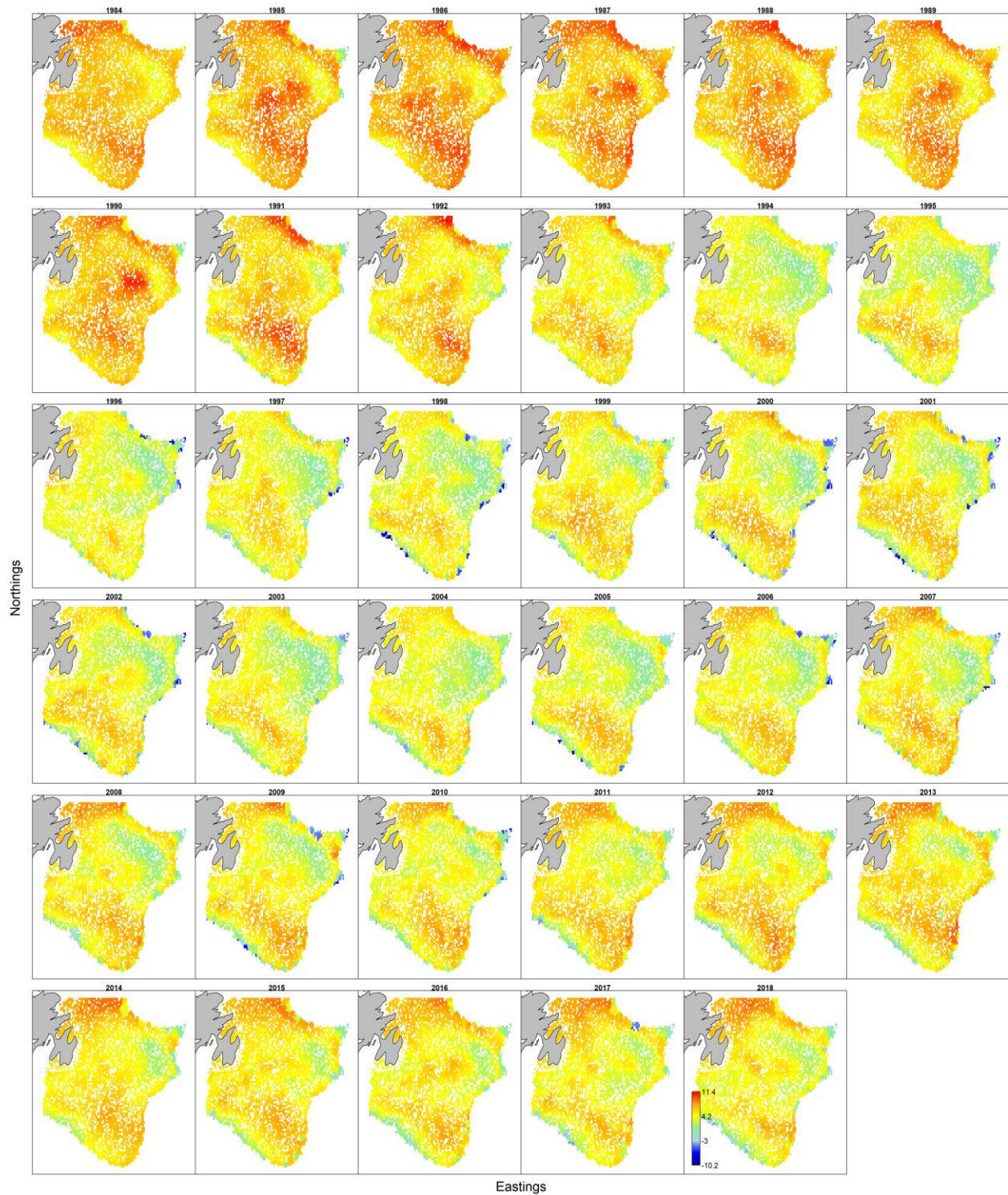
Figure 2.9 Natural log density distribution (standardized to kg/25 km^2) plot for Atlantic cod NAFO Div.3LNO Fall 1984-2018 from VAST. White cells indicate areas where no tows were done over the time series.
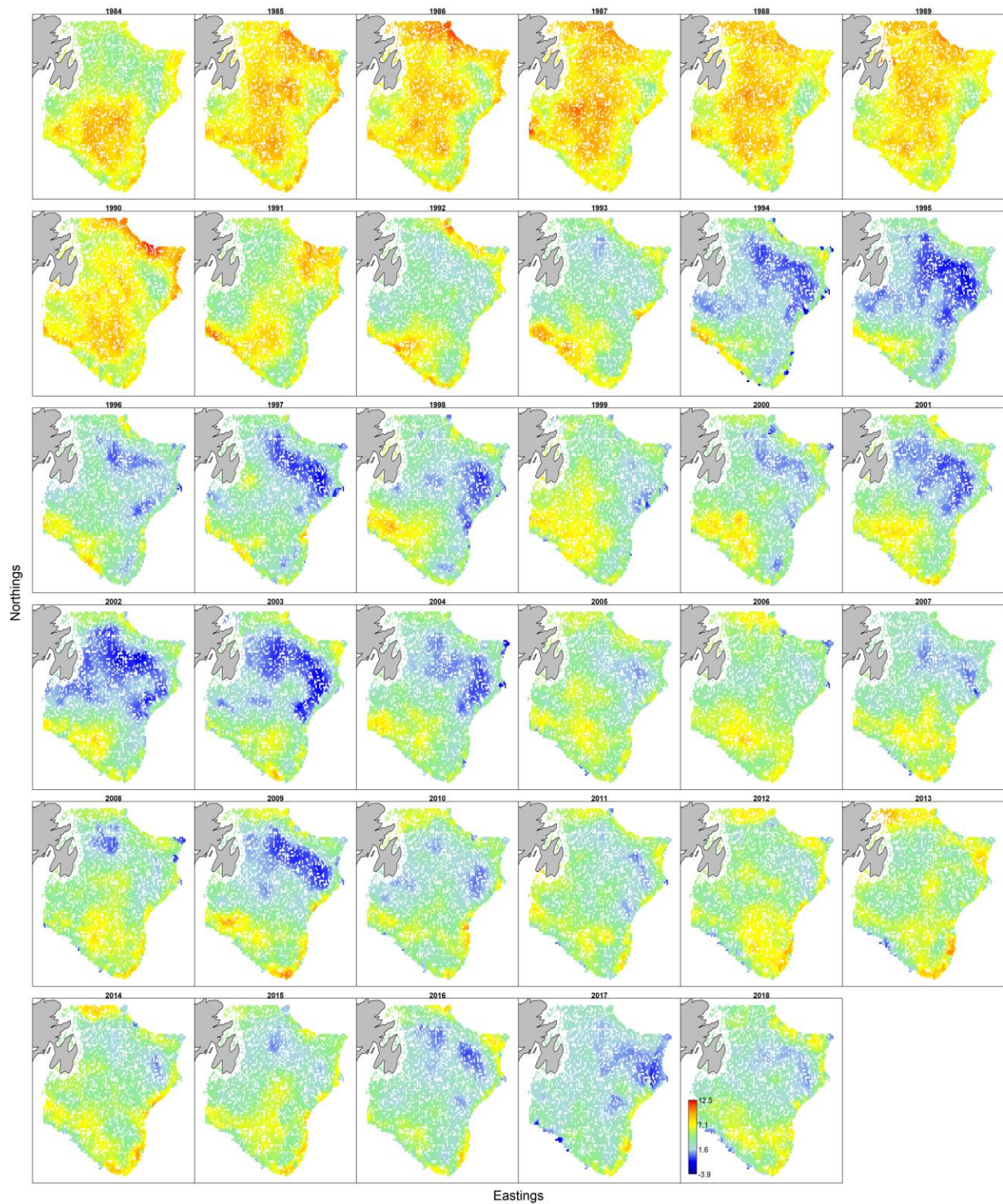
Figure 2.10 Natural log density distribution (standardized to kg/25 km^2) plot for Atlantic cod NAFO Div.3LNO Spring 1984-2018 from VAST. White cells indicate areas where no tows were done over the time series.
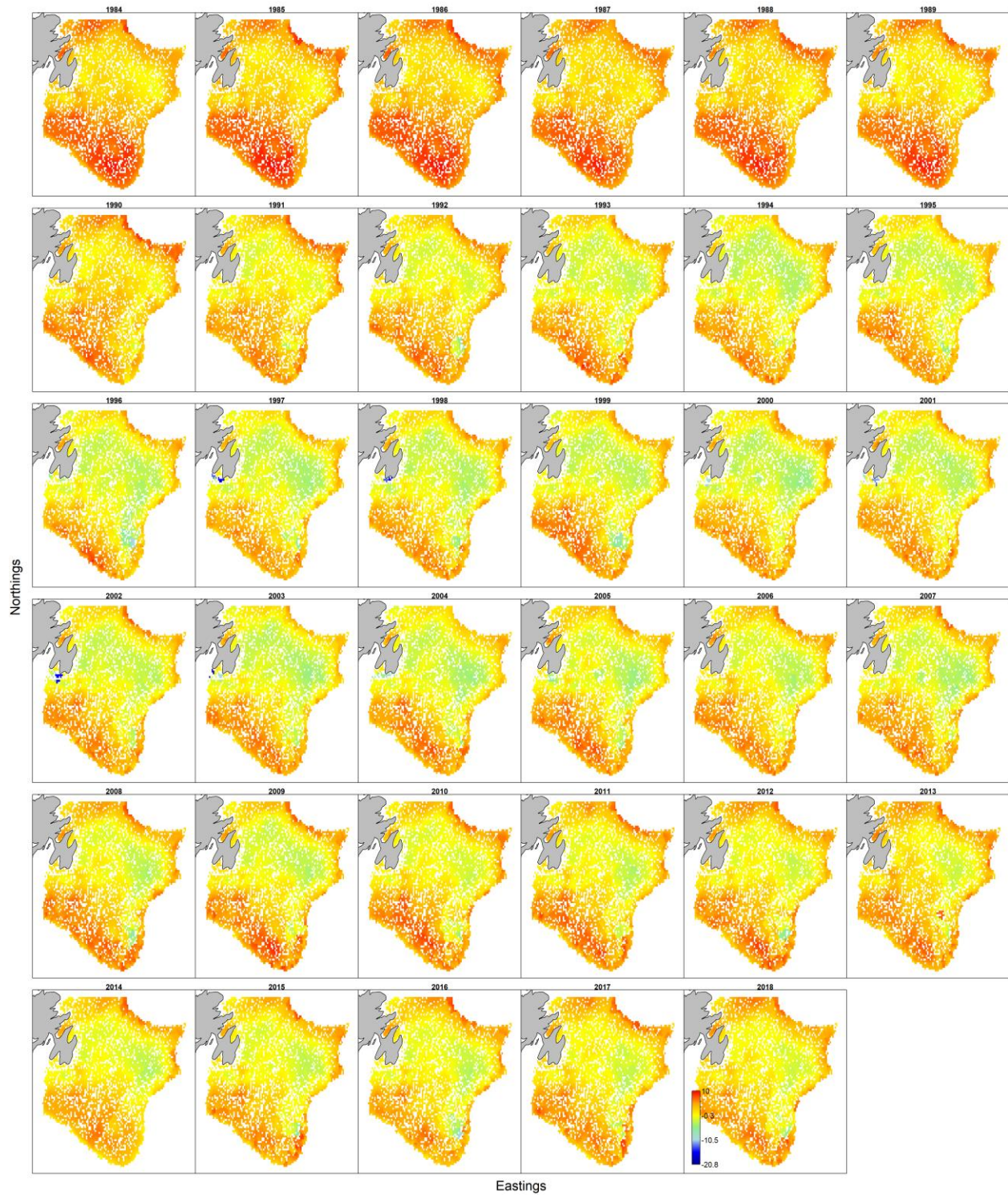
Figure 2.11 Natural log density distribution (standardized to kg/25 km^2) (kg/25 km^2) plot for witch flounder NAFO Div. 3LNO Fall 1984-2018 from VAST. White cells indicate areas where no tows were done over the time series.
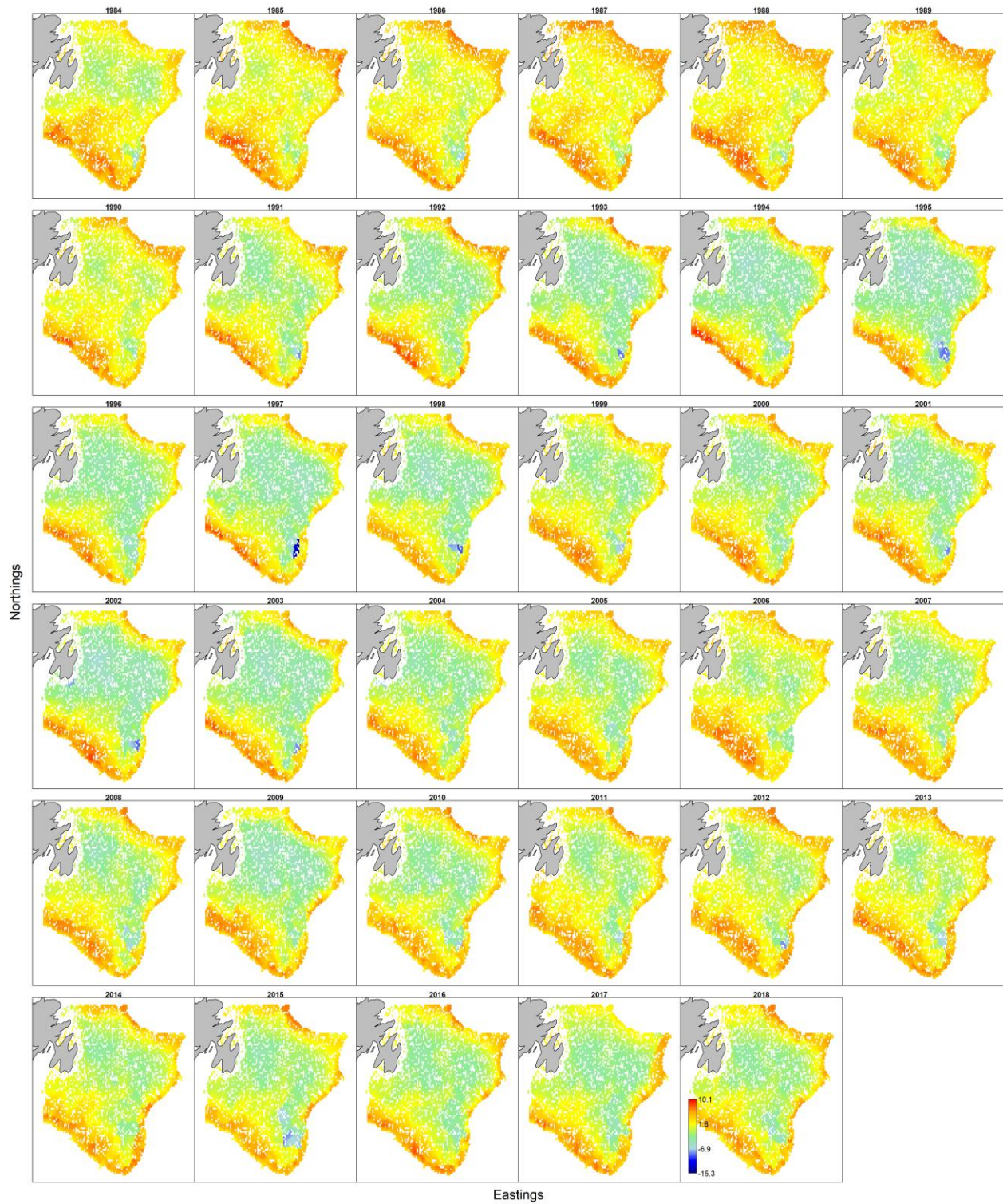
Figure 2.12 Natural log density distribution (standardized to kg/25 km^2) plot for witch flounder NAFO Div. 3LNO Spring 1984-2018 from VAST. White cells indicate areas where no tows were done over the time series.
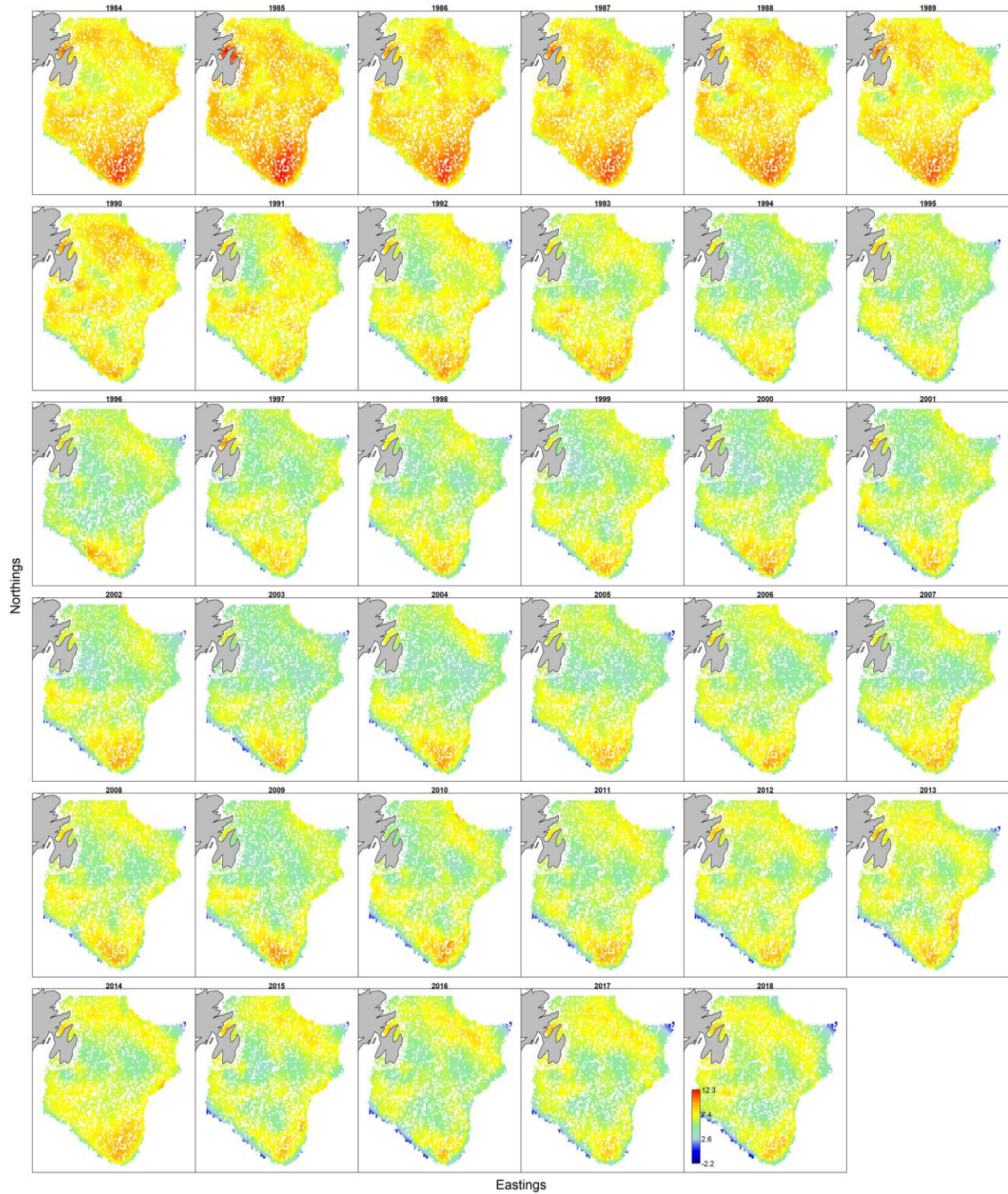
Figure 2.13 Natural log density distribution (standardized to kg/25 km^2) plot for American plaice NAFO Div. 3LNO Fall 1984-2018 from VAST. White cells indicate areas where no tows were done over the time series.
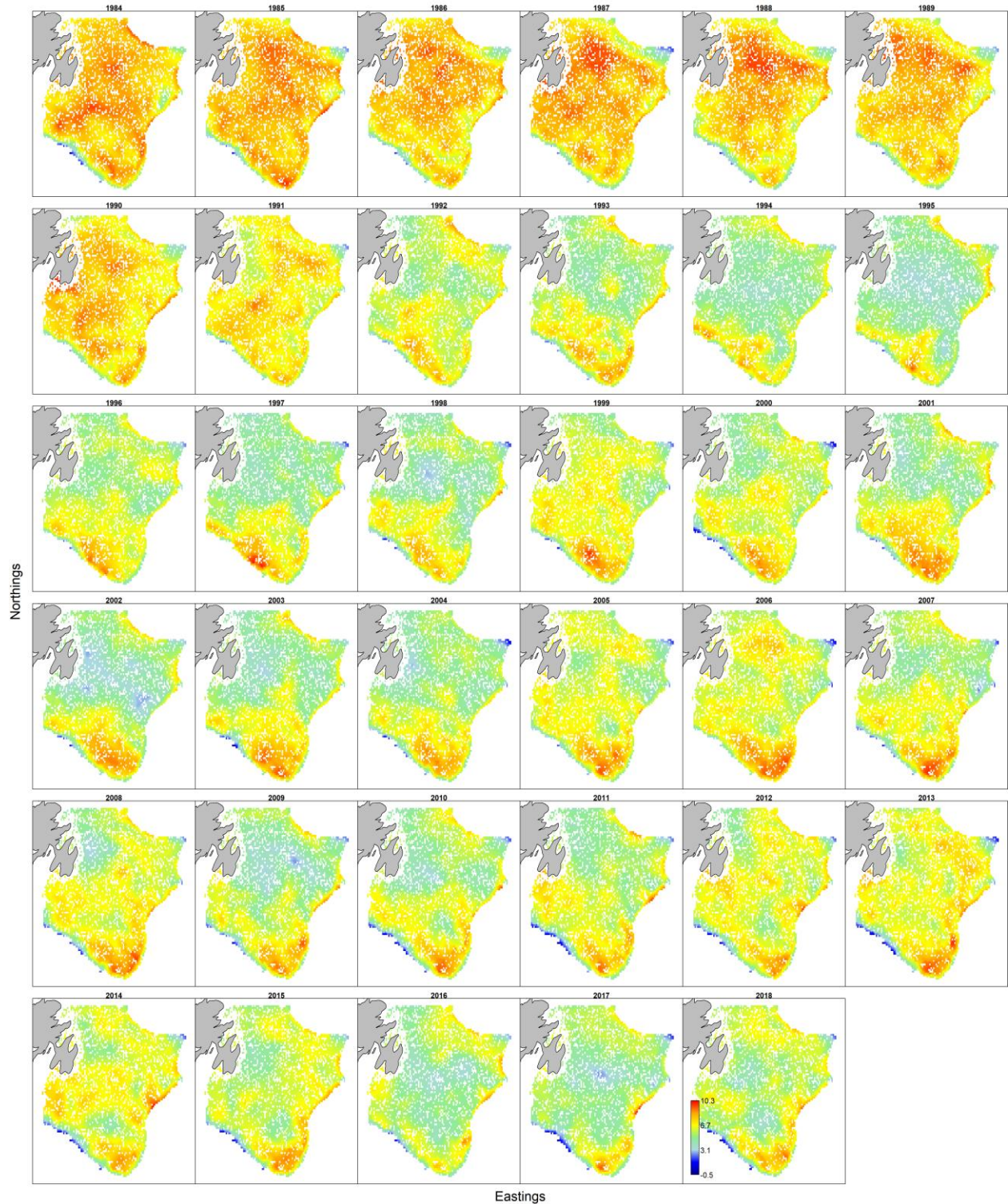
Figure 2.14 Natural log density distribution (standardized to kg/25 km^2) plot for American plaice NAFO Div.3LNO Spring 1984-2018 from VAST. White cells indicate areas where no tows were done over the time series.
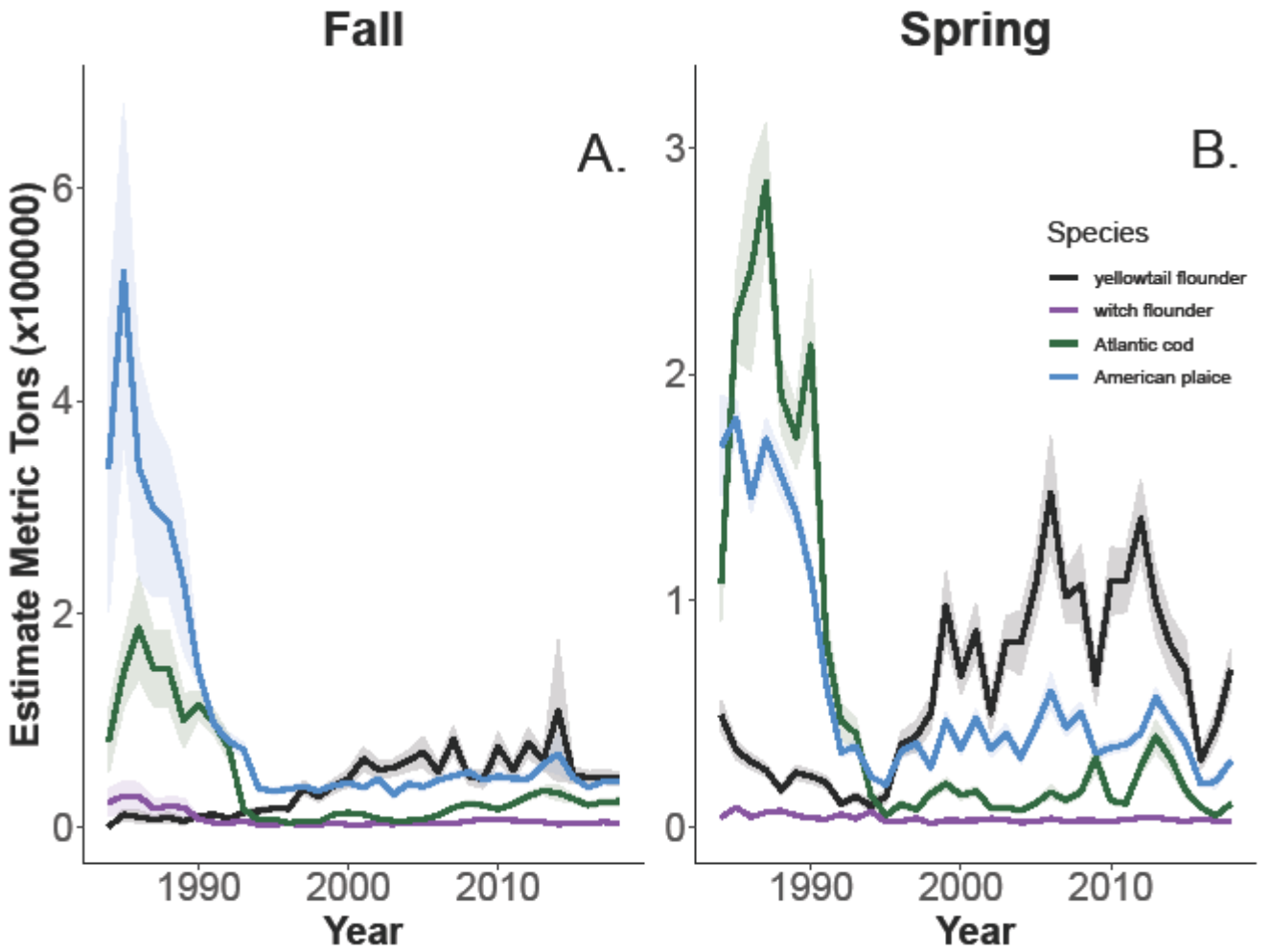
Figure 2.15 Estimated biomass in metric tons for each of the four species in the Fall (A) and Spring (B) from 1984-2018 for Div. 3LNO. Shaded area represents standard error.
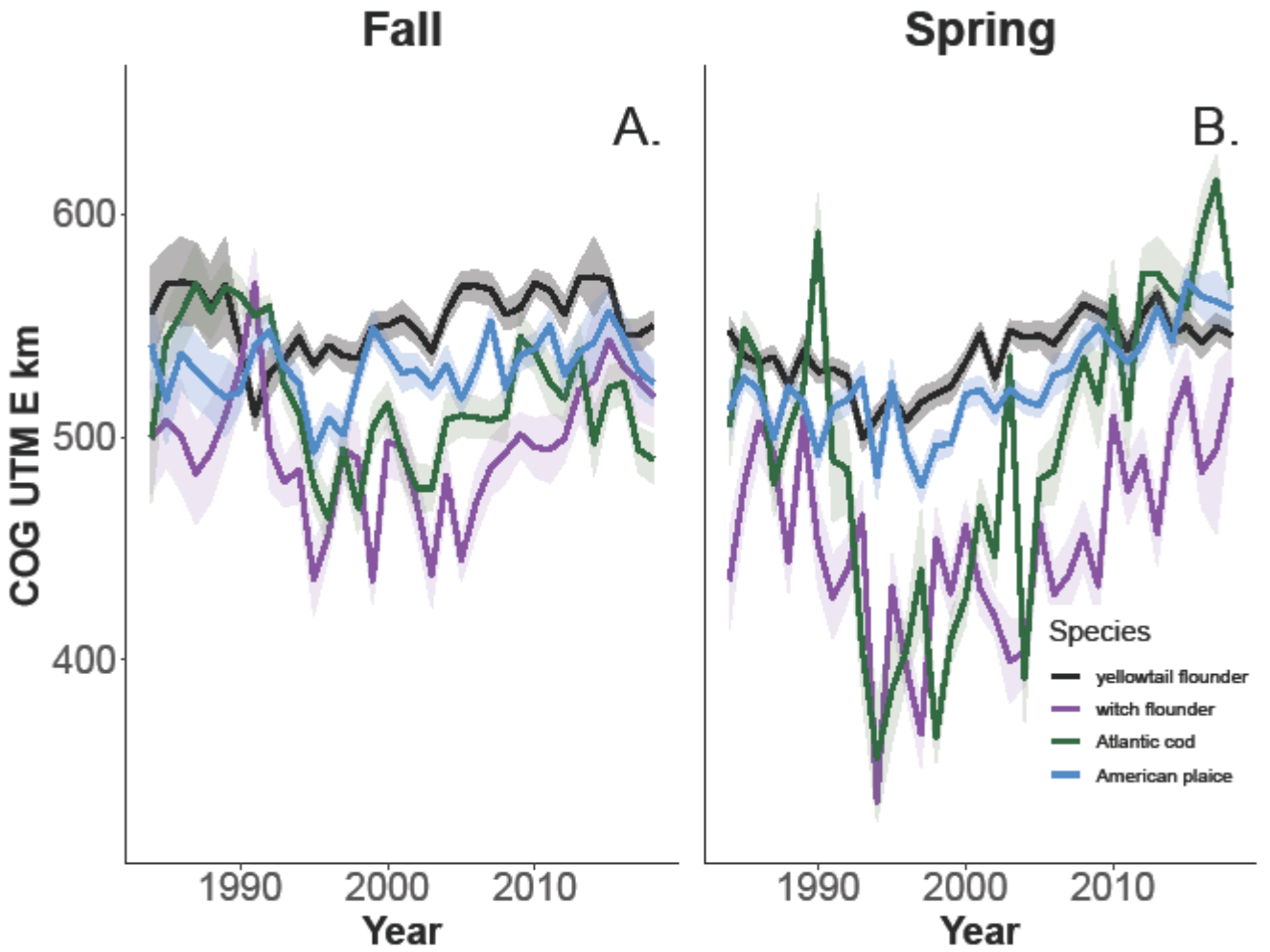
Figure 2.16 Estimated shift in Centre of Gravity East in UTM km for (A) Fall and (B) Spring for each of the four species from 1984-2018 for Div. 3LNO. Shaded area represents standard error.
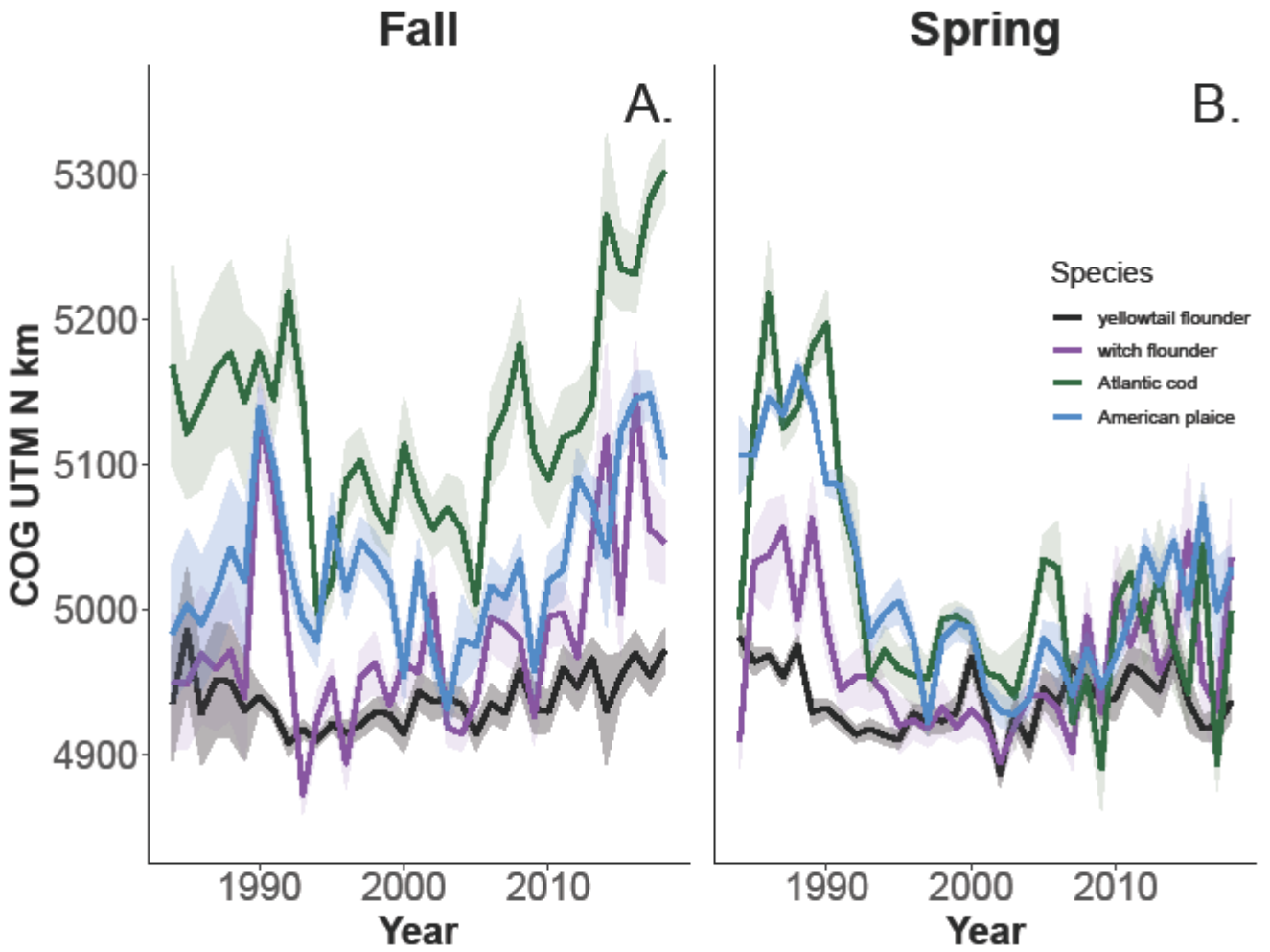
Figure 2.17 Estimated shift in Centre of Gravity North in UTM km for (A) Fall and (B) Spring for each of the four species from 1984-2018 for Div. 3LNO. Shaded area represents standard error.
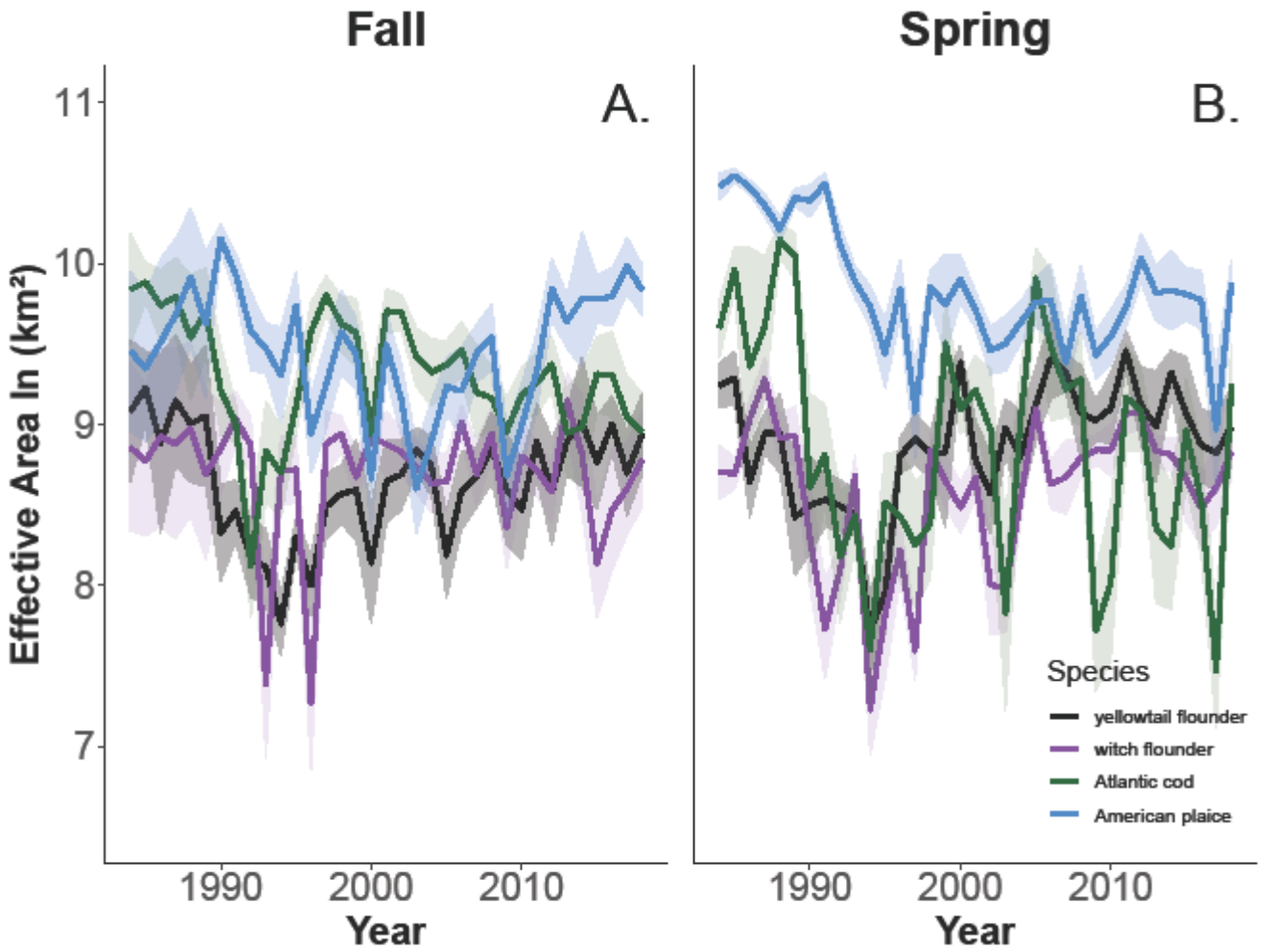
Figure 2.18 Estimated effective area in km² for each of the four species in the Fall (A) and Spring (B) from 1984-2018 for Div. 3LNO. Shaded area represents standard error.

2.7. Bibliography

Atkinson, D., Rose, G.A., Murphy, E., and Bishop, C.A. 1997. Distribution changes and abundance of northern cod (*Gadus morhua*). Canadian Journal of Fisheries and Aquatic Sciences **54**: 132–138. doi:10.1139/f96-158.

Bi, H., Peterson, W.T., and Strub, P.T. 2011. Transport and coastal zooplankton communities in the northern California Current system. Geophysical Research Letters **38**(12). doi:10.1029/2011GL047927.

Blyth-Skyrme, R., Atkinson, B., and Angel, J. 2015. MSC Sustainable Fishereies Certification: OCI Grand Bank Yellowtail Flounder Trawl Fishery. Public Certification Report, OCI.

Borregaard, M.K., and Rahbek, C. 2010. Causality of the Relationship between Geographic Distribution and Species Abundance. The Quarterly Review of Biology **85**(1): 3–25. doi:10.1086/650265.

Boudreau, S.A., Anderson, S.C., and Worm, B. 2015. Top-down and bottom-up forces interact at thermal range extremes on American lobster. Journal of Animal Ecology **84**(3): 840–850. doi:10.1111/1365-2656.12322.

Breivik, O.N., Storvik, G., and Nedreaas, K. 2016. Latent Gaussian models to decide on spatial closures for bycatch management in the Barents Sea shrimp fishery. Canadian Journal of Fisheries and Aquatic Sciences. NRC Research Press. doi:10.1139/cjfas-2015-0322.

Brodie, W.B., Walsh, S.J., and Atkinson, D.B. 1998. The effect of stock abundance on range contraction of yellowtail flounder (*Pleuronectes ferruginea*) on the Grand Bank of Newfoundland in the Northwest Atlantic from 1975 to 1995. Journal of Sea Research **39**(1): 139–152. doi:10.1016/S1385-1101(97)00056-7.

Brodie, W.B., Walsh, S.J., and Maddock Parsons, D. 2010. An evaluation of the collapse and recovery of the yellowtail flounder (*Limanda ferruginea*) stock on the Grand Bank. ICES Journal of Marine Science **67**(9): 1887–1895. doi:10.1093/icesjms/fsq121.

Combes, V., Chenillat, F., Di Lorenzo, E., Rivière, P., Ohman, M.D., and Bograd, S.J. 2013. Cross-shore transport variability in the California Current: Ekman upwelling vs. eddy dynamics. Progress in Oceanography **109**: 78–89. doi:10.1016/j.pocean.2012.10.001.

Cosandey-GodinAurelie, Teixeira, K., WormBoris, and Mills, F. 2014. Applying Bayesian spatiotemporal models to fisheries bycatch in the Canadian Arctic. Canadian Journal of Fisheries and Aquatic Sciences. NRC Research Press. doi:10.1139/cjfas-2014-0159.

Currie, J.C., Thorson, J.T., Sink, K.J., Atkinson, L.J., Fairweather, T.P., and Winker, H. 2019. A novel approach to assess distribution trends from fisheries survey data. Fisheries Research **214**: 98–109. doi:10.1016/j.fishres.2019.02.004.

Daufresne, M., Lengfellner, K., and Sommer, U. 2009. Global warming benefits the small in aquatic ecosystems. Proceedings of the National Academy of Sciences **106**(31): 12788–12793. doi:10.1073/pnas.0902080106.

Dulvy N.K., Rogers S.I., Jennings S., Stelzenmüller V., Dye S.R. & Skjoldal H.R. (2008). Climate change and deepening of the North Sea fish assemblage: a biotic indicator of regional warming. *Journal of Applied Ecology*, 45, 1029–1039. doi: 10.1111/j.1365-2664.2008.01488.x

Fisheries and Oceans Canada. 2019. Integrated Fisheries Management Plan: Groundfish Newfoundland and Labrador Region NAFO Subarea 2 + Divisions 3KLMNO.

Gao, J., Thorson, J.T., Szuwalski, C., and Wang, H.-Y. 2020. Historical dynamics of the demersal fish community in the East and South China Seas. Mar. Freshwater Res. **71**(9): 1073. doi:10.1071/MF18472.

Gaston, K.J., Blackburn, T.M., Greenwood, J.J.D., Gregory, R.D., Quinn, R.M., and Lawton, J.H. 2000. Abundance–occupancy relationships. Journal of Applied Ecology **37**(s1): 39–59. doi:10.1046/j.1365-2664.2000.00485.x.

Hall, M.A., Alverson, D.L., and Metuzals, K.I. 2000. By-Catch: Problems and Solutions. Marine Pollution Bulletin **41**(1–6): 204–219. doi:10.1016/S0025-326X(00)00111-9.

Keister, J.E., Lorenzo, E.D., Morgan, C.A., Combes, V., and Peterson, W.T. 2011. Zooplankton species composition is linked to ocean transport in the Northern California Current. Global Change Biology **17**(7): 2498–2511. doi:10.1111/j.1365-2486.2010.02383.x.

Knapman, P. 2017. OCI Grand Bank Yellowtail Flounder Trawl 2nd Surveillance Report.

Knapman, P., Cook, R., and Blyth-Skyrme, R. 2020. OCI Grand Bank Yellowtail Flounder Trawl: Public Comment Draft Report June 2020. : 180.

Kristensen, K., Nielsen, A., Berg, C.W., Skaug, H., and Bell, B.M. 2016. TMB: Automatic Differentiation and Laplace Approximation. Journal of Statistical Software **70**(1): 1–21. doi:10.18637/jss.v070.i05.

Latimer, A.M., Banerjee, S., Sang Jr, H., Mosher, E.S., and Silander Jr, J.A. 2009. Hierarchical models facilitate spatial analysis of large data sets: a case study on invasive plant species in the northeastern United States. Ecology Letters **12**(2): 144–154. doi:10.1111/j.1461-0248.2008.01270.x.

Lindgren, F. 2012. Continuous Domain Spatial Models in. The ISBA Bulletin 19, 14–20.: 8.

Lindgren, F., Rue, H., and Lindström, J. 2011. An explicit link between Gaussian fields and Gaussian Markov random fields: the stochastic partial differential equation approach. Journal of the Royal Statistical Society: Series B (Statistical Methodology) **73**(4): 423–498. doi:10.1111/j.1467-9868.2011.00777.x.

MacCall, A. 1990. Dynamic geography of marine fish populations. Washington University Press, Washington.

Maddock Parsons, D. 2013. Divisions 3LNO Yellowtail Flounder *(Limanda ferruginea)* in the 2011 and 2012 Canadian Stratified Bottom Trawl Surveys. NAFO SCR Doc.

Maddock Parsons, D., Morgan, J., Brodie, B., and Power, D. 2013. Assessment of NAFO Div. 3LNO Yellowtail Flounder, NAFO SCR Doc. 13/37, Serial No. N6192.

Martin, T.G., Wintle, B.A., Rhodes, J.R., Kuhnert, P.M., Field, S.A., Low-Choy, S.J., Tyre, A.J., and Possingham, H.P. 2005. Zero tolerance ecology: Improving ecological inference by modelling the source of zero observations. Ecology letters **8**(11): 1235–1246. Wiley-Blackwell. doi:10.1111/j.1461-0248.2005.00826.x.

Maunder, M.N., and Punt, A.E. 2013. A review of integrated analysis in fisheries stock assessment. Fisheries Research **142**: 61–74. doi:10.1016/j.fishres.2012.07.025.

Ovaskainen, O., Hottola, J., and Siitonen, J. 2010. Modeling species co-occurrence by multivariate logistic regression generates new hypotheses on fungal interactions. Ecology **91**(9): 2514–2521. doi:10.1890/10-0173.1.

Pérez Roda, M.A., Gilman, E., Huntington, T., Kennelly, S.J., Suuronen, P., Chaloupka, M., Medley, P.A.H., and Food and Agriculture Organization of the United Nations. 2019. A third assessment of global marine fisheries discards. FAO Fisheries and Aquaculture Technical Paper No. 633. Rome, FAO. 78 pp.

Perry, A.L., Low, P.J., Ellis, J.R., and Reynolds, J.D. 2005. Climate Change and Distribution Shifts in Marine Fishes. Science **308**(5730): 1912–1915. American Association for the Advancement of Science. doi:10.1126/science.1111322.

Pinsky, M.L., Worm, B., Fogarty, M.J., Sarmiento, J.L., and Levin, S.A. 2013. Marine Taxa Track Local Climate Velocities. Science **341**(6151): 1239–1242. American Association for the Advancement of Science. doi:10.1126/science.1239352.

Roberts, S.M., Boustany, A.M., and Halpin, P.N. 2020. Substrate-dependent fish have shifted less in distribution under climate change. Communications Biology **3**(1): 1–7. Nature Publishing Group. doi:10.1038/s42003-020-01325-1.

Robertson, M.D., Gao, J., Regular, P.M., Morgan, M.J., and Zhang, F. 2021. Lagged recovery of fish spatial distributions following a cold-water perturbation. Scientific Reports **11**(1): 9513. Nature Publishing Group. doi:10.1038/s41598-021-89066-x.

Rogers, L.A., Griffin, R., Young, T., Fuller, E., Martin, K.S., and Pinsky, M.L. 2019. Shifting habitats expose fishing communities to risk under climate change. Nature Climate Change **9**(7): 512–516. Nature Publishing Group. doi:10.1038/s41558-019-0503-z.

Selden, R.L., Thorson, J.T., Samhouri, J.F., Bograd, S.J., Brodie, S., Carroll, G., Haltuch, M.A., Hazen, E.L., Holsman, K.K., Pinsky, M.L., Tolimieri, N., and Willis-Norton, E. 2020. Coupled changes in biomass and distribution drive trends in availability of fish stocks to US West Coast ports. ICES J Mar Sci **77**(1): 188–199. Oxford Academic. doi:10.1093/icesjms/fsz211.

Simpson, M.R., and Walsh, S.J. 2004. Changes in the spatial structure of Grand Bank yellowtail flounder: testing MacCall's basin hypothesis. Journal of Sea Research: 12.

Sunday, J.M., Bates, A.E., and Dulvy, N.K. 2012. Thermal tolerance and the global redistribution of animals. Nature Clim Change **2**(9): 686–690. doi:10.1038/nclimate1539.

Swain, D.P., and Wade, E.J. 1993. Density-Dependent Geographic Distribution of Atlantic Cod (*Gadus morhua*) in the Southern Gulf of St. Lawrence. Canadian Journal of Fisheries and Aquatic Sciences **50**(4): 725–733.

Thorson, J. 2017. Three problems with the conventional delta-model for biomass sampling data, and a computationally efficient alternative. Canadian Journal of Fisheries and Aquatic Sciences **75**. doi:10.1139/cjfas-2017-0266.

Thorson, J.T. 2018. Forecast skill for predicting distribution shifts: A retrospective experiment for marine fishes in the Eastern Bering Sea. Fish and Fisheries **20**(1): 159–173. doi:10.1111/faf.12330.

Thorson, J.T. 2019a. Forecast skill for predicting distribution shifts: A retrospective experiment for marine fishes in the Eastern Bering Sea. Fish and Fisheries **20**(1): 159–173. doi:10.1111/faf.12330.

Thorson, J.T. 2019b. Guidance for decisions using the Vector Autoregressive Spatio-Temporal (VAST) package in stock, ecosystem, habitat and climate assessments. Fisheries Research **210**: 143–161. doi:10.1016/j.fishres.2018.10.013.

Thorson, J.T. 2021, May 5. Specify covariates and visualize responses. Available from https://github.com/James-Thorson-NOAA/VAST/wiki/Specify-covariates-and-visualize-responses.

Thorson, J.T., Adams, C.F., Brooks, E.N., Eisner, L.B., Kimmel, D.G., Legault, C.M., Rogers, L.A., and Yasumiishi, E.M. 2020. Seasonal and interannual variation in spatio-temporal models for index standardization and phenology studies. ICES Journal of Marine Science **77**(5): 1879–1892. doi:10.1093/icesjms/fsaa074.

Thorson, J.T., and Barnett, L.A.K. 2017. Comparing estimates of abundance trends and distribution shifts using single- and multispecies models of fishes and biogenic habitat. ICES Journal of Marine Science **74**(5): 1311–1321. doi:10.1093/icesjms/fsw193.

Thorson, J.T., Ianelli, J.N., Larsen, E.A., Ries, L., Scheuerell, M.D., Szuwalski, C., and Zipkin, E.F. 2016a. Joint dynamic species distribution models: a tool for community ordination and spatio-temporal monitoring. Global Ecology and Biogeography **25**(9): 1144–1158. doi:10.1111/geb.12464.

Thorson, J.T., Pinsky, M.L., and Ward, E.J. 2016b. Model-based inference for estimating shifts in species distribution, area occupied and centre of gravity. Methods in Ecology and Evolution **7**(8): 990–1002. doi:10.1111/2041-210X.12567.

Thorson, J.T., Rindorf, A., Gao, J., Hanselman, D.H., and Winker, H. 2016c. Density-dependent changes in effective area occupied for sea-bottom-associated marine fishes. Proc. R. Soc. B **283**(1840): 20161853. doi:10.1098/rspb.2016.1853.

Thorson, J.T., Scheuerell, M.D., Shelton, A.O., See, K.E., Skaug, H.J., and Kristensen, K. 2015a. Spatial factor analysis: a new tool for estimating joint species distributions and correlations in species range. Methods in Ecology and Evolution **6**(6): 627–637. doi:10.1111/2041-210X.12359.

Thorson, J.T., Shelton, A.O., Ward, E.J., and Skaug, H.J. 2015b. Geostatistical delta-generalized linear mixed models improve precision for estimated abundance indices for West Coast groundfishes. ICES Journal of Marine Science **72**(5): 1297–1310. doi:10.1093/icesjms/fsu243.

Thorson, J.T., Skaug, H., Kristensen, K., Shelton, A.O., Ward, E.J., Harms, J.H., and Benante, J.A. 2015c. The importance of spatial models for estimating the strength of density dependence. Ecology 96, 1202–1212. doi:doi:10.1890/14-0739.1.

Vert-pre, K.A., Amoroso, R.O., Jensen, O.P., and Hilborn, R. 2013. Frequency and intensity of productivity regime shifts in marine fish stocks. Proceedings of the National Academy of Sciences **110**(5): 1779–1784. doi:10.1073/pnas.1214879110.

Walsh, S.J., and Brodie, W.B. 2006. Exploring relationships between bottom temperatures and spatial and temporal patterns in the Canadian fishery for yellowtail flounder on the Grand Bank. NAFO SCR Doc 06/26, Serial No. N5245.

Walsh, S.J., Simpson, M., and Morgan, M.J. 2004. Continental shelf nurseries and recruitment variability in American plaice and yellowtail flounder on the Grand Bank: insights into stock resiliency. Journal of Sea Research **51**(3–4): 271–286. doi:10.1016/j.seares.2003.10.003.

Warren, W., Brodie, W.B., Stansbury, S., Walsh, S.J., Morgan, J., and Orr, D. 1997. Analysis of the 1996 Comparative Fishing Trial between the Alfred Needier with the Engel 145 trawl and the Wilfred Templeman, with the Campelen 1800 trawl.

Warren, W.G. 1996. Report on the Comparative Fishing Trial Between the Gadus Atlantica and Teleost.

Warton, D.I., Blanchet, F.G., O'Hara, R.B., Ovaskainen, O., Taskinen, S., Walker, S.C., and Hui, F.K.C. 2015. So Many Variables: Joint Modeling in Community Ecology. Trends in Ecology & Evolution **30**(12): 766–779. doi:10.1016/j.tree.2015.09.007.

Wilderbuer, T., Stockhausen, W., and Bond, N. 2013. Updated analysis of flatfish recruitment response to climate variability and ocean conditions in the Eastern Bering Sea. Deep Sea Research Part II: Topical Studies in Oceanography **94**: 157–164. doi:10.1016/j.dsr2.2013.03.021.

Chapter 3:
Retrospective Forecasting of Seasonal Spatiotemporal Dynamics to Identify Bycatch Hotspots in the Yellowtail flounder Fishery on the Grand Banks

3.1. Introduction

Many marine species spatial distributions have been shown to be particularly sensitive to changing climate over multi-annual to decadal scales (Nye et al. 2009; Pinsky et al. 2013; Poloczanska et al. 2013; Bell et al. 2015; Thorson et al. 2016). Therefore, there is a recent interest in forecasting species distribution shifts as an ecosystem management tool, because many ecosystems worldwide are shifting in response to rapid changes in environmental conditions. Ecosystem resource management requires forecasting species distributions over various short- and long-term timescales to ensure the most sustainable management of that particular resource. Long-term forecasts can be used to make industry decisions such as long-term capitalization of profit and develop strategies for long-term sustainability of the respective fishery (Tommasi et al. 2017). Whereas short-term seasonal forecasts can be used to modify fleet behaviour to ensure the most effective and efficient fishing strategies such as bycatch reduction (Tommasi et al. 2017). Integration of nowcasting (real-time) (Hobday and Hartmann 2006; Howell et al. 2008, 2015) and short-term forecasts incorporating oceanic conditions into habitat preference models are being pursued to forecast spatial distributions of species and to set dynamic time-area closures to decrease bycatch (Hobday et al. 2011; Dunn et al. 2016).

Static spatial management strategies restrict fishing access to a specific area and potentially limits bycatch when fishing gear cannot be modified. However, fish are not static; they are dynamic. They move to remain in optimal environments to suite their physical needs causing

81

their distribution and phenology's to vary with oceanic dynamics and life stages (Perry et al. 2005; Nye et al. 2009; Pinsky et al. 2013; Asch 2015). Therefore, static time-area closures can be ineffective for dynamic processes like bycatch avoidance (Hobday and Hartmann 2006; Howell et al. 2008, 2015; Hobday et al. 2011). Also, abundance estimates generally lack spatial structure and therefore provide no capability to forecast changes in stock distribution as habitat conditions shift the distribution of the stock. Therefore, a dynamic spatial modelling approach is needed for short-term forecast to mitigate bycatch.

Thorson (2019) investigated three forecasting models (AR, HE and VAST) and found that VAST models had the most appropriate width for forecasting intervals (predicted uncertainty) and explained the highest variance in poleward movement. VAST has been used as a forecasting tool to predict the dynamics of future distribution shifts within and between species of 20 fish and crab species in the Eastern Bering sea for 1-, 2-, and 30- year periods, proving to be a powerful short-term forecasting tool for commercial fisheries under new environmental conditions (Thorson 2019). However, VAST has not been yet been used to explain distribution shifts in the North Atlantic.

In chapter two, I found that including quality habitat covariates improves the performance of VAST multispecies distribution models. In chapter three, I use the model described in chapter two to perform multispecies short-term retrospective forecasts over 1-5 years to hindcast the seasonal spatiotemporal distribution patterns of yellowtail flounder, and bycatch species such as American plaice, Atlantic cod and witch flounder. Retrospective skill testing involves fitting ecological models to historical data, hindcasting changes and comparing hindcasts with historical

observations. Using our retrospective forecast models, I will estimate biomass, density and bycatch hotspot trends and use these as tools to assess the accuracy of our retrospective forecast models for both Fall and Spring surveys to predict season-specific dynamic bycatch hotspots. By using a multispecies VAST model, I hope to provide a framework for short-term seasonal forecasts to identify dynamic bycatch hotspots. Thus, increasing the efficiency and sustainability of the yellowtail flounder fishery.

3.2. Methods

3.2.1. Data Collection

Refer to section 2.2.1.

3.2.2. Model Components

Refer to section 2.2.2.

3.2.3. Model Fit

Refer to section 2.2.3.

3.2.4. Predictive Process

Using the model I developed in chapter two, I use a "predictive process" approximation to simplify computation for spatial and spatiotemporal variation similar to (Thorson 2019) with 100 knots in a stochastic partial differential equation approximation to the sparse precision matrix that approximates a Matern correlation function (Lindgren et al. 2011). Spatiotemporal variation

is still independent and also follows random walk across years, the same as the best model selected in section 2.2.3.

Our full data set includes data from 1984-2018 for both spring and fall surveys. I ran a series of retrospective forecast models for 1-, 2-,3-,4- and 5- years (Table 3.1); all models converged. The 6-year retrospective forecast model predicting 2013, 2014, 2015, 2016, 2017 and 2018 using data for 1984-2012 did not converge for both Spring and Fall surveys; therefore, our longest prediction is 5- years, predicting 2014, 2015, 2016, 2017, and 2018 for both Fall and Spring.

3.2.5. Metrics of Forecast Ability: Density

I evaluated each model's forecast ability by comparing estimated density and biomass trends between the full model and the retrospective forecast models. VAST estimates the relative density instead of the true density, thus comparing the retrospective forecast model to the model with the full data set represents a fair and straightforward metric to assess the accuracy of predictions.

Predicted biomass density $d\ (c, s, t)$ for each location for each species c_i every year t_i were calculated from each model the same way as equation 2.9 in section 2.2.5. Predicted density was compared between the full model and retrospective forecast models using Pearson correlation separately between the years to determine the accuracy of the density predictions. Scatter plots were also made to visualize the residual variation.

3.2.6. Metrics of Forecast Ability: Biomass

Density is used to predict total biomass $I(c, s, t)$ for the entire domain for each species to estimate temporal trends in biomass way as equation 2.8 in section 2.2.6. Predicted biomass including sd was compared between the full model and retrospective forecast model as a separate metric to determine model accuracy. Line plots of estimated density were made per species by each season to show model accuracy. I plotted the five most recent years; 2018, 2017, 2016, 2015, and 2014 for the full model and our model predicting 2014 & 2015 & 2016 & 2017 & 2018 for both Fall (Figure 3.3) and Spring (Figure 3.4) as an example. Other years were not plotted to conserve time.

3.2.7. Bycatch Hotspot Visualization

Predicted biomass density $d(c, s, t)$ derived from our model was used to plot species density ratios relative to yellowtail flounder (species density (standardized to kg/25 km^2) / (species density (standardized to kg/25 km^2) + yellowtail flounder density (standardized to kg/25 km^2))) for my three bycatch species of interest including American plaice, witch flounder and Atlantic cod. I plotted the model predicting 2014 & 2015 & 2016 & 2017 & 2018 for both Fall (Figure 3.7-3.9) and Spring (Figure 3.10-3.12) to identify bycatch hotspots between the bycatch species and yellowtail flounder.

3.3. Results

3.3.1. Comparing Density

Across all models, the Pearson correlation for density decreased as the number of years predicted increased (Figure 3.1 & 3.2). Yellowtail flounder density had highest predictability measured by

Pearson correlation amongst all four species across density for all retrospective forecast models for both Fall and Spring (Figure 3.1& 3.2). Using the 5-year predictive model, predicting 2014-2018, as an example, our model over predicts density for yellowtail flounder in both the Spring and Fall as the slope of the data is greater than 1(Figure 3.3 & 3.4). Witch flounder density has a higher Pearson correlation in the Fall than in the spring (Figure 3.1 & 3.2). Using the 5-year predictive model (predicting 2014-2018) witch flounder density is over predicted in the Fall as the slope is greater than 1, in contrast, witch flounder density is fairly evenly disturbed for Spring as the slope is close to 1 (Figure 3.3 & 3.4). American plaice density has stronger Pearson correlation in the fall than in the spring (Figure 3.1 & 3.2). With the 5-year predictive model, American plaice density is slightly under predicted for spring as the slope is below 1, and over predicted for Fall as the slope is above 1 (Figure 2.4 & 3.5). Atlantic cod density had the lowest Pearson correlation amongst all four species for all retrospective forecast models for both Fall and Spring (Figure 3.1 & 3.2). With the 5-year predictive model, Atlantic cod density is underpredicted for both Fall and Spring as the slope is below 1.

3.3.2. Comparing Biomass

All retrospective forecast models standard error increased for all species as the number of predictive years increased (Figure 3.5 & 3.6). Yellowtail flounder biomass had the largest predictive error of all four species in both seasons (Figure 3.5 & 3.6). For the Fall, the retrospective forecast models for yellowtail flounder, witch flounder and American plaice over-estimated the biomass, while Atlantic cod biomass estimates were slightly below as the model was trying to converge to the respective means (Figure 3.5 & 3.6). For the Spring, the retrospective forecast models over-estimated again for Yellowtail flounder, were fairly close for

witch flounder and American plaice, and under-estimated for Atlantic cod biomass as the model was trying to converge to the respective means (Figure 3.5 & 3.6).

3.3.3. *Bycatch Hotspot Visualization*

Species density ratios relative to yellowtail flounder for the 5-year predictive model for both Fall (Figure 3.9) and Spring (Figure 3.10) were plotted and clear patterns emerged. Other predicted models were not plotted to conserve time. The highest values (darkest colours) on these plots indicate areas where yellowtail flounder is found the least. The highest values for all plots are on the edges on the Grand Bank (Figure 3.7-3.12). The lowest values (lightest colours) on these plots indicate areas where yellowtail flounder is found the most. The lowest values for all plots are on the southeast shoal (figure 3.7-3.12). The species with the highest overlap for both seasons with yellowtail flounder was American plaice (Figure 3.7 &3.10). The species with the lowest overlap for both seasons with yellowtail flounder was witch flounder (Figure 3.8 &3.11).

3.4. Discussion

In chapter two, I performed a multispecies VAST to determine the seasonal spatiotemporal dynamics of yellowtail flounder, and three of its bycatch species, and with important environmental covariates. In chapter three, I used this model to perform multispecies short-term hindcasts over 1-, 2- and 3-, 4- and 5- years to predict the seasonal spatiotemporal distribution patterns of these species. Using our retrospective forecast models, I estimated density, biomass and bycatch hotspot trends and used these to assess the accuracy of our retrospective forecast models for both Fall and Spring to predict season-specific dynamic bycatch hotspots.

Pearson correlation in density estimates decreased (Figure 3.1 & 3.2) and biomass sd increased (Figure 3.5 and 3.6) as the number of years predicted increased as the model uncertainty increased as the model lost the ability to detect variation in species distribution over time. This maybe due to the models intercepts having a lack of flexibility. The random spatiotemporal component forecasts are zero (because they are independent), spatial effects are constant, and temporal effects are random walk; therefore, the forecasted random walk is derived from 2013 (the last full year with data). I selected these intercepts because this model set up yielded the lowest AIC in chapter two (Table 2.3 & 2.4); however, other model intercepts may be investigated to decrease model uncertainty and increase predictability. This model output also may have been observed because I only had one dynamic habitat covariate, temperature (as depth and substrate are static habitat covariates). Therefore, adding more dynamic habitat covariates would also strengthen the models predictivity allowing the density estimates to be anchored to a dynamic variable. Thus, model flexibility could be increased by investigating different temporal, spatial and spatiotemporal effects and including more dynamic variables.

Generally, the model predicted density in the Fall fit better than predicted density in the spring (Figure 3.1 & 3.2). Predictability is influenced by a combination of factors in our model including intraspecies interactions and habitat covariates. I found in chapter two that all species in our model are generally highly correlated with stronger correlation in the Spring than in the Fall (Figure 2.4 & 2.5). Therefore, interspecies effects maybe weaker than habitat effects for predictably as species were more highly correlated in the Spring; yet, predicted density estimates fit better in the Fall. Single species hindcasts should be performed to see if the predictability increases or decreases to dissect the effect of species associations. Spring predictability may

possibly be restricted to spawning habitat which may be associated with a habitat covariate that I have not identified. Thus, the habitat covariates I tested may be fitting better for Fall than Spring. The species may also have more seasonal movement in the Fall compared to the Spring as previously recorded in the literature as they are not restricted to the spawning areas, resulting in them being more selective with the habitat covariates I tested, resulting in a higher predictability for the Fall estimated density per tow.

The Pearson correlation for density estimates between the full model and the predictive models were highest for yellowtail and lowest for Atlantic cod (Figure 3.1 & 3.2). Yellowtail flounder (DFO 2000), witch flounder (Bigelow and Schroeder 1953) and American plaice (Pitt 1969) tend to be rather sedentary. However, the Atlantic cod 2J3KL stock is highly migratory as they overwinter near the edge of the continental shelf and spend spring and summers in shallow waters along the coast onto the plateau of the grand banks (Fisheries and Oceans Canada 2019). Also, the Atlantic cod 3NO stock stays in the shallower parts of the banks in summer (mostly the SE shoal in 3N), and the slopes of the Grand Bank in the winter when cooling occurs (Rideout et al. 2015). When spawning, Atlantic cod also forms 'spawning columns' (Knickle and Rose 2012) which may cause the spring surveys to have more variability as some of the fish might be missed as the fish are less likely to be at sea floor level where the tows occur. Therefore, the flatfish in our study are more sedentary than Atlantic cod resulting in less change in their density distribution over time. This may be why the Pearson correlations were higher for our flatfish species, and lower for Atlantic cod; as Atlantic cod is more dynamic than the other flatfish species, therefore the model had difficulty predicting dynamic distribution shifts due to its rigidity in its intercepts as described above (Figure 3.1 & 3.2).

Yellowtail flounder had the highest Pearson correlation across density for all retrospective forecast models for both Fall (Figure 3.1) and Spring (Figure 3.2), and the values were over predicted as the slope was above 1 (Figure 3.3 & 3.4). Whereas Atlantic cod had the lowest Pearson correlation across density for all retrospective forecast models for both Fall (Figure 3.1) and Spring (Figure 3.2), and the values were under predicted as the slope was below 1 (Figure 3.3 & 3.4). American plaice was slightly under predicted in the Spring and more underpredicted in the Fall (Figure 3.3 &3.4). It is unclear why some species are over predicted, and some are underpredicted. It is not a systematic error within VAST as it has been proven to be reliable for multispecies models (ie. Gao et al. 2020, Thorson & Barnett 2017); however, it may be an issue with out data that was not accounted for. This warrants further investigation.

For species in which the biomass does not fluctuate over recent years, the estimated biomass for the predictive models had a lower sd (Figure 3.5 & 3.6). This is because the model converges to the mean, and if there is not much variation then the mean is closer to the estimated biomass. Estimated biomass for witch flounder, American plaice and Atlantic cod in the Fall, and Atlantic cod in the spring fit well (Figure 3.7 & 3.8); as the biomass did not fluctuate that much over recent years. Estimated biomass for with flounder, American plaice and yellowtail flounder in the Spring, and yellowtail flounder in the fall fit worse (Figure 3.7 & 3.8); as the biomass has varied more over the recent years, therefore the mean of the model was not close to the estimated biomass.

As our Pearson correlations for Fall and Spring density being relatively high (Figure 3.1 & 3.2), we can infer that the bycatch hotspots from our retrospective forecast model predicting years 2014-2018 (Figure 3.7 to 3.12) are similar to the full model. Clear patterns emerge from plotting. Species density ratios relative to yellowtail flounder for the 5-year predictive model for both Fall (Figure 3.9) and Spring (Figure 3.10) were plotted and clear patterns emerged. The highest values on these plots indicate areas where yellowtail flounder is found the least, therefore any fishery targeting the yellowtail flounder would presumably avoid these areas. The highest values for all plots are on the edges on the Grand Bank (Figures 3.7-3.12). The lowest values on these plots indicate areas where yellowtail flounder is found the most, therefore any fishery targeting the yellowtail flounder would presumably target these areas. An area with constantly higher densities of yellowtail flounder compared to the other three species is the Southeast Shoal for both season (Figures 3.7 to 3.12). This is consistent with what is in the literature as the Southeast Shoal has a high concentration of many groundfish species (Fisheries and Oceans Canada 2019). The lowest values for all plots are on the southeast shoal (Figures 3.7-3.12). This would also suggest that the areas that the fishery targets have inherently lower bycatch levels.

The species with the highest overlap for both seasons with yellowtail flounder was American plaice (Figures 3.7 & 3.10). This is consistent with what is in the literature, as American plaice is the bycatch species caught the most in the yellowtail flounder fishery (Table 1.1) (Knapman et al. 2020). Further research should focus on American plaice bycatch as a "choke" bycatch species within the yellowtail founder fishery. The species with the lowest overlap for both seasons with yellowtail flounder was witch flounder as it is concentrated mor on the edges of the Grand Banks (Figures 3.8 & 3.11). This is congruent with their being less witch flounder caught

91

as bycatch compared to the other three species (Table 1.1) (Knapman et al. 2020). Further research should include forecasting bycatch hotspots into the future so that industry can use similar models to identify areas of potential high bycatch before they even occur so that they can avoid them.

By using a retrospective forecast multispecies VAST model, I provided a framework for short-term seasonal forecasts in this region and identify dynamic bycatch hotspots. By identifying bycatch hotspots before fishermen actively fish in these areas, fishermen can actively avoid them therefore avoiding areas with high bycatch. This in turn increases the efficiency and sustainability of the yellowtail flounder fishery. I focused mainly on predicting spatiotemporal distribution as that is what matters at the bycatch management level, whereas the density estimates and biomass trends were primarily used as a model comparison tool. I demonstrated how difficult it is to predict overall indices such as estimated total biomass; even at the local level (estimated density per tow) there needs to be more effort into increasing the accuracy of spatiotemporal models. This is the first time this kind of model has been applied to 3LNO and there are many other approaches to explore.

3.5. Tables

Table 3.1 Description of retrospective forecast models and their respective data inputs. Each model was run for both Spring and Fall separately.

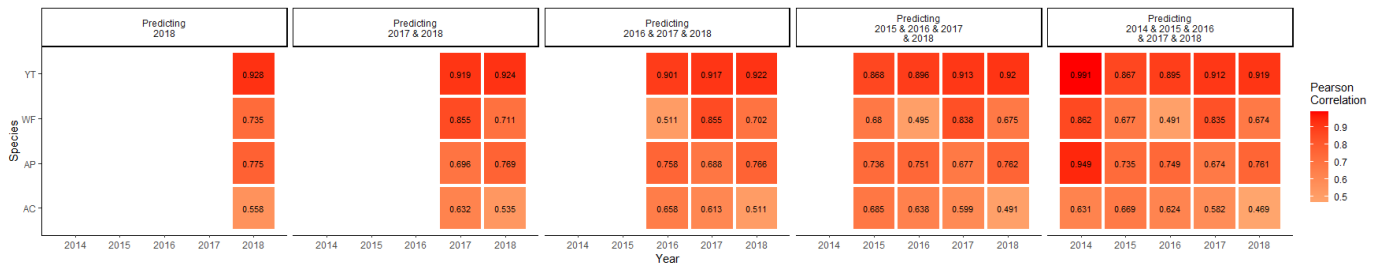| Model	Data	Predicting years
Full model	1984-2018	0
Predicting 2018	1984-2017	1
Predicting 2017 & 2018	1984-2016	2
Predicting 2016 & 2017 & 2018	1984-2015	3
Predicting 2015 & 2016 & 2017 & 2018	1984-2014	4
Predicting 2014 & 2015 &2016 & 2017 & 2018	1984-2013	5

3.6. Figures

Figure 3.1 Fall Pearson correlation for all models density (standardized to kg/ 25 km^2) for all four species; YT = yellowtail flounder, WF=witch flounder, AP=American plaice, and AC=Atlantic cod.
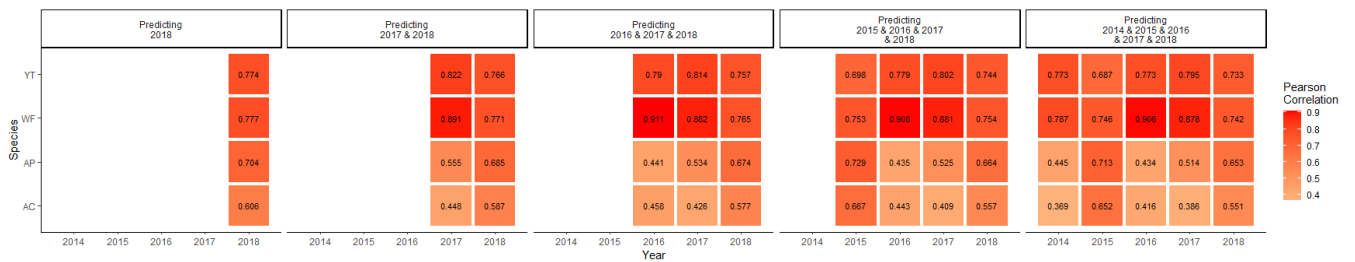

Figure 3.2 Spring Pearson correlation for all models density (standardized to kg/25 km^2) for all four species; YT = yellowtail flounder, WF=witch flounder, AP=American plaice, and AC=Atlantic cod.

Figure 3.3 Fall density (standardized to kg/25 km^2) of model predicting 2014 & 2015 & 2016 & 2017 & 2018 versus the full model showing Pearson correlation for all four species; yellowtail flounder, witch flounder, American plaice, and Atlantic cod.
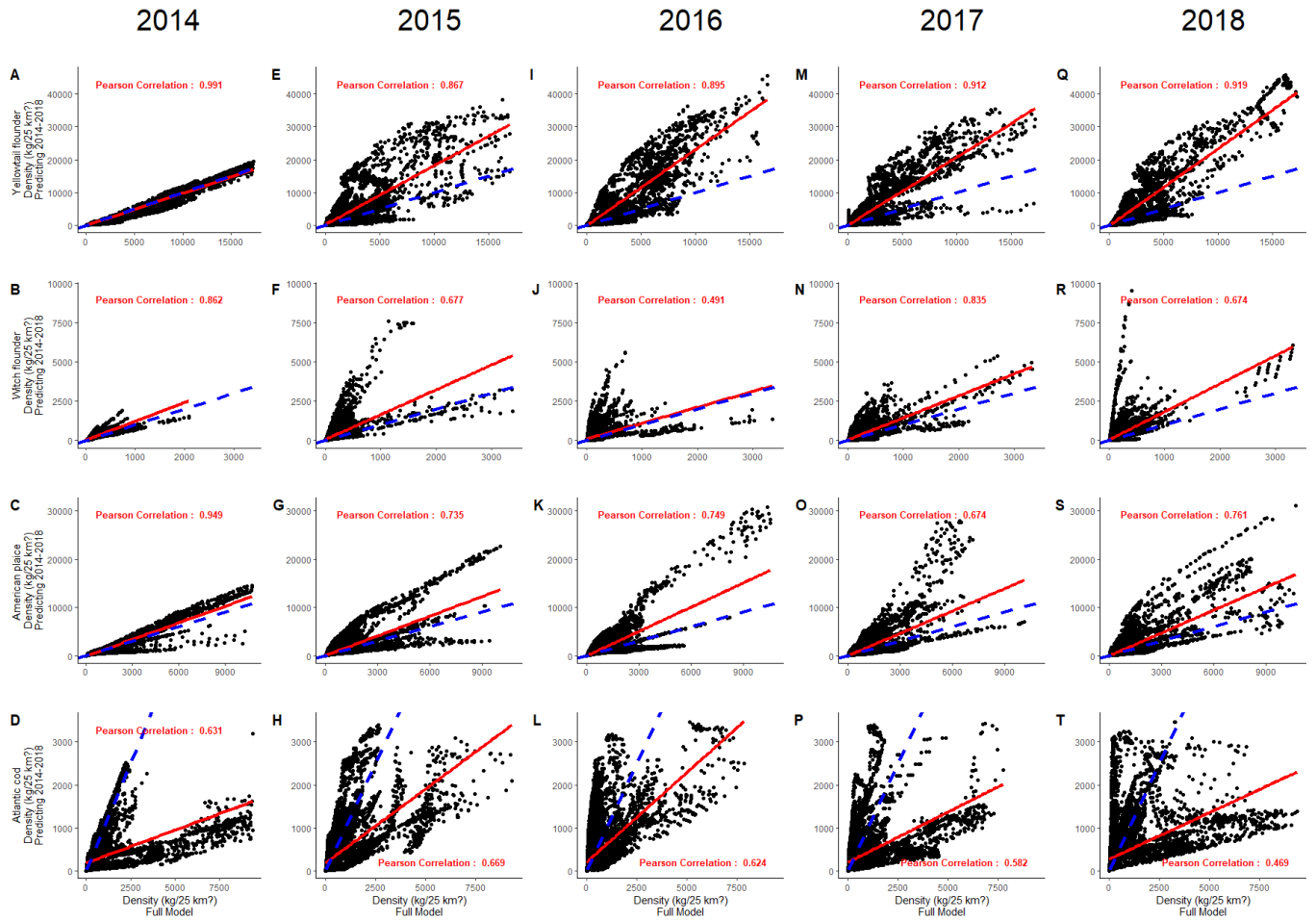
Figure 3.4 Spring density (standardized to kg/25 km^2) of model predicting 2014 & 2015 & 2016 & 2017 & 2018 versus the full model showing Pearson correlation for all four species; yellowtail flounder, witch flounder, American plaice, and Atlantic cod.
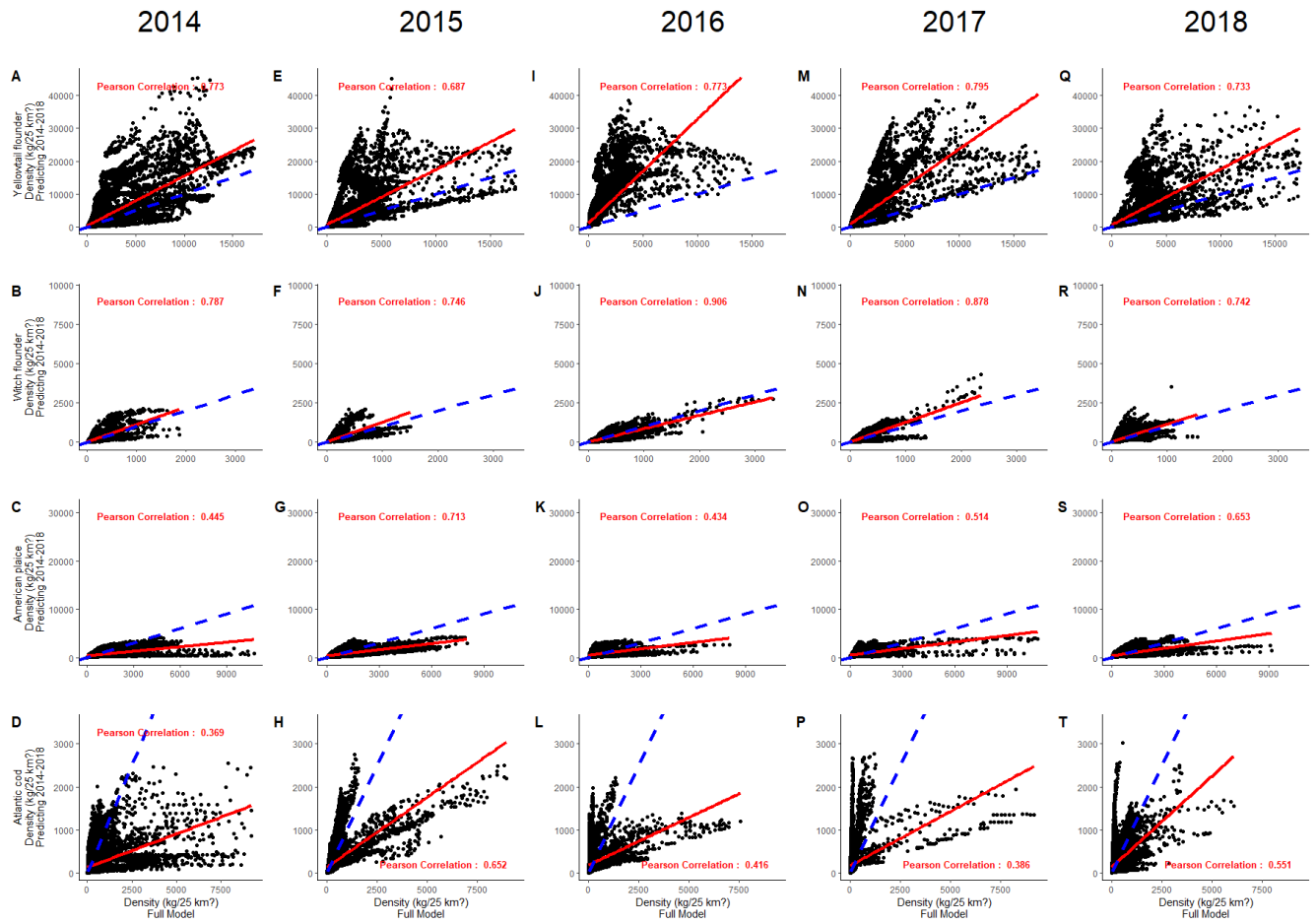
Figure 3.5 Fall biomass plots for 2010-2018 for all models and all four species: (A) yellowtail flounder, (B) Atlantic cod, (C) American plaice, and (D) witch flounder. Shaded area represents +/- 1 standard deviation.
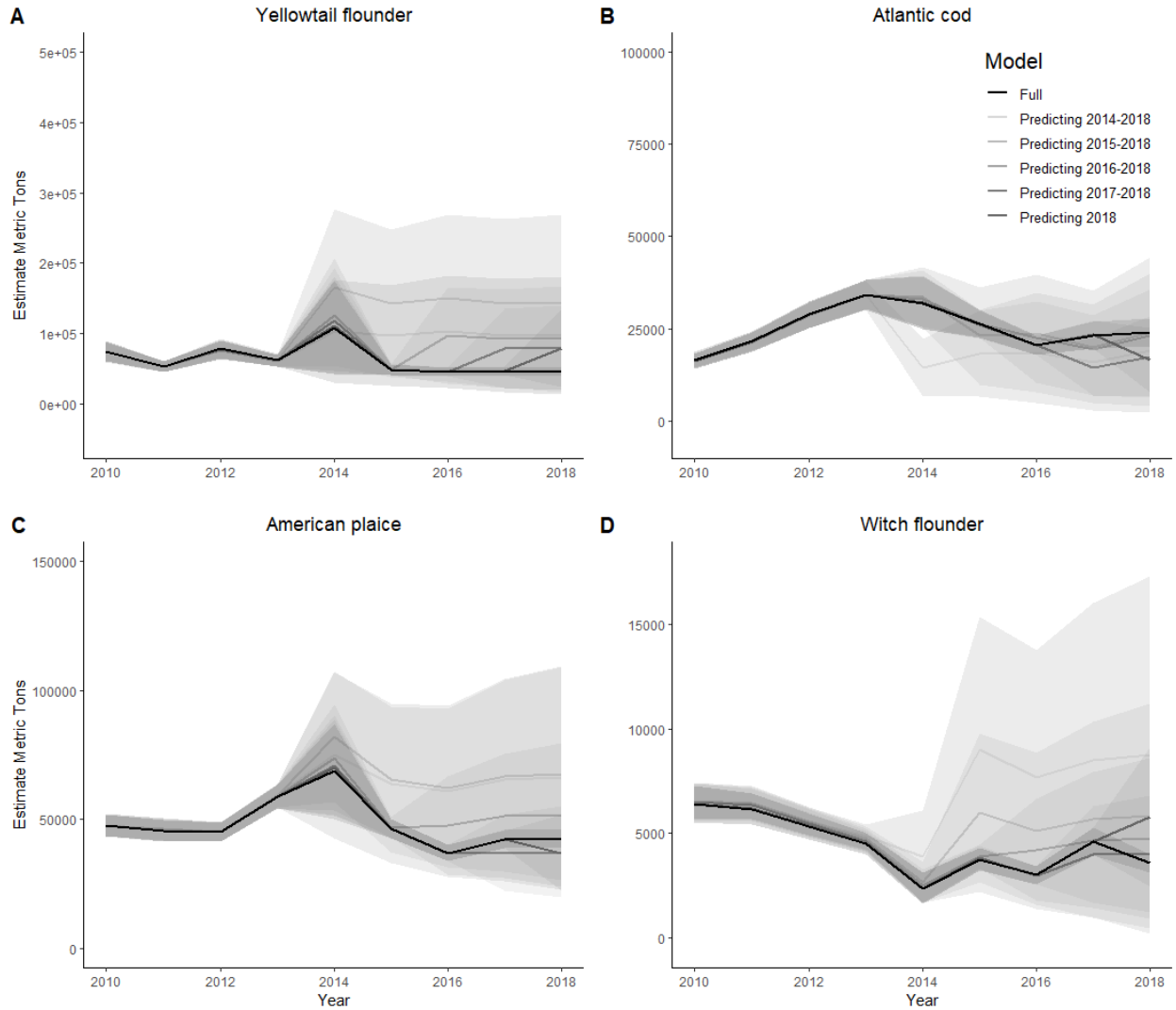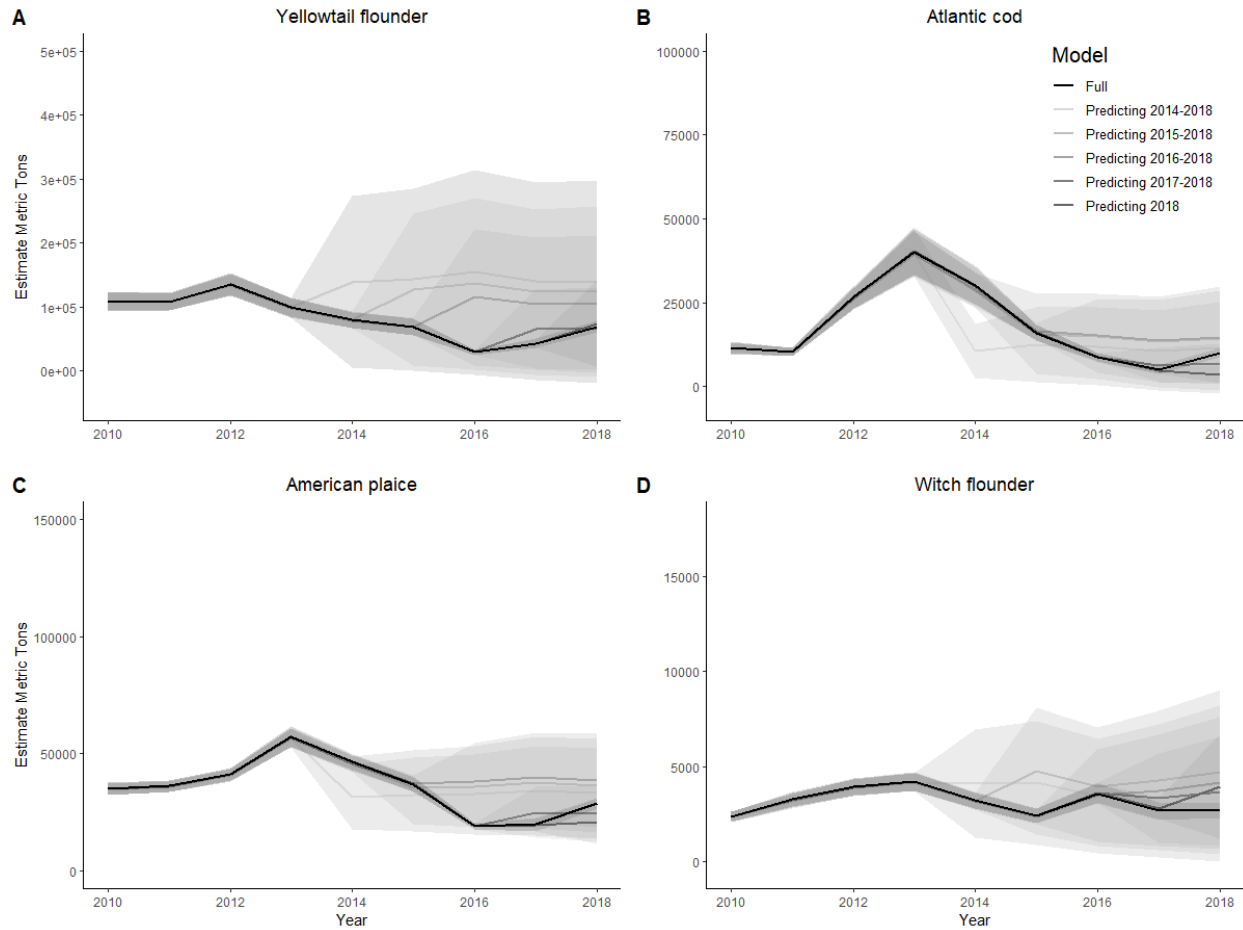
Figure 3.6 Spring biomass plots for 2010-2018 for all models and all four species: (A) yellowtail flounder, (B) Atlantic cod, (C) American plaice, and (D) witch flounder. Shaded area represents +/- 1 standard deviation.
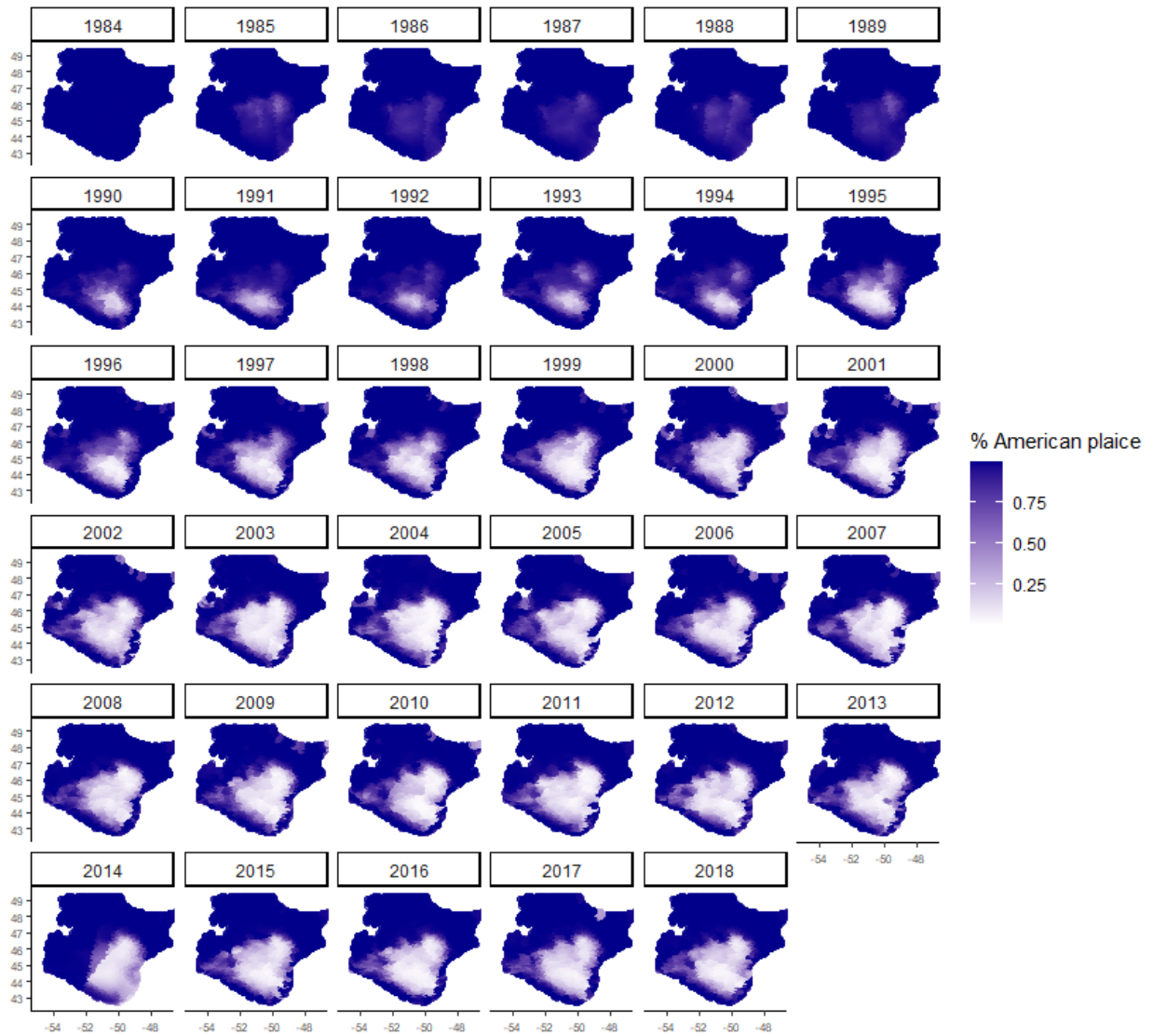
Figure 3.7 Fall American plaice density (standardized to kg/25 km^2) relative to yellowtail flounder density (standardized to kg/25 km^2) (American plaice density (standardized to kg/25 km^2) / (American plaice density (standardized to kg/25 km^2) + yellowtail flounder density (standardized to kg/25 km^2))) for 1984-2018 for the model predicting 2014 & 2015 & 2016 & 2017 & 2018.

Figure 3.8 Fall witch flounder density (standardized to kg/25 km^2) relative to yellowtail flounder density (standardized to kg/25 km^2) (witch flounder density (standardized to kg/25 km^2) / (witch flounder density (standardized to kg/25 km^2) + yellowtail flounder density (standardized to kg/25 km^2))) for 1984-2018 for the model predicting 2014 & 2015 & 2016 & 2017 & 2018.
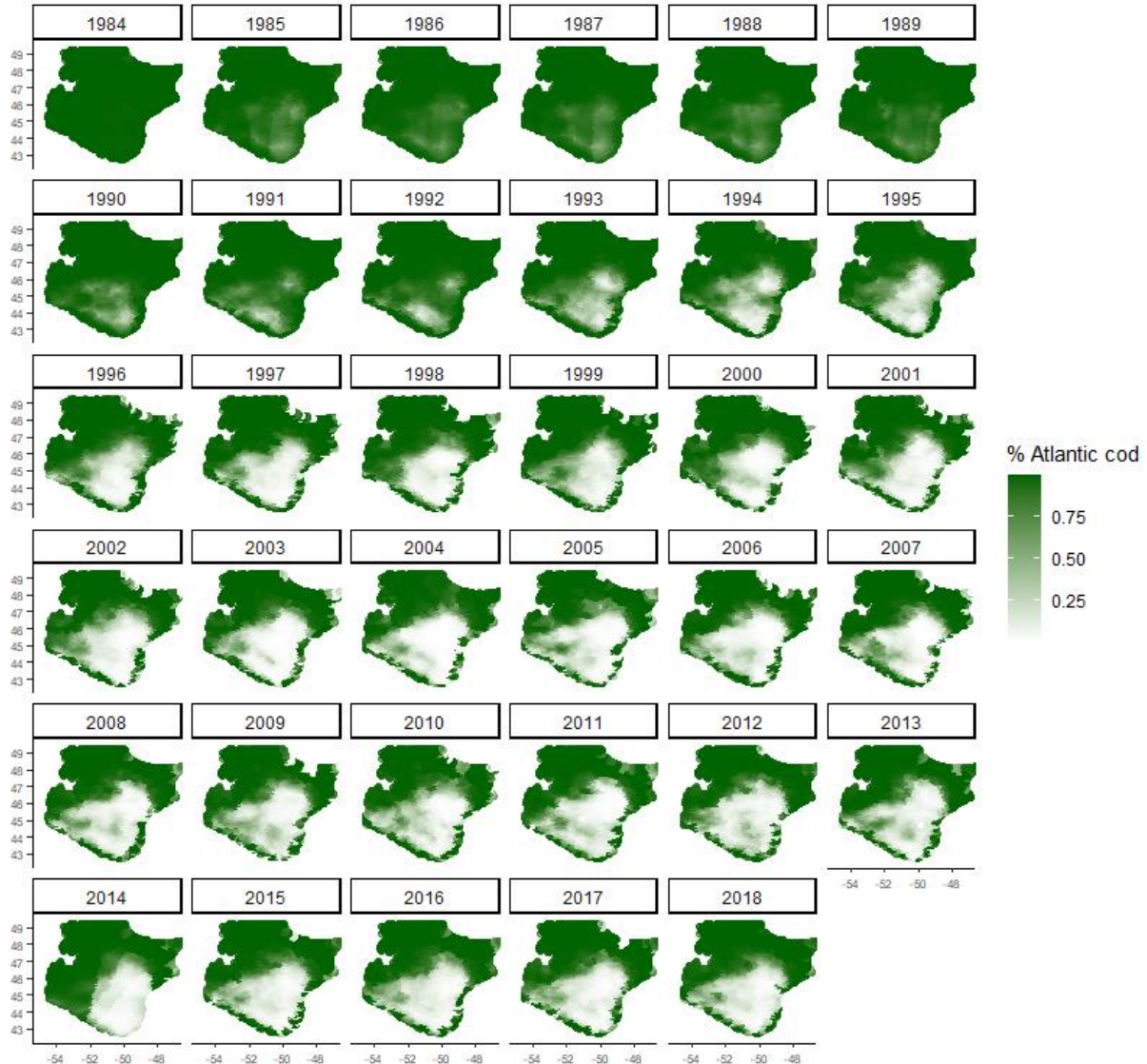
Figure 3.9 Fall Atlantic cod density (standardized to kg/25 km^2) relative to yellowtail flounder density (standardized to kg/25 km^2) (Atlantic cod density (standardized to kg/25 km^2) / (Atlantic cod density (standardized to kg/25 km^2) + yellowtail flounder density (standardized to kg/25 km^2))) for 1984-2018 for the model predicting 2014 & 2015 & 2016 & 2017 & 2018.
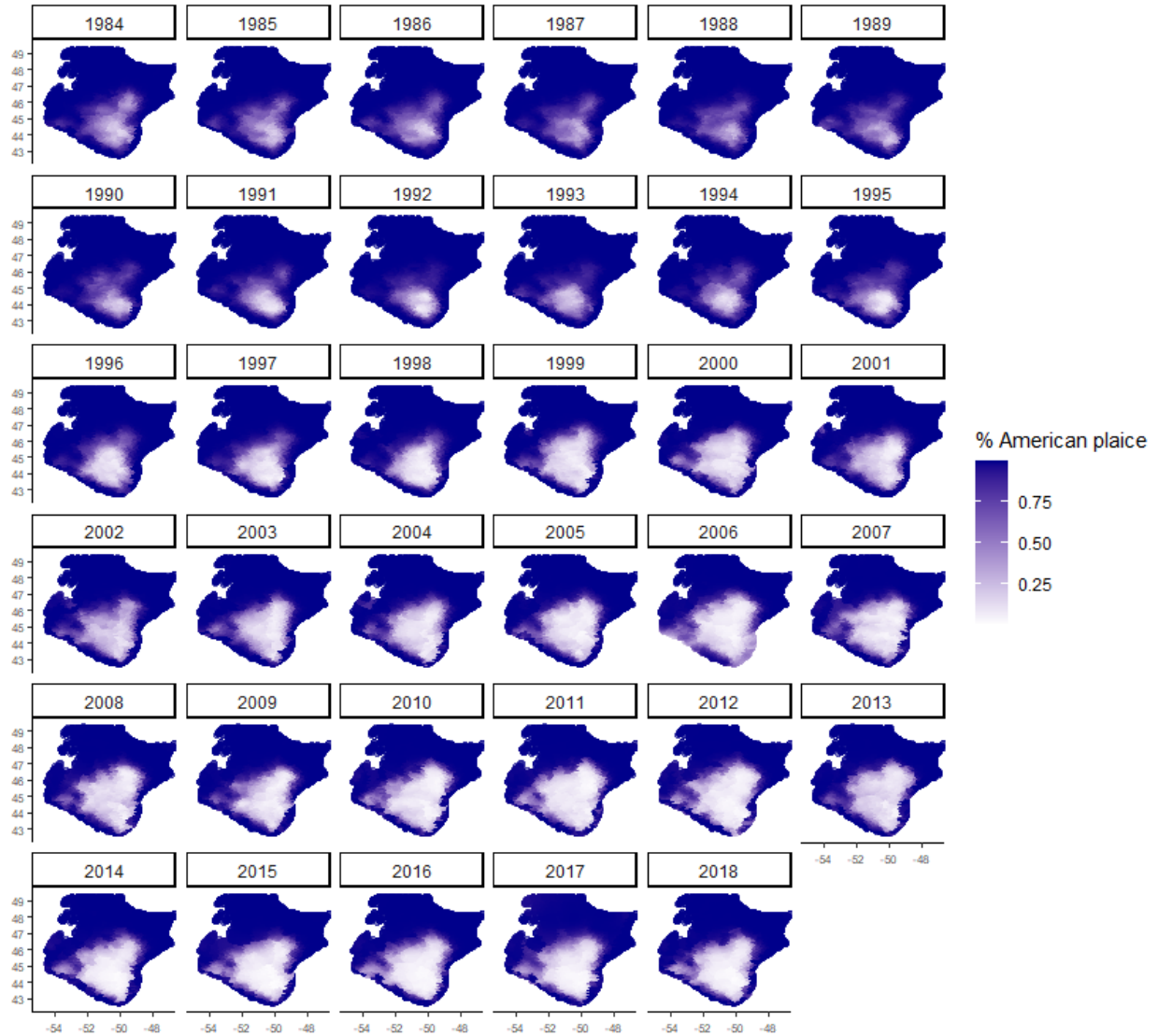
Figure 3.10 Spring American plaice density (standardized to kg/25 km^2) relative to yellowtail flounder density (standardized to kg/25 km^2) (American plaice density (standardized to kg/25 km^2) / (American plaice density (standardized to kg/25 km^2) + yellowtail flounder density (standardized to kg/25 km^2))) for 1984-2018 for the model predicting 2014 & 2015 & 2016 & 2017 & 2018.
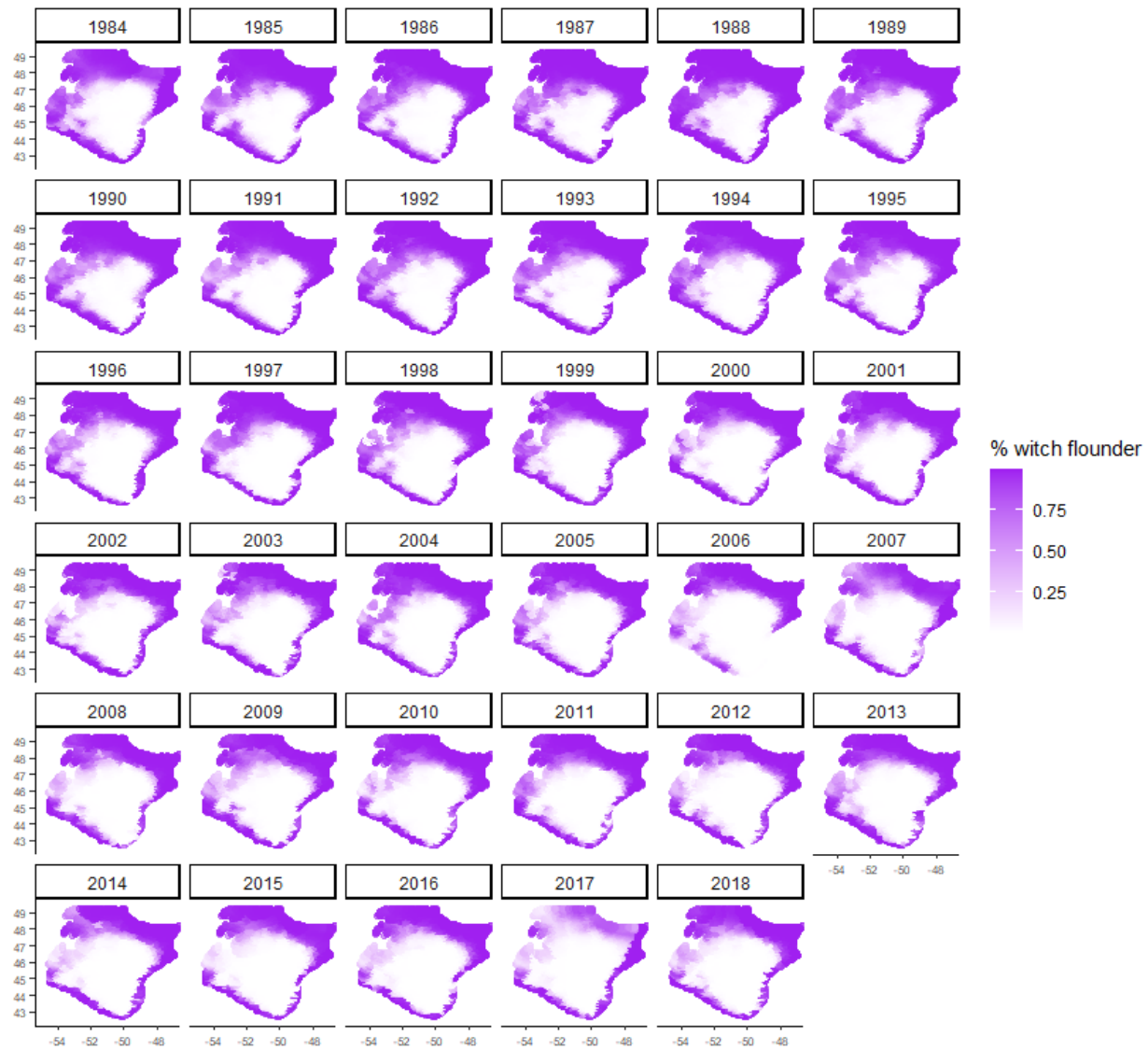
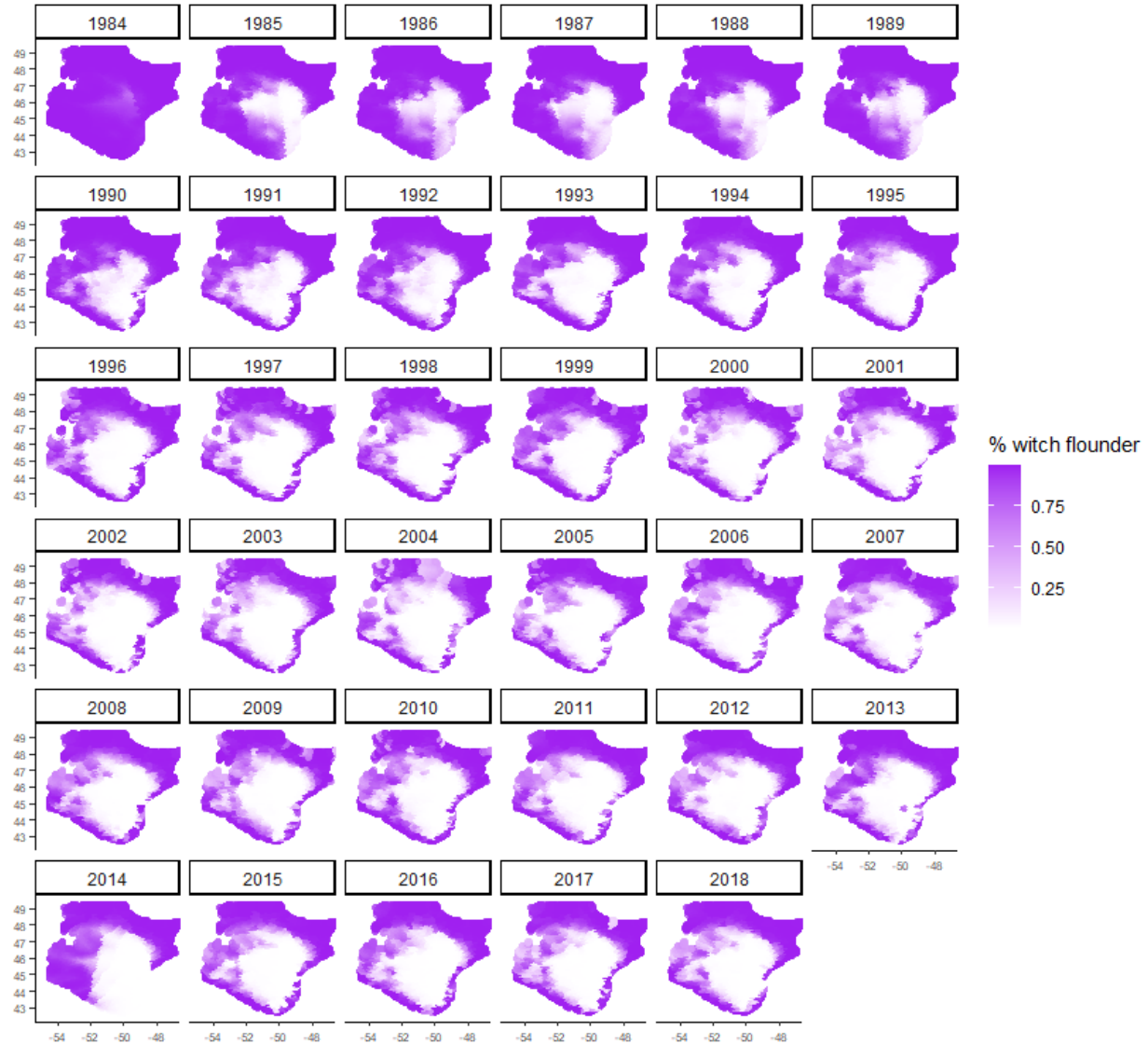Figure 3.11Spring witch flounder density (standardized to kg/25 km^2) relative to yellowtail flounder density (standardized to kg/25 km^2) (witch flounder density (standardized to kg/25 km^2) / (witch flounder density (standardized to kg/25 km^2) + yellowtail flounder density (standardized to kg/25 km^2))) for 1984-2018 for the model predicting 2014 & 2015 & 2016 & 2017 & 2018.

Figure 3.12 Spring Atlantic cod density (standardized to kg/25 km^2) relative to yellowtail flounder density (standardized to kg/25 km^2) (Atlantic cod density (standardized to kg/25 km^2) / (Atlantic cod density (standardized to kg/25 km^2) + yellowtail flounder density (standardized to kg/25 km^2))) for 1984-2018 for the model predicting 2014 & 2015 & 2016 & 2017 & 2018.

3.7. Bibliography
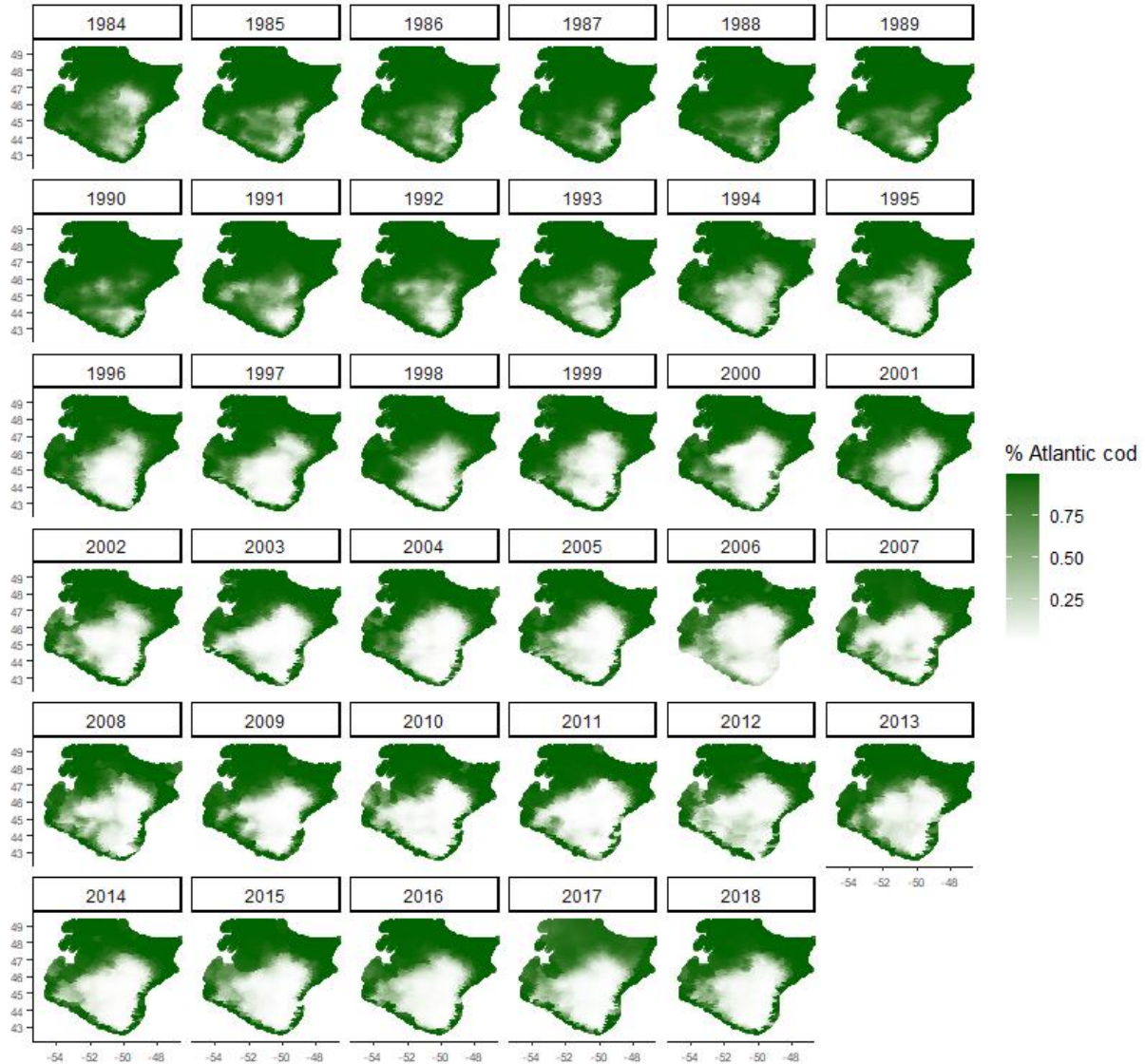
Asch, R.G. 2015. Climate change and decadal shifts in the phenology of larval fishes in the California Current ecosystem. Proc Natl Acad Sci USA **112**(30): E4065–E4074. doi:10.1073/pnas.1421946112.

Bell, R.J., Richardson, D.E., Hare, J.A., Lynch, P.D., and Fratantoni, P.S. 2015. Disentangling the effects of climate, abundance, and size on the distribution of marine fish: an example based on four stocks from the Northeast US shelf. ICES J Mar Sci **72**(5): 1311–1322. Oxford Academic. doi:10.1093/icesjms/fsu217.

Bigelow, H.B., and Schroeder, W.C. 1953. Fishes of the Gulf of Maine. U.S. Fish Wildl. Serv., Fish. Bull. 53(74), 577 p.

DFO. 2000. Yellowtail Flounder on Georges Bank. DFO Sci. Stock Status Rep. A3- 15.

Dunn, D.C., Maxwell, S.M., Boustany, A.M., and Halpin, P.N. 2016. Dynamic ocean management increases the efficiency and efficacy of fisheries management. PNAS **113**(3): 668–673. National Academy of Sciences. doi:10.1073/pnas.1513626113.

Gao, J., Thorson, J.T., Szuwalski, C., and Wang, H.-Y. 2020. Historical dynamics of the demersal fish community in the East and South China Seas. Mar. Freshwater Res. **71**(9): 1073. doi:10.1071/MF18472.

Fisheries and Oceans Canada. 2019. Integrated Fisheries Management Plan: Groundfish Newfoundland and Labrador Region NAFO Subarea 2 + Divisions 3KLMNO.

Hobday, A.J., and Hartmann, K. 2006. Near real-time spatial management based on habitat predictions for a longline bycatch species. Fisheries Management and Ecology **13**(6): 365–380. doi:10.1111/j.1365-2400.2006.00515.x.

Hobday, A.J., Hartog, J.R., Spillman, C.M., and Alvesc, O. 2011. Seasonal forecasting of tuna habitat for dynamic spatial management. Canadian Journal of Fisheries and Aquatic Sciences **68**(5): 898–911. doi:https://doi.org/10.1139/f2011-031.

Howell, E.A., Hoover, A., Benson, S.R., Bailey, H., Polovina, J.J., Seminoff, J.A., and Dutton, P.H. 2015. Enhancing the TurtleWatch product for leatherback sea turtles, a dynamic habitat model for ecosystem-based management. Fisheries Oceanography **24**(1): 57–68. doi:10.1111/fog.12092.

Howell, E.A., Kobayashi, D.R., Parker, D.M., Balazs, G.H., and Polovina, J.J. 2008. TurtleWatch: a tool to aid in the bycatch reduction of loggerhead turtles Caretta caretta in the Hawaii-based pelagic longline fishery. Endangered Species Research **5**(2–3): 267–278. doi:10.3354/esr00096.

Knapman, P., Cook, R., and Blyth-Skyrme, R. 2020. OCI Grand Bank Yellowtail Flounder Trawl: Public Comment Draft Report June 2020. 1-180.

Knickle, D., Rose, G., 2012. Acoustic markers of Atlantic cod (*Gadus morhua*) spawning in coastal Newfoundland. Fisheries Research **129-130**:8-16.

Lindgren, F., Rue, H., and Lindström, J. 2011. An explicit link between Gaussian fields and Gaussian Markov random fields: the stochastic partial differential equation approach. Journal of the Royal Statistical Society: Series B (Statistical Methodology) **73**(4): 423–498. doi:10.1111/j.1467-9868.2011.00777.x.

Nye, J.A., Link, J.S., Hare, J.A., and Overholtz, W.J. 2009. Changing spatial distribution of fish stocks in relation to climate and population size on the Northeast United States continental shelf. Marine Ecology Progress Series **393**: 111–129. doi:10.3354/meps08220.

Perry, A.L., Low, P.J., Ellis, J.R., and Reynolds, J.D. 2005. Climate Change and Distribution Shifts in Marine Fishes. Science **308**(5730): 1912–1915. American Association for the Advancement of Science. doi:10.1126/science.1111322.

Pinsky, M.L., Worm, B., Fogarty, M.J., Sarmiento, J.L., and Levin, S.A. 2013. Marine Taxa Track Local Climate Velocities. Science **341**(6151): 1239–1242. American Association for the Advancement of Science. doi:10.1126/science.1239352.

Pitt, T.K. 1969. Migrations of American Plaice on the Grand Bank and in St. Mary's Bay, 1954, 1959, and 1961. Journal of the Fisheries Board of Canada. NRC Research Press Ottawa, Canada. doi:10.1139/f69-115.

Poloczanska, E.S., Brown, C.J., Sydeman, W.J., Kiessling, W., Schoeman, D.S., Moore, P.J., Brander, K., Bruno, J.F., Buckley, L.B., Burrows, M.T., Duarte, C.M., Halpern, B.S., Holding, J., Kappel, C.V., O'Connor, M.I., Pandolfi, J.M., Parmesan, C., Schwing, F., Thompson, S.A., and Richardson, A.J. 2013. Global imprint of climate change on marine life. Nature Climate Change **3**(10): 919–925. Nature Publishing Group. doi:10.1038/nclimate1958.

Rideout, R.M., Ings, D.W., Brattey, J., and Dwyer, K. 2015. An Assessment of the Cod Stock in NAFO Divisions 3NO. : 51.

Thorson, J.T. 2019. Forecast skill for predicting distribution shifts: A retrospective experiment for marine fishes in the Eastern Bering Sea. Fish and Fisheries **20**(1): 159–173. doi:10.1111/faf.12330.

Thorson, J.T., and Barnett, L.A.K. 2017. Comparing estimates of abundance trends and distribution shifts using single- and multispecies models of fishes and biogenic habitat. ICES Journal of Marine Science **74**(5): 1311–1321. doi:10.1093/icesjms/fsw193.

Thorson, J.T., Pinsky, M.L., and Ward, E.J. 2016. Model-based inference for estimating shifts in species distribution, area occupied and centre of gravity. Methods in Ecology and Evolution **7**(8): 990–1002. doi:10.1111/2041-210X.12567.

Tommasi, D., Stock, C.A., Hobday, A.J., Methot, R., Kaplan, I.C., Eveson, J.P., Holsman, K., Miller, T.J., Gaichas, S., Gehlen, M., Pershing, A., Vecchi, G.A., Msadek, R., Delworth, T., Eakin, C.M., Haltuch, M.A., Séférian, R., Spillman, C.M., Hartog, J.R., Siedlecki, S., Samhouri, J.F., Muhling, B., Asch, R.G., Pinsky, M.L., Saba, V.S., Kapnick, S.B., Gaitan, C.F., Rykaczewski, R.R., Alexander, M.A., Xue, Y., Pegion, K.V., Lynch, P., Payne, M.R., Kristiansen, T., Lehodey, P., and Werner, F.E. 2017. Managing living marine resources in a dynamic environment: The role of seasonal to decadal climate forecasts. Progress in Oceanography **152**: 15–49. doi:10.1016/j.pocean.2016.12.011.

Chapter 4:
Summary

Using the yellowtail flounder fishery as a case study, the overarching goal of this thesis was to incorporate interspecific bycatch species dynamics and habitat variables to identify and hindcast seasonal spatiotemporal bycatch hotspots. This thesis will assist in providing a framework for bycatch forecast models in the yellowtail flounder fishery to mitigate bycatch and increase the sustainability and economic efficiency of the fishery.

In my first chapter, I summarized the history of the yellowtail flounder fishery in 3LNO. I highlighted yellowtail flounder life history traits, stock management, stock history and bycatch problems. By doing so, I identified some of the knowledge gaps within the fishery. First, there is a knowledge gap in understanding the dynamic seasonal spatiotemporal relationships between yellowtail flounder and its bycatch species. I addressed this knowledge gap in chapter two. Second, there is a need for improved forecasts of seasonal spatiotemporal bycatch hotspots. I addressed this knowledge gap in chapter three.

In chapter two, I used interspecies relationships and habitat variables to identify distribution patterns for the yellowtail flounder and three of its bycatch species: American plaice, Atlantic cod and witch flounder, using a multispecies VAST (vector-autoregressive spatiotemporal) model. I found that that including quality habitat covariates improves the performance of my VAST multispecies distribution models. I found high spatial interspecies correlation between yellowtail flounder and the three respective bycatch species. I also identified seasonal trends in: biomass, density distribution, effective area and centre of gravity associated with all species. For example, all four species centre of gravity has shifted northwards since the moratoria in the

1990s. Also, there was range contraction patterns for yellowtail flounder and American plaice under low population levels.

I demonstrated how difficult it is to estimate overall indices such as total biomass; even at the local level there needs to be more effort into increasing the accuracy of spatiotemporal models. I recognize attempting to summarize these complex effects in a model is extremely difficult. The model framework I have presented here is a developmental point for multispecies spatiotemporal models including habitat covariates. Further research should include dissecting the influence of different habitat covariates on species distributions. Also, including different habitat covariates (such as temperature anomalies) and covariates like catchability and fishing pressures to increase the model's accuracy.

In chapter three, I used retrospective forecast models testing to evaluate the forecast ability of the model developed in chapter two. By using a retrospective forecast multispecies VAST model, I provided a framework for short-term seasonal forecasts in this region and identify dynamic bycatch hotspots to increase the efficiency and sustainability of the yellowtail flounder fishery. Overall, the further I forecasted into the future, the Pearson correlation for density estimates across all species decreased and the biomass sd increased. Also, VAST made good predictions at higher resolution (ie. density level) as the Pearson correlation for density between our full models and our predictive models is high; but at a lower resolution (ie. total biomass), the predictions are not as good as the biomass sd for each predictive model is quite large. I also identified areas with high densities of yellowtail flounder and lower densities of the other three

bycatch species in question. Thus, identifying areas where fisherman could potential fish to yield the most efficient and sustainable catch of yellowtail flounder.

Attempting to summarize these complex effects in a model is extremely difficult, and a better understanding of the drivers of spatiotemporal models including habitat covariate variation and lower trophic level interactions will improve the forecast ability. Investigation into other oceanographic and biological covariates is needed. I did not account for ontogenetic shifts in our model due to processing time constraints. Ontogenetic effects should also be separated as juveniles may have different habitat preferences than adults. Exploration into the effects of different developmental stages to account for ontogenetic shifts may affect individuals respond to climate variables effecting the predictability of the model. I was unable to run bias-correction due to time constraints and computing power; however, this may not affect the model's predictability since I only compared between model outputs. If the goal is to forecast indices for stock assessment, then bias-correction is definitely recommended. Future work should also include trying different spatial scales for forecasting to choose the optimum resolution. I used 100 knots for my VAST model as that was the largest number of knots computationally possibly with the technology that I had. Increasing the number of knots would increase the fine scale ability of the model. Exploration in developing a joint fall-spring survey model would be beneficial for bycatch management, where a one-step seasonal forecast would provide accurate bycatch hotspot predictions ie. use the Spring survey to predict the subsequent Fall bycatch hotspots.

Currently in the literature, there is a need for more spatiotemporal modelling applications to mitigate bycatch. Building upon our retrospective forecast model, future research should include VAST as a tool to project areas of bycatch hotspots in the yellowtail flounder fishery before fishing occurs. VAST has been used to predict the dynamics as forecasting future distribution shifts is important to predict interactions within and between species of 20 fish and crab species in the Eastern Bering sea of 1-, 2-, and 30 year periods, proving to be a powerful short-term forecasting tool for commercial fisheries under novel environmental conditions (Thorson 2019). By comparing VAST to other commonly used forecasting models such as habitat envelopes and annual regressions, VAST models have been shown to have the most appropriate width for forecasting intervals and explained the highest variance in poleward movement out of the three models (Thorson 2019). Therefore, VAST has the potential to be a spatiotemporal forecasting tool to mitigate bycatch in the yellowtail flounder fishery.

4.1. Bibliography

Asch, R.G. 2015. Climate change and decadal shifts in the phenology of larval fishes in the California Current ecosystem. Proc Natl Acad Sci USA **112**(30): E4065–E4074. doi:10.1073/pnas.1421946112.

Dunn, D.C., Boustany, A.M., and Halpin, P.N. 2011. Spatio-temporal management of fisheries to reduce by-catch and increase fishing selectivity. Fish and Fisheries **12**(1): 110–119. doi:10.1111/j.1467-2979.2010.00388.x.

Hall, M.A., Alverson, D.L., and Metuzals, K.I. 2000. By-Catch: Problems and Solutions. Marine Pollution Bulletin **41**(1–6): 204–219. doi:10.1016/S0025-326X(00)00111-9.

Hobday, A.J., and Hartmann, K. 2006. Near real-time spatial management based on habitat predictions for a longline bycatch species. Fisheries Management and Ecology **13**(6): 365–380. doi:10.1111/j.1365-2400.2006.00515.x.

Hobday, A.J., Hartog, J.R., Spillman, C.M., and Alvesc, O. 2011. Seasonal forecasting of tuna habitat for dynamic spatial management. Canadian Journal of Fisheries and Aquatic Sciences **68**(5): 898–911. doi:https://doi.org/10.1139/f2011-031.

Howell, E.A., Hoover, A., Benson, S.R., Bailey, H., Polovina, J.J., Seminoff, J.A., and Dutton, P.H. 2015. Enhancing the TurtleWatch product for leatherback sea turtles, a dynamic habitat model for ecosystem-based management. Fisheries Oceanography **24**(1): 57–68. doi:10.1111/fog.12092.

Howell, E.A., Kobayashi, D.R., Parker, D.M., Balazs, G.H., and Polovina, J.J. 2008. TurtleWatch: a tool to aid in the bycatch reduction of loggerhead turtles Caretta caretta in the Hawaii-based pelagic longline fishery. Endangered Species Research **5**(2–3): 267–278. doi:10.3354/esr00096.

Nye, J.A., Link, J.S., Hare, J.A., and Overholtz, W.J. 2009. Changing spatial distribution of fish stocks in relation to climate and population size on the Northeast United States continental shelf. Marine Ecology Progress Series **393**: 111–129. doi:10.3354/meps08220.

Pérez Roda, M.A., Gilman, E., Huntington, T., Kennelly, S.J., Suuronen, P., Chaloupka, M., Medley, P.A.H., and Food and Agriculture Organization of the United Nations. 2019. A third assessment of global marine fisheries discards. FAO Fisheries and Aquaculture Technical Paper No. 633. Rome, FAO. 78 pp.

Perry, A.L., Low, P.J., Ellis, J.R., and Reynolds, J.D. 2005. Climate Change and Distribution Shifts in Marine Fishes. Science **308**(5730): 1912–1915. American Association for the Advancement of Science. doi:10.1126/science.1111322.

Pinsky, M.L., Worm, B., Fogarty, M.J., Sarmiento, J.L., and Levin, S.A. 2013. Marine Taxa Track Local Climate Velocities. Science **341**(6151): 1239–1242. American Association for the Advancement of Science. doi:10.1126/science.1239352.

Thorson, J.T. 2019. Forecast skill for predicting distribution shifts: A retrospective experiment for marine fishes in the Eastern Bering Sea. Fish and Fisheries **20**(1): 159–173. doi:10.1111/faf.12330.

Appendix A: Calculating Standard Tow Area

Table A.1 Tow distance (Nm), tow duration (min) and wind spread(ft) for Engle and Campelen trawls from personal correspondence, Truong Nguyen (Department of Fisheries and Oceans Canada; truong.nguyen@dfo-mpo.gc.ca).

	Tow Distance (Nm)	Tow Duration(min)	Wing Spread(ft)
Engel	1.8	30	45
Campelen	0.8	15	55.25

The converted DFO multispecies bottom trawl data set is converted to Campelen standards.

Therefore, I calculated the Campelen area per tow by:

$$wing\ spread \rightarrow\ 55.25\ ft * \frac{0.305\ m}{1\ ft} * \frac{1\ km}{1000\ m} = 0.0168\ km$$

$$Tow\ length \rightarrow\ 0.8\ Nm * \frac{1.852\ km}{1\ Nm} = 1.482\ km$$

$$Tow\ area \rightarrow 0.0168\ km * 1.482\ km = 0.0230\ km^2$$

Therefore, I used $0.02\ km^2$ for area per tow in our VAST models.

Appendix B: Compare Traditional Log-link to Poisson-link

Historically, delta models are commonly used in fisheries for biomass sampling with lots of zeroes. Delta models are fitted to data by estimating parameters for two separate and independent generalizes linear models: one for encounter probability and one for positive catch rates. Predictions from these two generalized linear models can be multiplied together to predict local density and local abundance. Traditionally, this is done with a logit-link.

(B.1) $p(c, s, t) = logit^{-1}(n(c, s, t))$

The odds ratio is the encounter probability over non-encounter probability:

(B.2) $logit(n(c, s, t)) = \log\left(\frac{n(c,s,t)}{1-n(c,s,t)}\right)$

(B.3) $r(c, s, t) = a_i * log^{-1}(w(c, s, t))$

However, it is not easy to summarize the average effect of covariates on logit(p) on population density because this effect depends upon the value of the covariates and samples. Three draw backs to the conventional delta model include (Thorson 2017):

(1) Difficulty interpreting covariates: it has difficulties summarizing fixed and random effects for logit(p) for encounter probability as this effect depends on all covariates sample by relying on the odds ratio. The model also assumes that area swept only effects catch rates and not encounter probability. However, increase in area swept for many species will increase the probability of sampling more than one individual.

(2) Assumed independence between model comparisons: logit-link also assumes independence among components; which is not the case. For example; abundant species that have wide ranges frequently encounter species at higher densities and increase in local density will decrease the probability of failing to detect a species that is present.

Therefore, encounter probability and positive catch rates are not independent, but in reality are related.

(3) Biologically implausible form when removing covariates: for example, a covariate representing local density of eel grass might be slated for group density but not for average weight. Thus a reduction in the # of estimated parameters still retains a biologically meaningful impacts on eel grass on both encounter probability and catch rates.

Therefore, I use a poison-link function with a Tweedie Distribution as it solves these three problems.

The poisson-link delta model (Equations 4 & 5) decreases residual spatial variation, improves fit and estimates covariates that are similar and biologically interoperable (Thorson 2017). Predicted encounter probability pi is defined in the Poisson-link delta model given the assumption that individuals are randomly distributed in the geographic sampling area, such that he probability of encountering at least on individual is:

(B.4) $p(c, s, t) = 1 - \exp(-\alpha \times n(c, s, t))$

Where α_i is the area sampled (area swept by each operation of a bottom trawl sample) for the ith sample. Predicted biomass density for positive encounter rates r_i is defined from the biomass:

$$(B.5)\ r(c,s,t) = \frac{\alpha \times n(c,s,t)}{p(c,s,t)} \times w(c,s,t)$$

Bibliography

Thorson, J. 2017. Three problems with the conventional delta-model for biomass sampling data, and a computationally efficient alternative. Canadian Journal of Fisheries and Aquatic Sciences **75**. doi:10.1139/cjfas-2017-0266.

Appendix C: Fall Atlantic Cod 2J3KL and 3NO

The Div. 3LNO yellowtail flounder fishery intersects two stocks of Atlantic Cod, Div. 2J3KL and Div. 3NO. Therefore, to understand the distribution shifts (especially in the Fall) in Atlantic cod in the Div. 3LNO multispecies model, I ran a Fall VAST for Atlantic cod Div. 2J3KL and Div. 3NO with no habitat covariates to represent the two stocks of Atlantic cod that intersect our model (I used fine_scale= FALSE, with 100 knots). The spring DFO multi species bottom trawl survey data that I had was incomplete and only included survey data from Div. 3L and not Div. 2J3K, therefore I did not include the results of the Spring VAST for comparison.

In our multispecies model I observed Atlantic cods centre of gravity shifting northward the fastest of the four species in the Fall from about 2005 - 2018. This shift could be because the Div. 2J3KL stock is recovering faster than the Div. 3NO stock for unknown reasons. The Div. 2J3KL stock is highly migratory as they overwinter near the edge of the continental shelf and spend spring and summers in shallow waters along the coast onto the plateau of the grand banks (Fisheries and Oceans Canada 2019). By the 1990s off shore overwintering components were barely detectable; aggregations inshore in Div. 3L and southern 3K (Fisheries and Oceans Canada 2019). Inshore stock productivity is greater than offshore productivity (Fisheries and

Oceans Canada 2019). Offshore biomass of cod has increased in most stock areas in the past decade except in southern Div. 3L (Fisheries and Oceans Canada 2019).

The Atlantic cod Div. 3NO stock stays in the shallower parts of the banks in summer particularity the SE shoal in 3N, and the slopes of the Banks in the winter when cooling occurs (Fisheries and Oceans Canada 2019). There is some seasonal mixing between Div. 3O and Div. 3Ps. The stock biomass is widely distributed in the fall (Fisheries and Oceans Canada 2019). Spring biomass abundance is low in both Div. 3N and Div. 3O from 1994 to 2006 and the biomass is increasing in Div. 3N since 2011(Fisheries and Oceans Canada 2019). Moratorium is still in place for Div. 3NO stock since 1995. 95% of the total Canadian catch of Atlantic cod Div. 3NO is taken by the Div. 3LNO Yellowtail flounder fishery in 2013-2014 (Rideout et al. 2015).

According to our Fall Atlantic cod single species VAST results, the Div. 2J3KL stock's centre of gravity is moving northward (Figure C.1 & C.2), whereas the Div. 3NO stock is staying in relatively the same spot in Div. 3N over the time period (Figure C.3 & C.4). This is cohesive with what is in the literature as explained above.
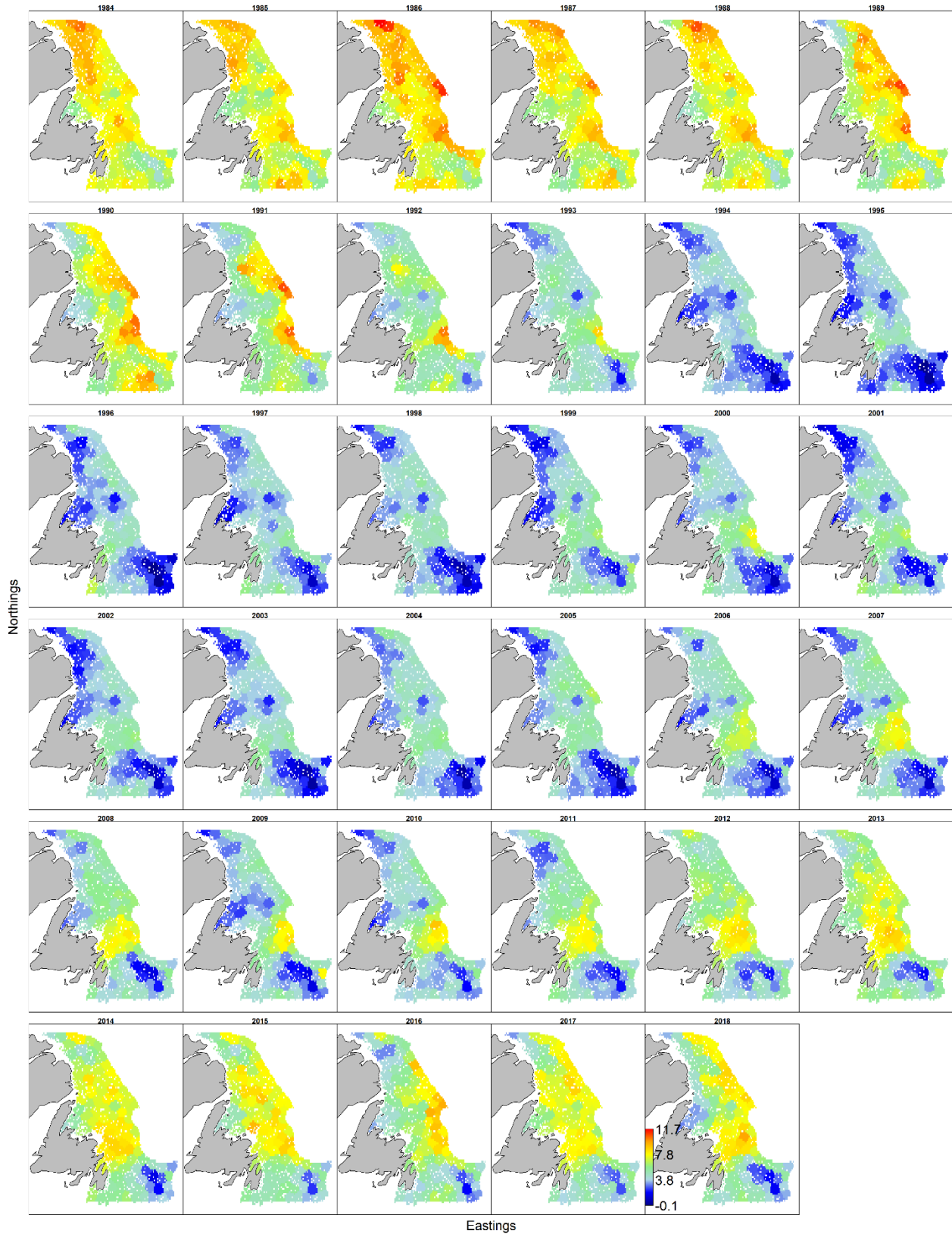
Figure C.1 Density distribution plot for the Atlantic cod stock in Div. 2J3KL during the Fall,

1984-2018, from VAST. White cells indicate areas where no tows were done over the time series.
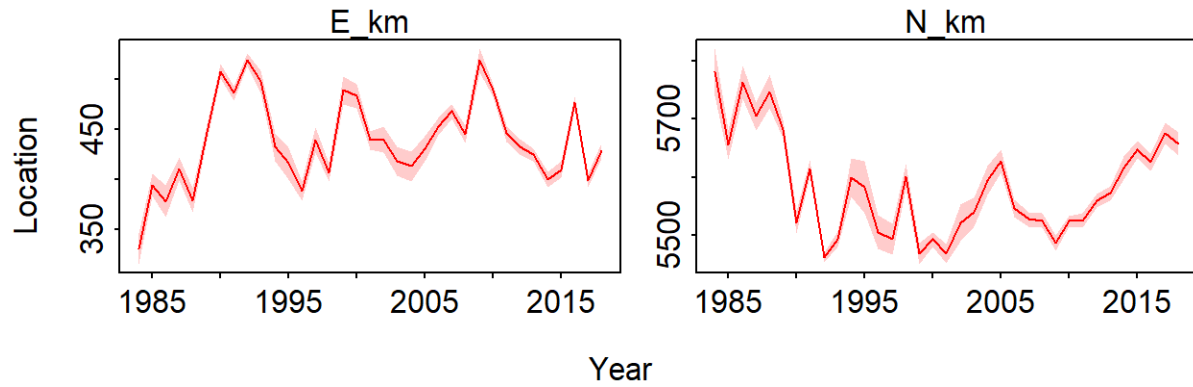
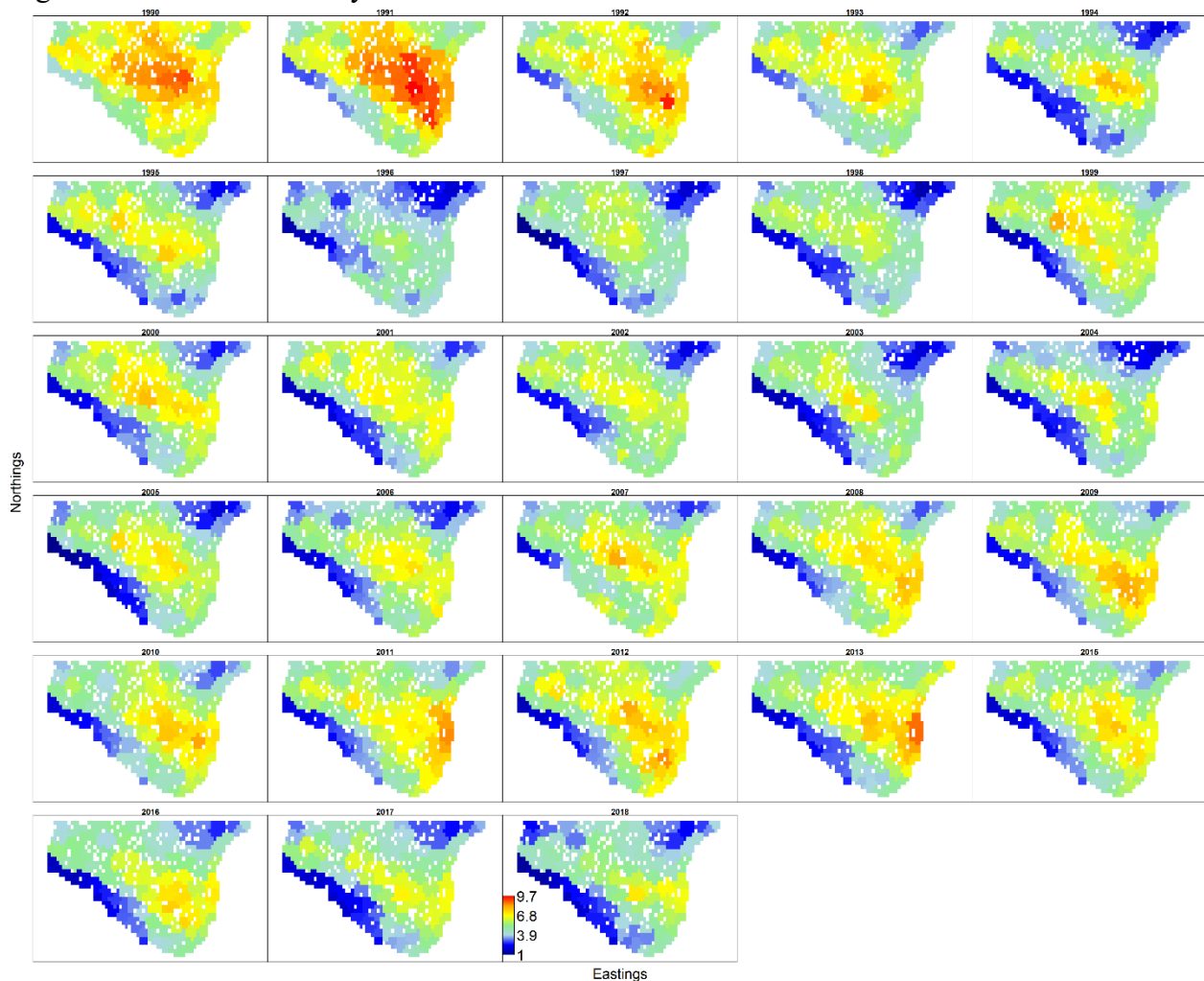Figure C.2 Centre of Gravity for the Atlantic cod Div. 2J3KL for Fall 1984-2018 from VAST.

Figure C.3 Density distribution plot for Atlantic cod Div. 3NO for Fall 1984-2018 from VAST. White cells indicate areas where no tows were done over the time series.
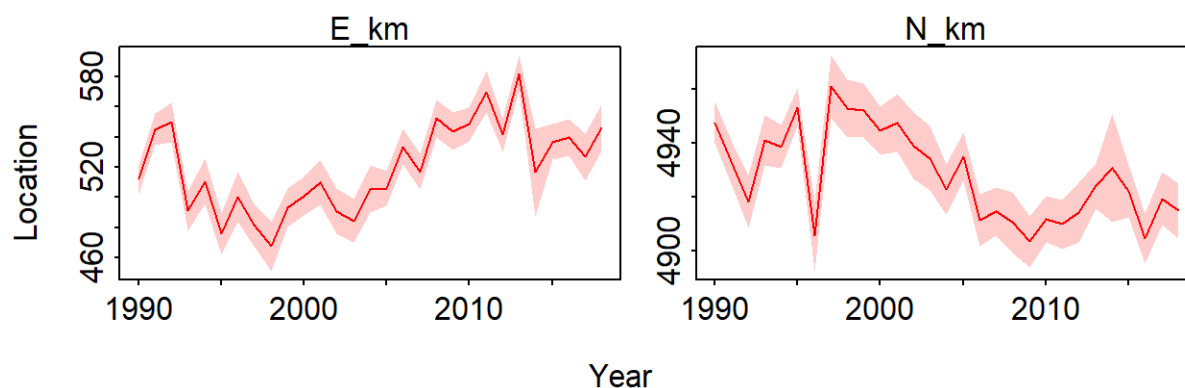
Figure C.4 Centre of Gravity for Atlantic cod Div. 3NO for Fall 1984-2018 from VAST.

Bibliography

Fisheries and Oceans Canada. 2019. Integrated Fisheries Management Plan: Groundfish Newfoundland and Labrador Region NAFO Subarea 2 + Divisions 3KLMNO.

Rideout, R.M., Ings, D.W., Brattey, J., and Dwyer, K. 2015. An Assessment of the Cod Stock in NAFO Divisions 3NO.51.

Appendix D: Fall Witch Flounder 2J3KL and 3NO

The Div. 3LNO yellowtail flounder fishery intersects two stocks of witch flounder in Div. 2J3KL and Div. 3NO. Therefore, to understand the distribution shifts (especially in the Fall) in witch flounder in the Div. 3LNO multispecies model, I ran a Fall VAST for witch flounder Div. 2J3KL and Div. 3NO with no habitat covariates to represent the two stocks of witch flounder that intersect our model (I used fine_scale= FALSE, with 100 knots). The spring DFO multi species bottom trawl survey data that I had was incomplete and only included survey data from Div. 3L and not Div. 2J3K, therefore I did not include the results of the Spring VAST for comparison.

In our multispecies model I observed witch flounder centre of gravity shifting northward in the Fall from about 2005 -2018. Div. 2J and Div. 3L biomass indices have been showing an overall increase since 2004 and reached a high in 2015. Div. 3K generally accounts for the majority of

the biomass for this stock with an average of 51% being located in this division from 1983-2017 (Wheeland et al. 2019). By the early 1990'distrubiton was limited to very small catches along the continental shelf slope, and more to the southern area of the stock boundary (Wheeland et al. 2019). As the biomass indices have increased over the last several years, a redistribution of the stock has been observed, with biomass once again spread across portions of the shelf and deeper channels primarily in 3K, in addition to the slope waters (Wheeland et al. 2019).The distribution of Div. 2J3KL biomass by depth favours deep waters towards the northern extent of the stock area (Wheeland et al. 2019).

There was no directed fishery on witch flounder Div. 3NO 1994-2014 with a moratorium placed in 1995 (Wheeland et al. 2019). Spring Div. 3NO stock indices are variable are primarily driven by the overall higher abundance and biomass in Div. 3O(Wheeland et al. 2019). It is likely that some witch flounder may be distributed outside the survey area (too deep), particularly in the spring, following spawning in deeper waters contributing to variability in survey estimates (Wheeland et al. 2019). Fall Div. 3NO stock indices are less variable with a generally increasing trend in biomass and abundance from 1997-2004 and have increased or remained stable since 2016. Div. 3O also dominates the majority of the biomass estimates in the fall surveys (83% on average) (Brodie 2019).

According to my VAST results, the Div. 2J3KL stock's centre of gravity is moving slightly northward (dominated by 2J and 3K) (Figure D.1 & D.2), whereas the Div. 3NO stock is staying in relatively the same spot over the time period (dominated by 3O) (Figure D.3 & D.4). This is cohesive with what is in the literature as explained above.
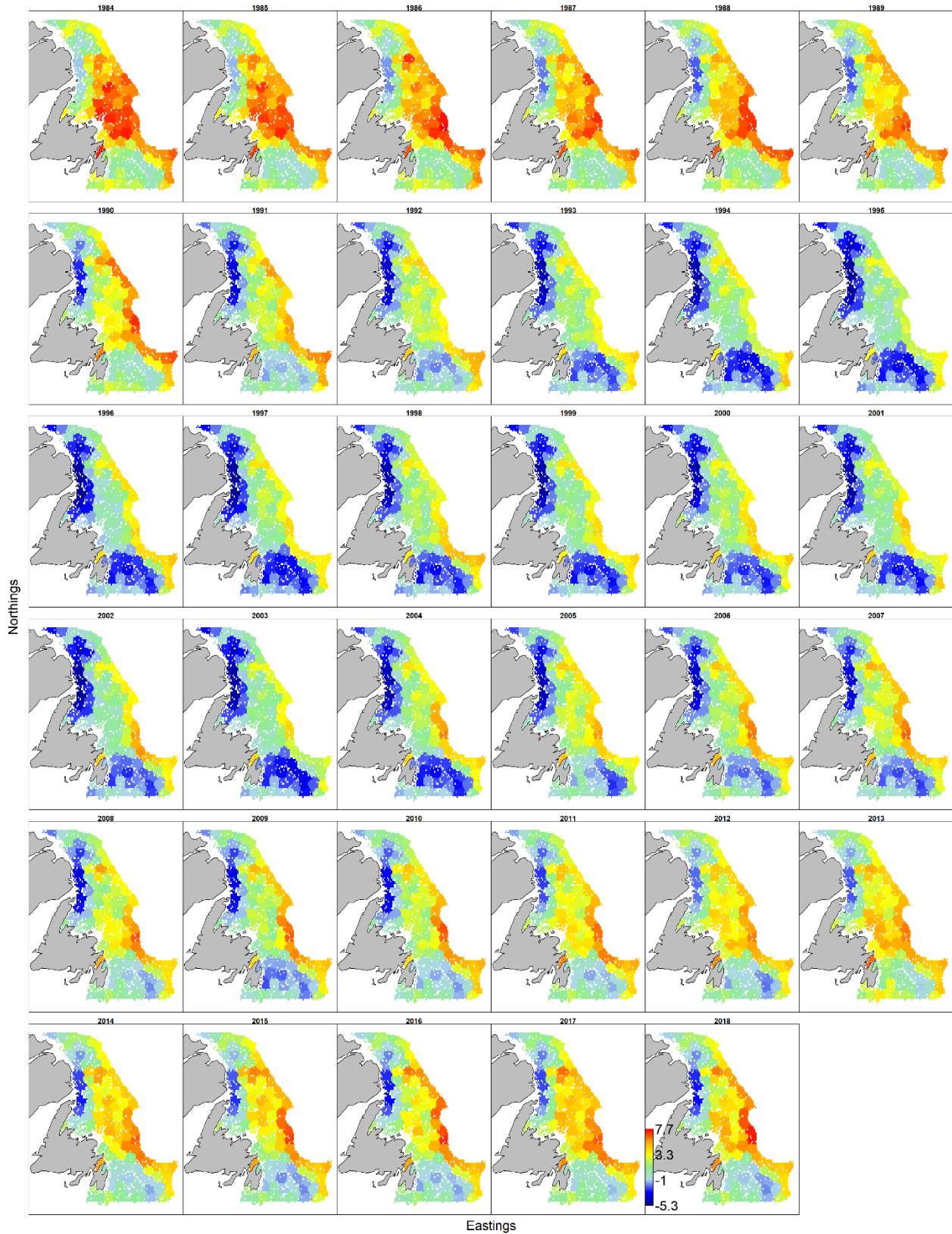
Figure D.1 Density distribution plot for witch flounder Div. 2J3KL for Fall 1984-2018 from VAST. White cells indicate areas where no tows were done over the time series.
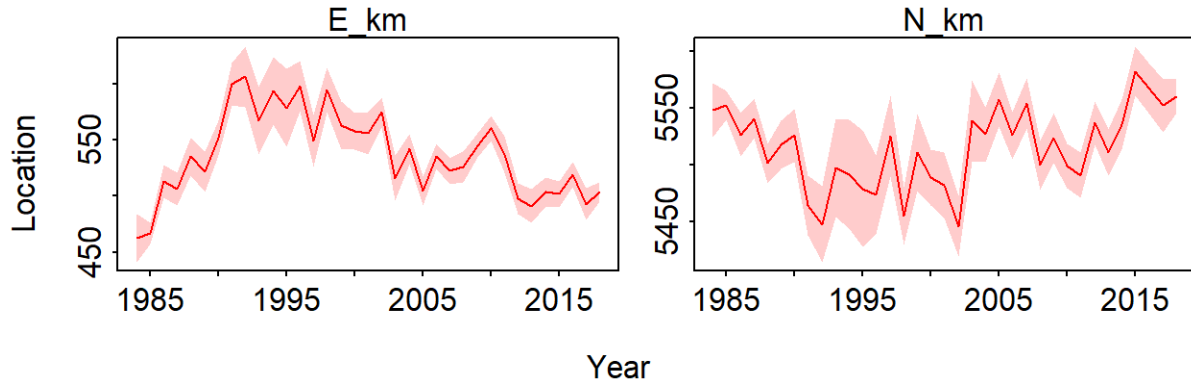
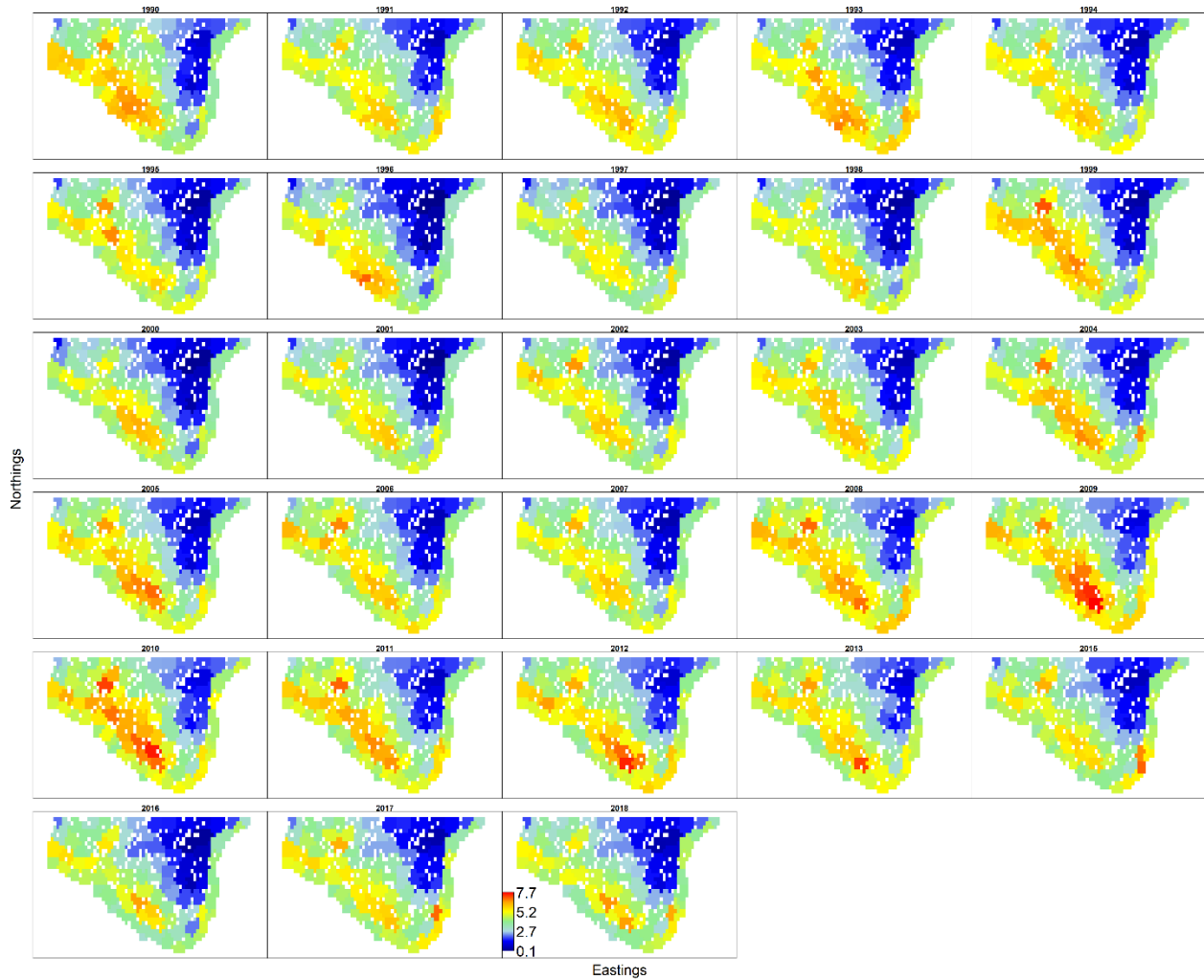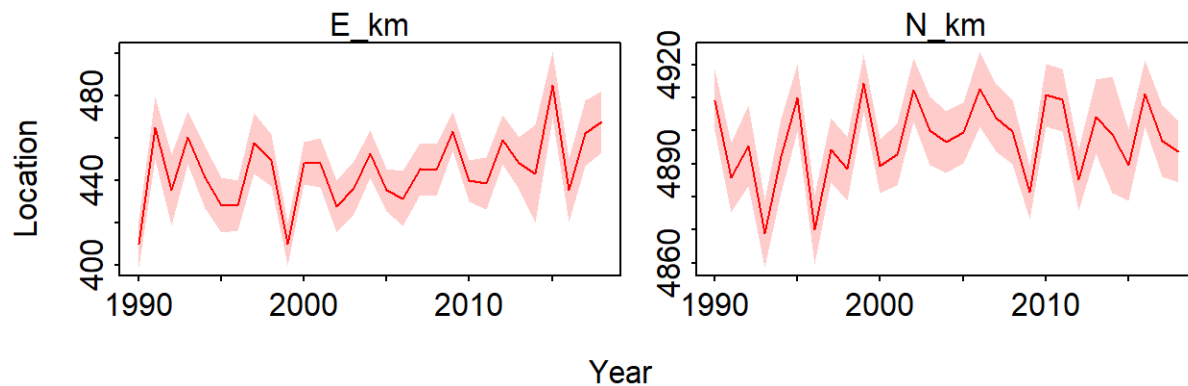Figure D.2 Centre of Gravity for witch flounder Div. 2J3KL for Fall 1984-2018 from VAST.

Figure D.3 Density distribution plot for witch flounder Div.3NO for Fall 1984-2018 from VAST. White cells indicate areas where no tows were done over the time series.

Figure D.4 Centre of Gravity for witch flounder Div. 3NO for Fall 1984-2018 from VAST.

Bibliography

Brodie, W. 2019. An assessment of the witch flounder resource in NAFO Divisions 3NO. : 35.

Wheeland, L., Rogers, B., Rideout, R., and Maddock Parsons, D. 2019. Assessment of Witch
    Flounder (*Glyptocephalus cynoglossus*) NAFO Divisions 2J3KL. Canadian Science
    Advisory Secretariat(CSAS) Research Document 2019/066, St. John's NL.

Appendix E: Habitat Covariates

My thesis used habitat covariates to make my model predictions stronger. Bottom temperature, depth, and substrate type had significant effects on my model (Table 2.4). Relating habitat variables to trends in species distribution was not the goal of my thesis and warrants further research. However, I did some preliminary investigation into these relationships.

I have included plots of the raw trawl catch data (kg) for each species vs. bottom temperature (Figure E.1 & 2), bottom depth (Figure E.3 & 4) and substrate type (Figure E.5 & 6) for both Fall and Spring. These plots do not account for spatiotemporal variation. These plots show variations between seasons and species that require further investigation. I also plotted the

bottom temperature (Figure E.7 & 8), depth (Figure E.9 & 10) and substrate (Figure E.11 & 12) corresponding to each tow location for both Fall and Spring. Depth and substrate are static habitat covariates; however, the tow locations were different between the Fall and Spring which is why I decided to plot both separately. Bottom temperature appears to be warmest on the edges and south part of the Grand Bank (Figure E.7 & 8). The deepest parts of the Grand Bank appear to be around the edges (Figure E.9 & 10). There appears to be no apparent pattern with substrate type on the Grand Banks at this scale (Figure E.11 & 12).

I cannot define the suitable spatiotemporal habitat variables for each species using a VAST model. That is beyond the scope of my thesis and would require additional modelling. However, I do recognize that the strong interspecies correlation (Figure 2.5 & 2.6) hint that the species may be occupying similar habitats. I created habitat covariate performance curves (Figure E.13-15) using the estimates found in Table 2.5 & 2.6 and arbitrary habitat covariate values. Some of the values of the habitat covariate performance curves (Figure E.13-15) between species cover similar ranges in covariates suggesting similar preference in habitat. These overlaps differ by season, linear predator, habitat variable and species. The performance curves are difficult to disentangle because the covariate effects are separated by linear predictor. Additionally, they do not represent dynamic spatiotemporal effects which is the focus of my thesis. These relationships should be further investigated.
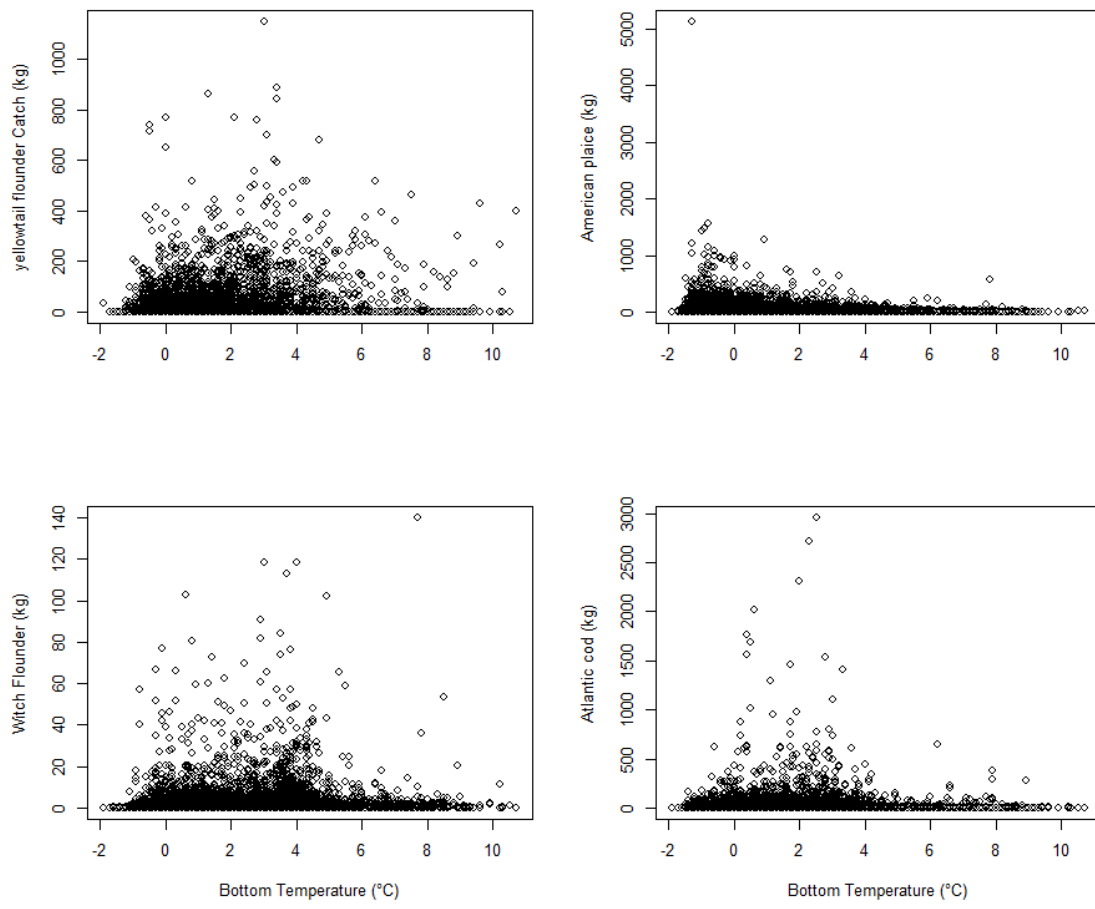
Figure E.1 Fall bottom water temperature in NAFO Div. 3LNO for 1984-2018 for the DFO multispecies bottom trawl survey data used in the VAST model for all four species.
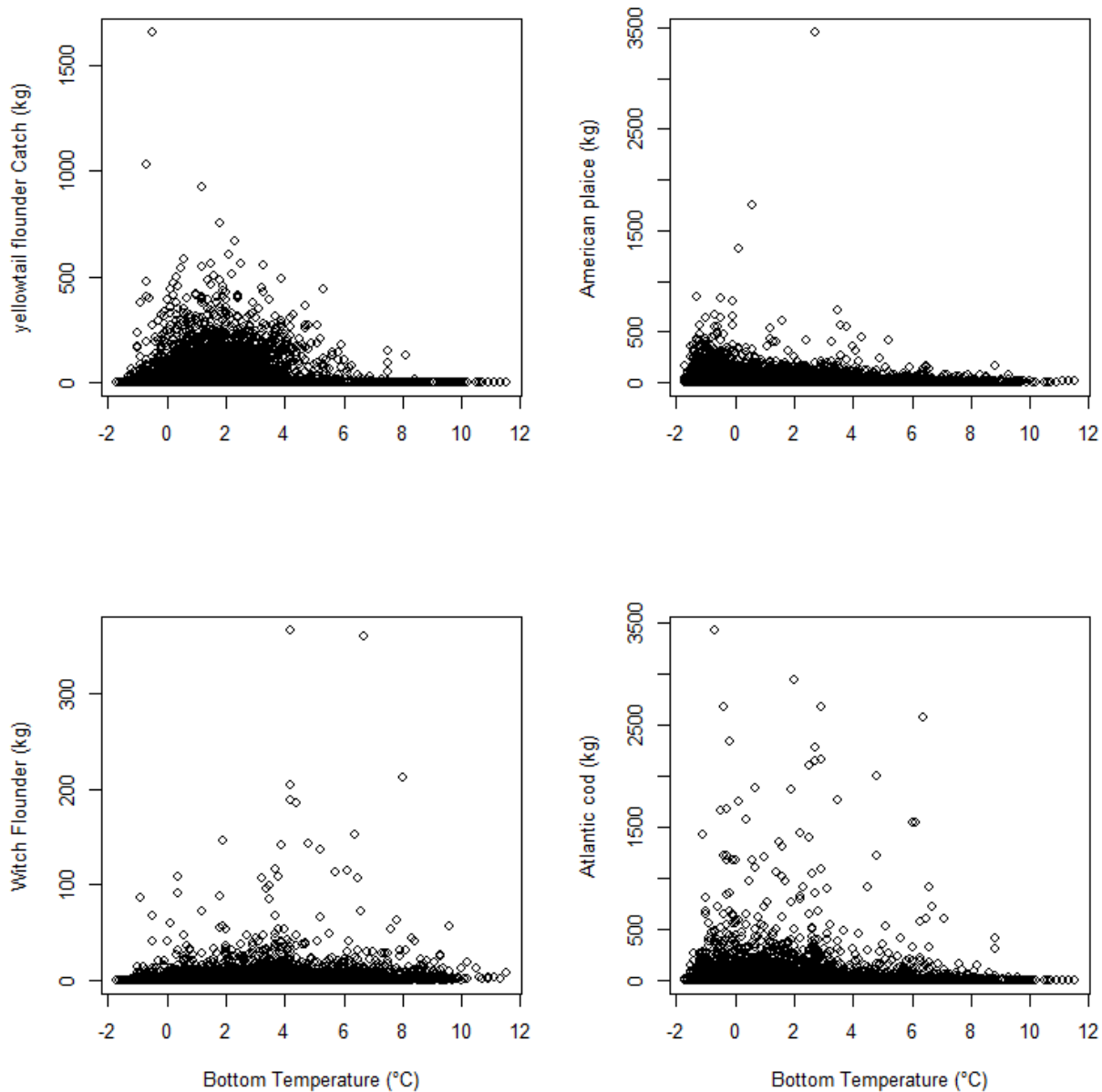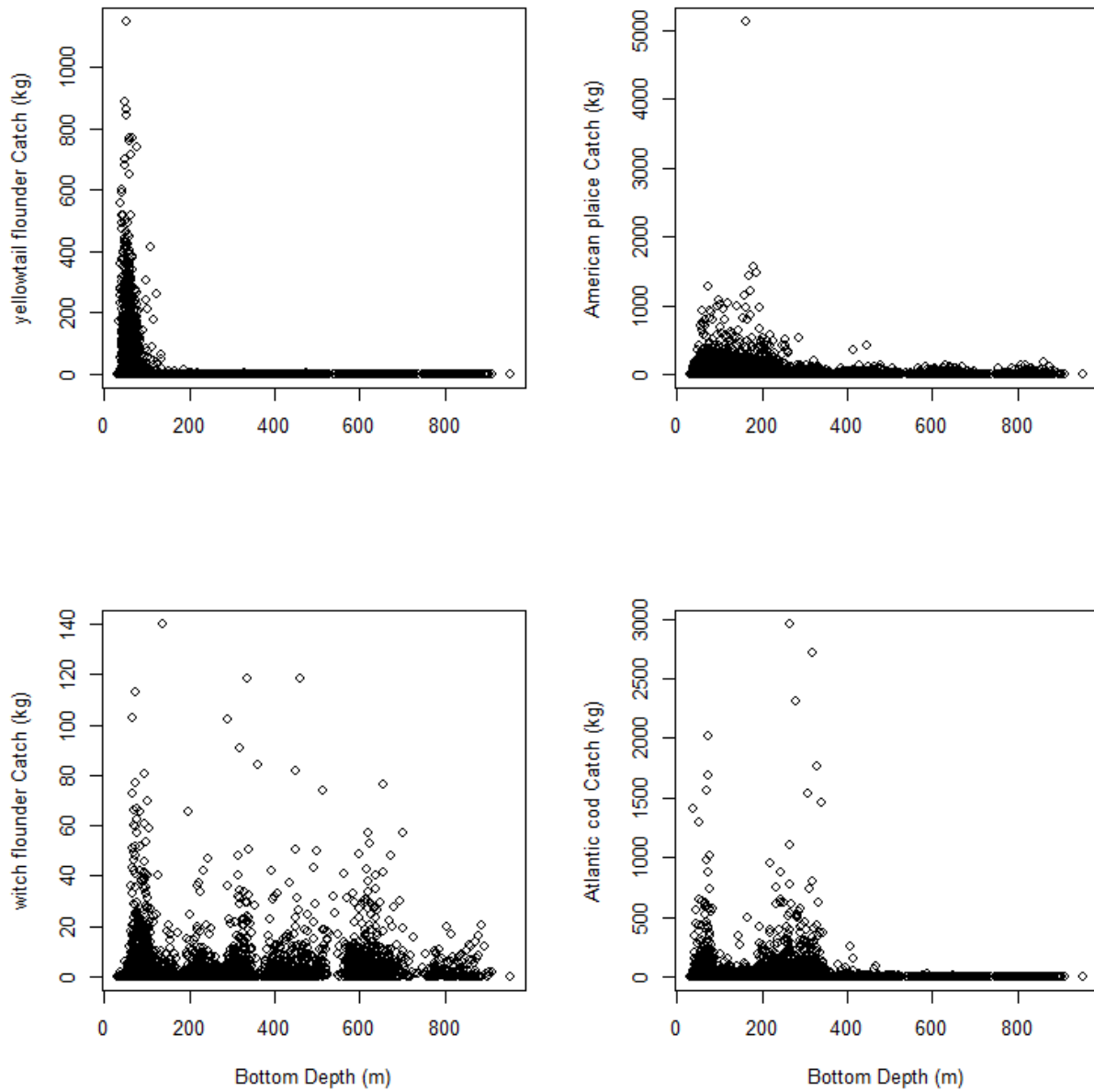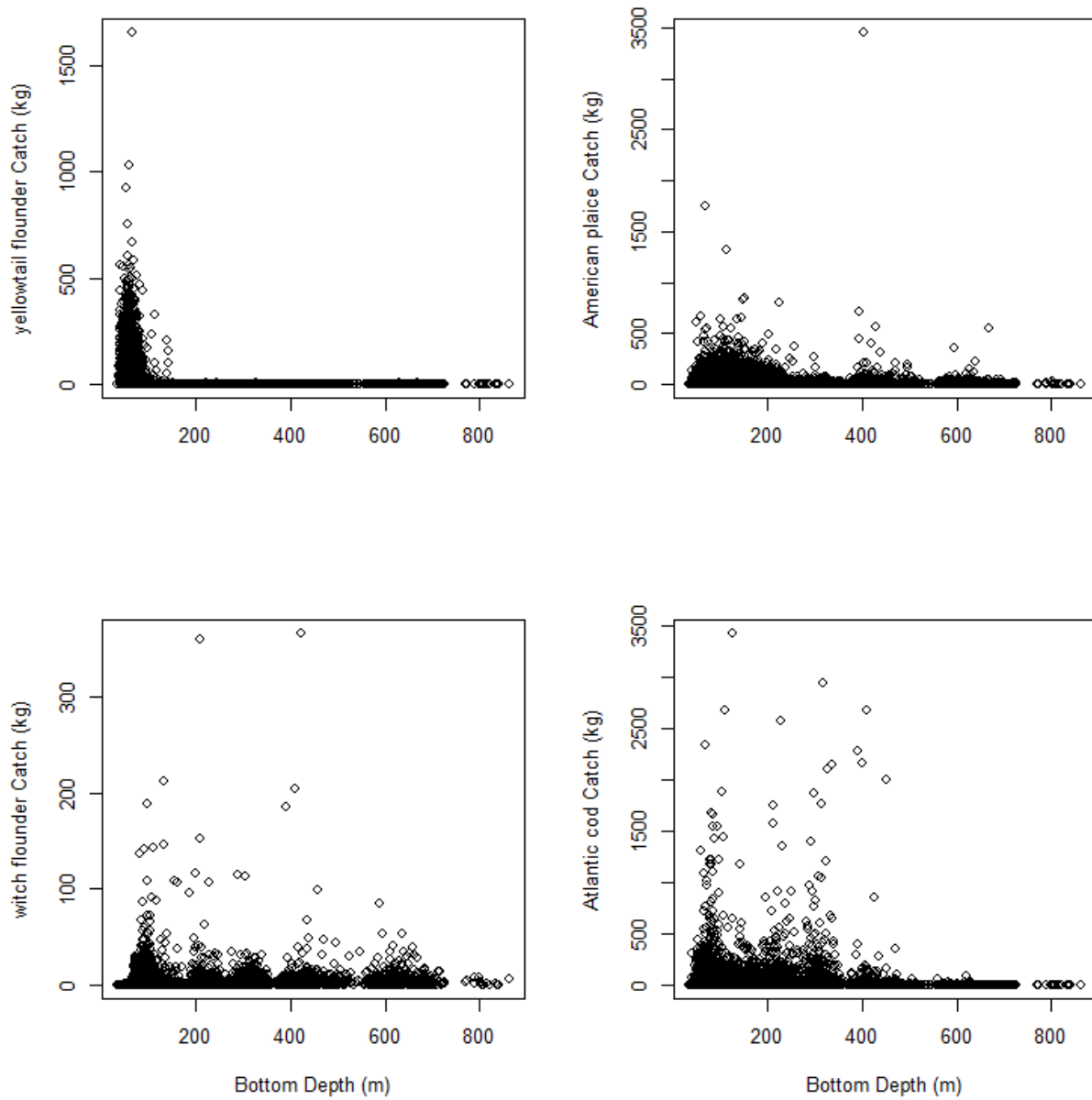
Figure E.2 Spring bottom water temperature in NAFO Div. 3LNO for 1984-2018 for the DFO multispecies bottom trawl survey data used in the VAST model for all four species

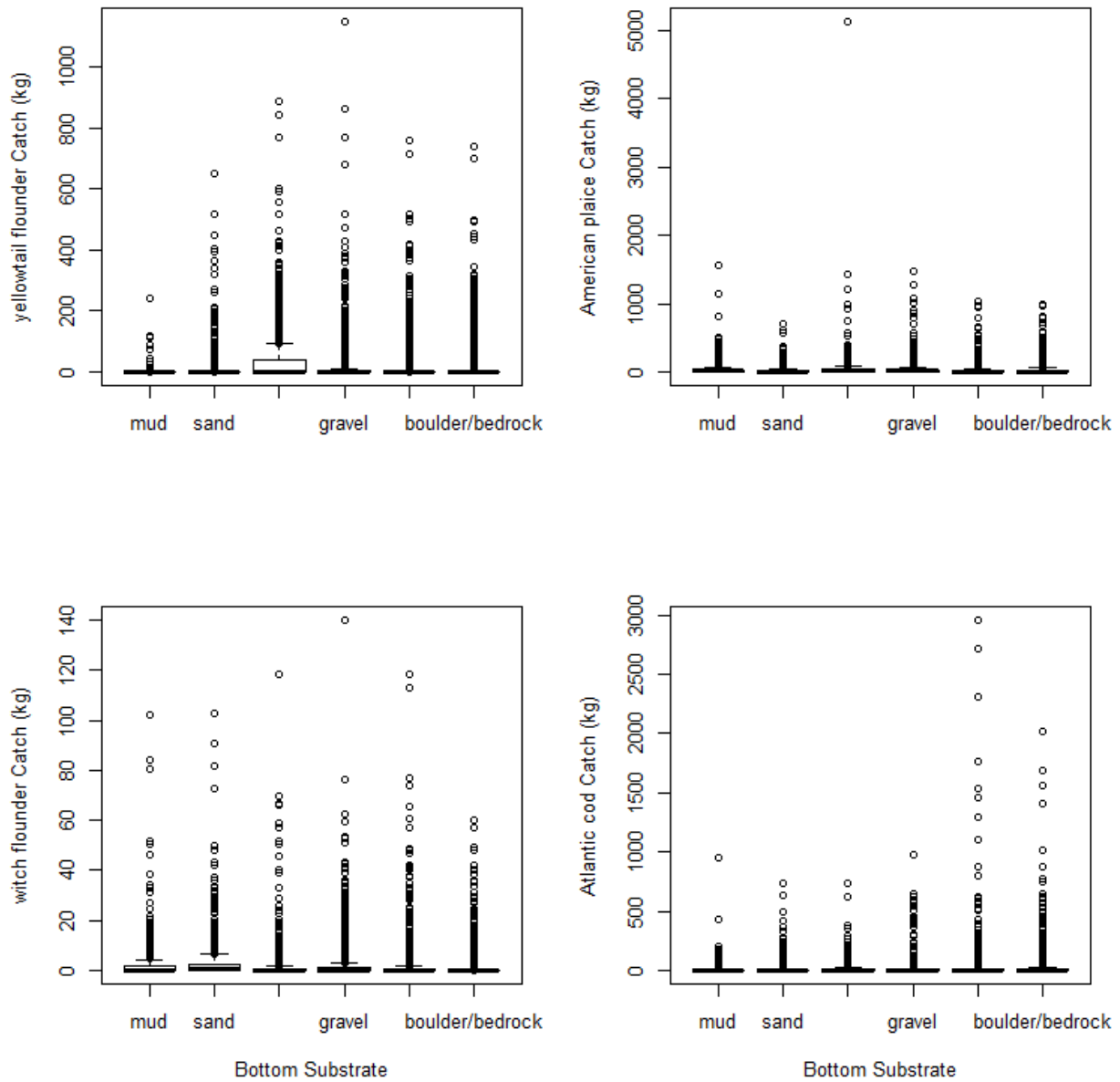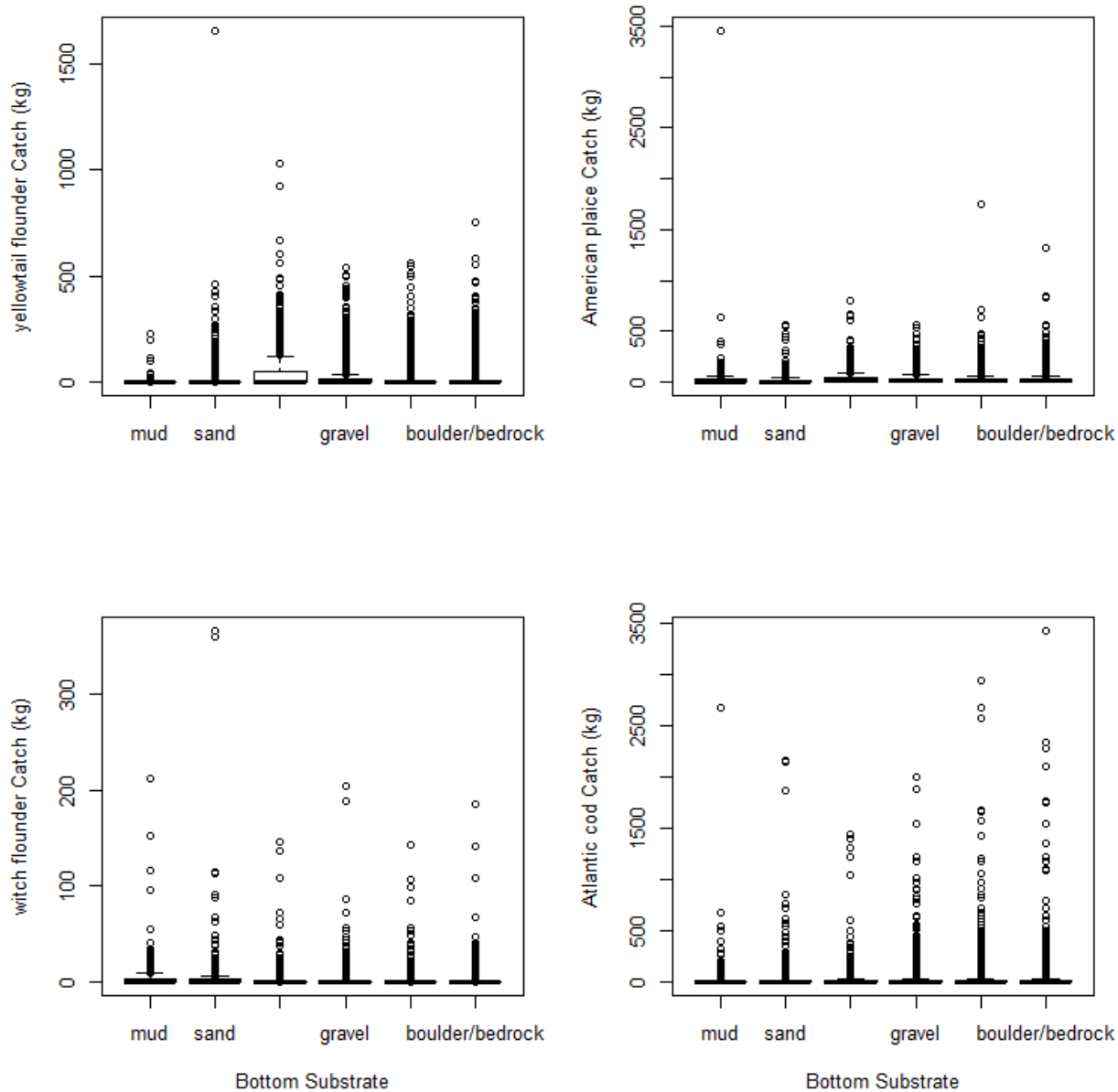Figure E.3 Fall bottom depth in NAFO Div. 3LNO for 1984-2018 for the DFO multispecies bottom trawl survey data used in the VAST model for all four species

Figure E.4 Spring bottom depth in NAFO Div. 3LNO for 1984-2018 for the DFO multispecies bottom trawl survey data used in the VAST model for all four species

Figure E.5 Fall substrate type in NAFO Div. 3LNO for 1984-2018 for the DFO multispecies bottom trawl survey data used in the VAST model for all four species

Figure E.6 Spring substrate type in NAFO Div. 3LNO for 1984-2018 for the DFO multispecies bottom trawl survey data used in the VAST model for all four species
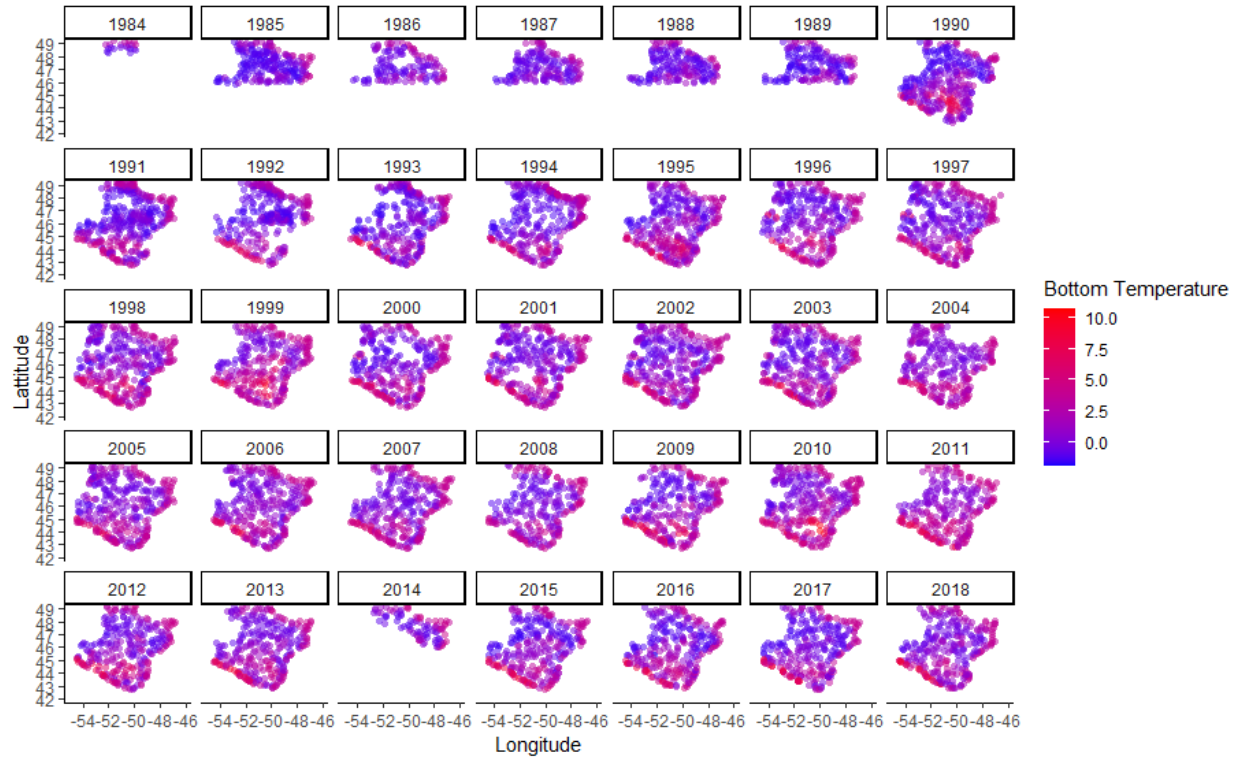
Figure E.7 Fall bottom temperature for all DFO multispecies bottom trawls inputted into the VAST model for 1984-2018 NAFO Div. 3LNO.
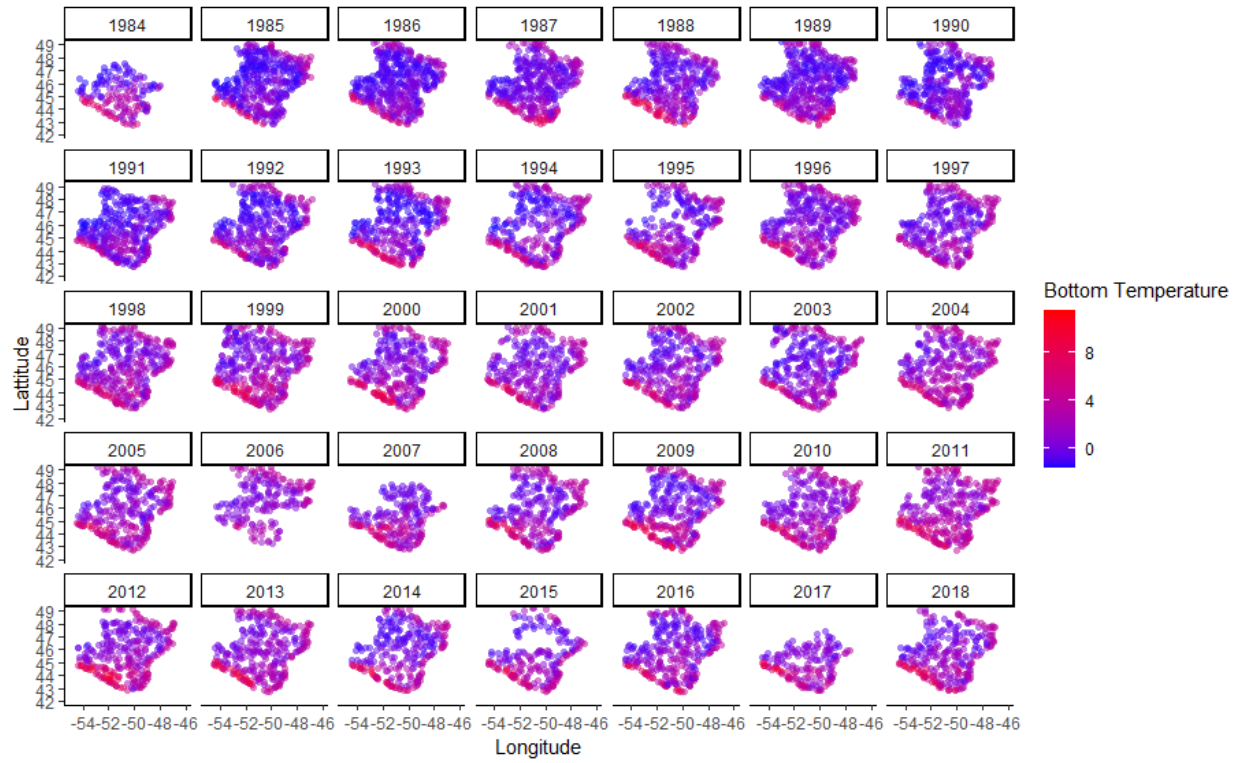
Figure E.8 Spring bottom temperature for all DFO multispecies bottom trawls inputted into the VAST model for 1984-2018 NAFO Div. 3LNO.
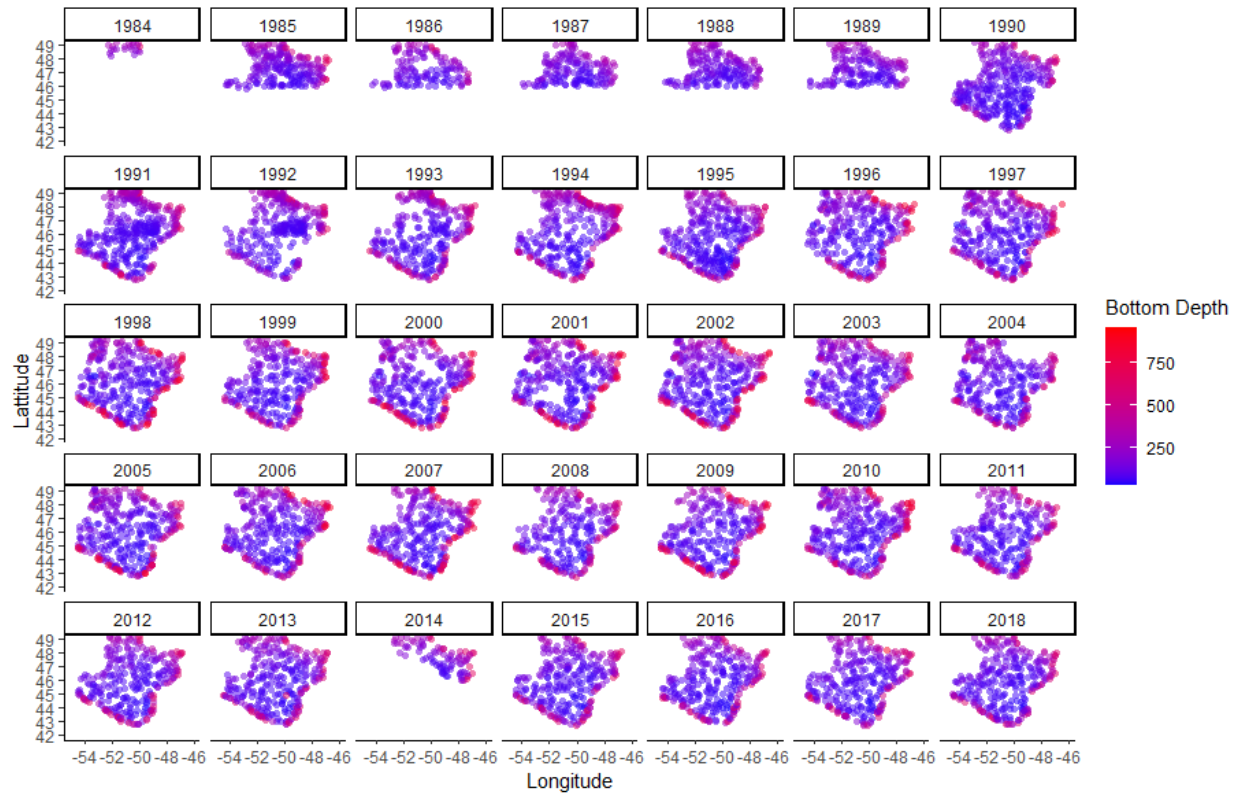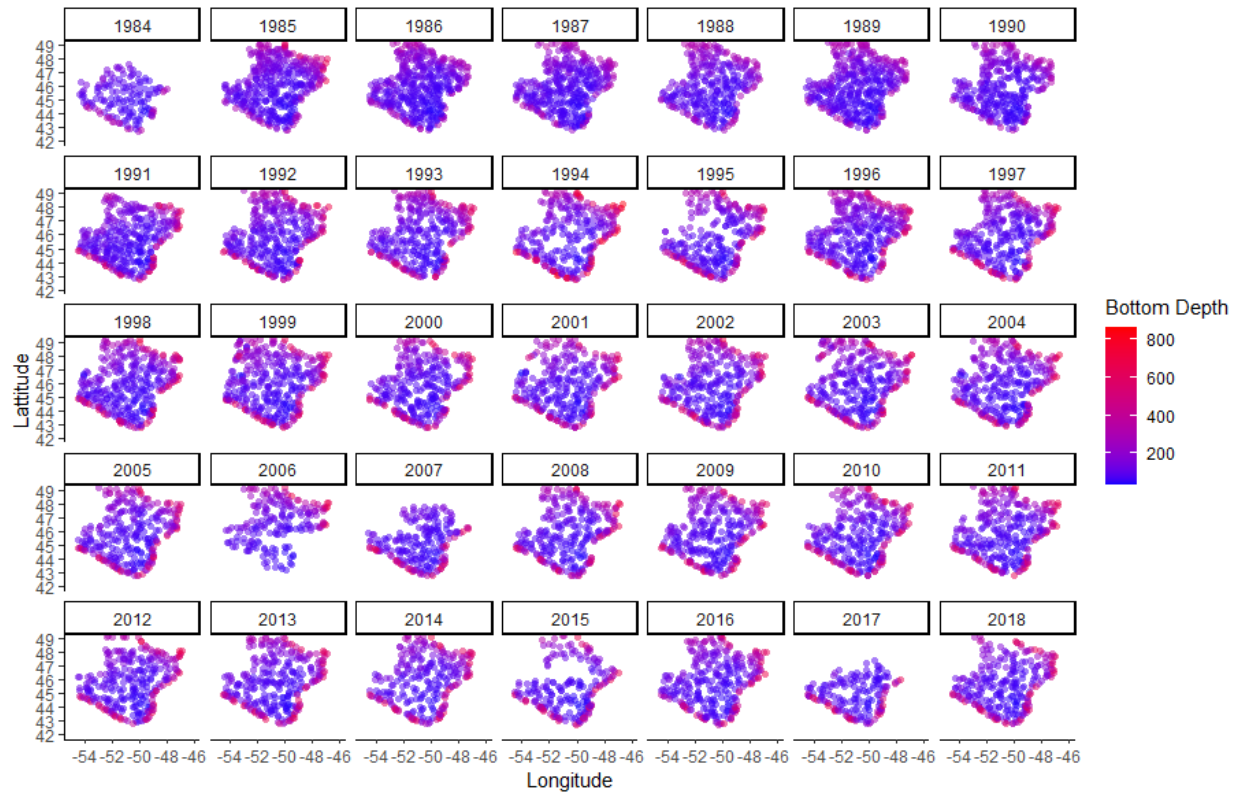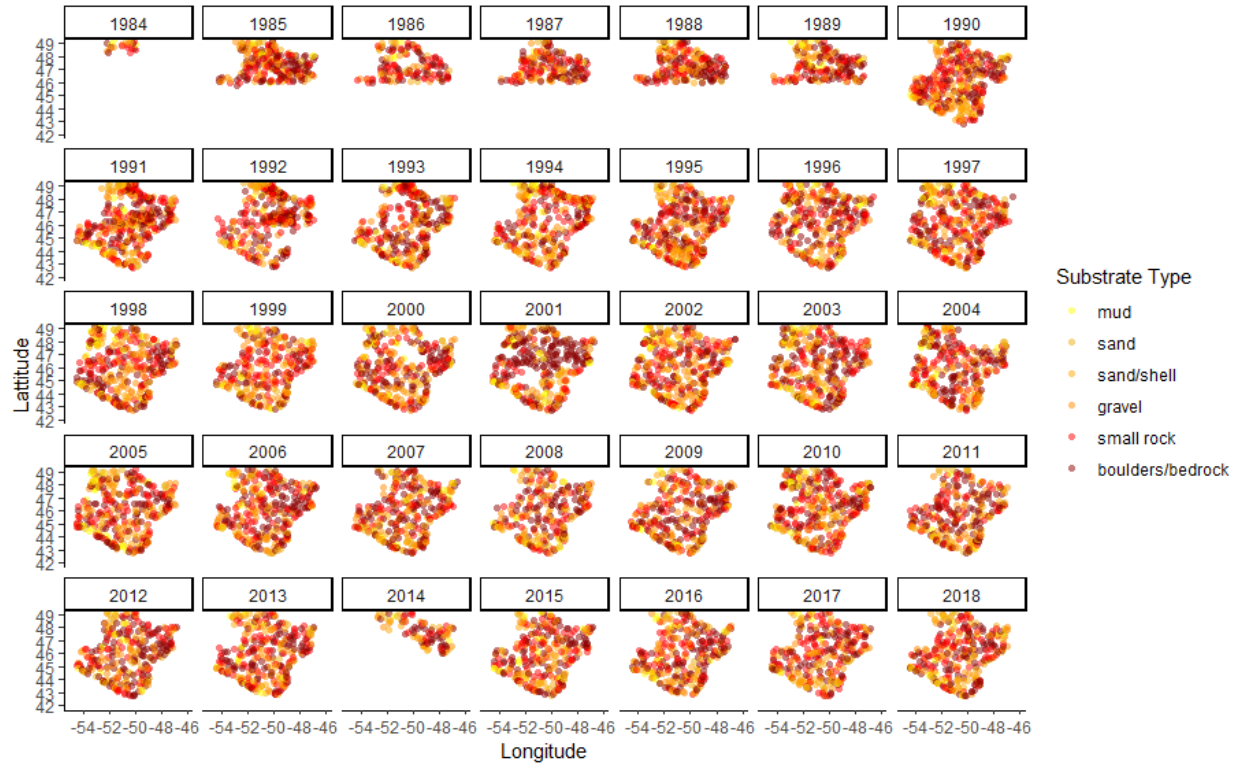
Figure E.9 Fall bottom temperature for all DFO multispecies bottom trawls inputted into the VAST model for 1984-2018 NAFO Div. 3LNO.

Figure E.10 Spring bottom depth for all DFO multispecies bottom trawls inputted into the VAST model for 1984-2018 NAFO Div. 3LNO.

Figure E.11 Fall substrate type for all DFO multispecies bottom trawls inputted into the VAST model for 1984-2018 NAFO Div. 3LNO.
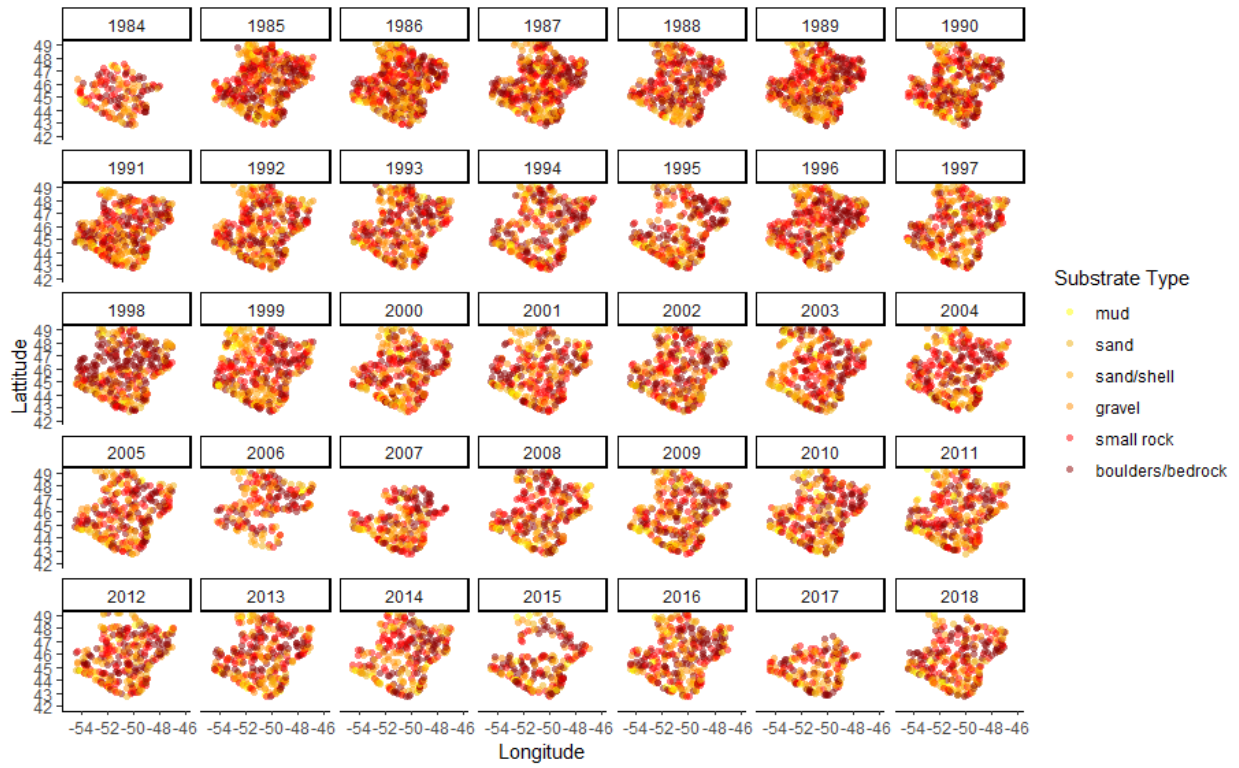
Figure E.12 Spring substrate type for all DFO multispecies bottom trawls inputted into the VAST model for 1984-2018 NAFO Div. 3LNO.
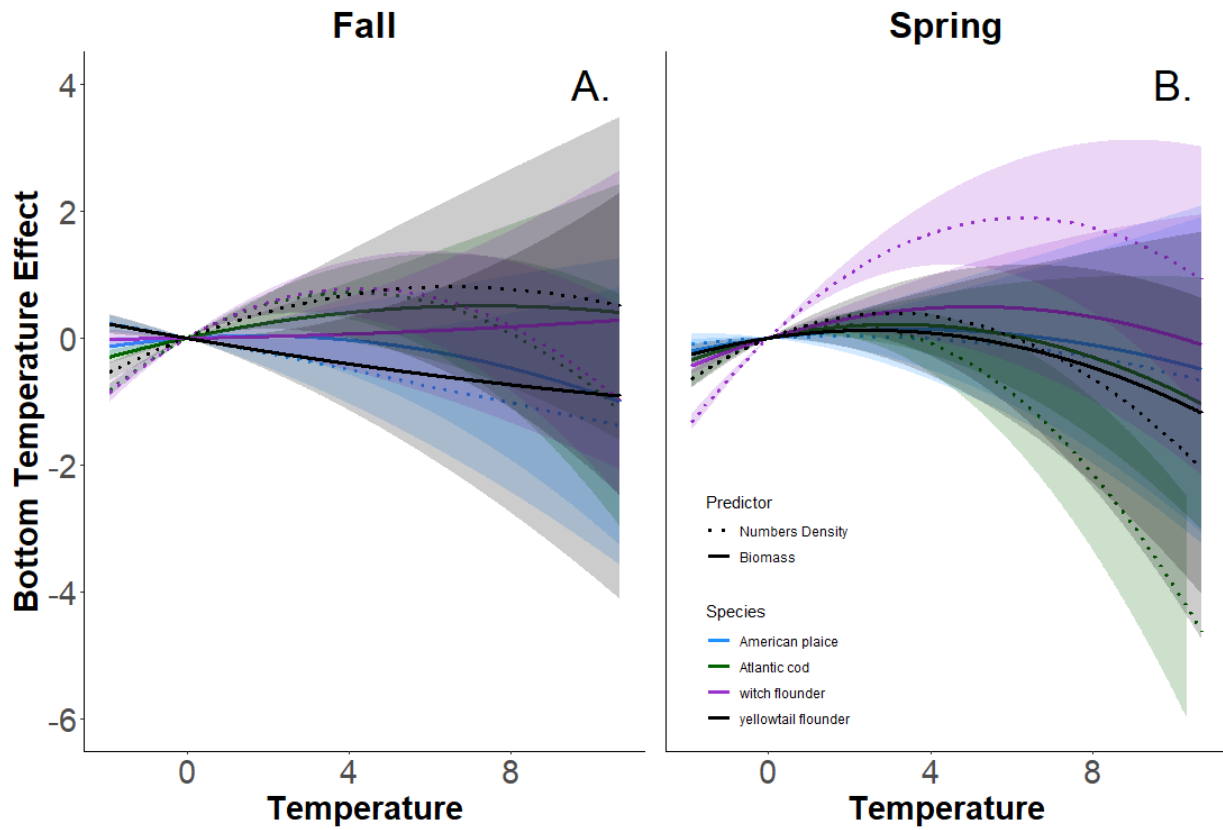
Figure E.13 Performance curves for bottom temperature effect on American plaice, Atlantic cod, witch flounder and yellowtail flounder for (A) Fall and (B) Spring in NAFO Div. 3LNO for 1984-2018 for the first (numbers density) and second (biomass) linear predictors of the VAST model.
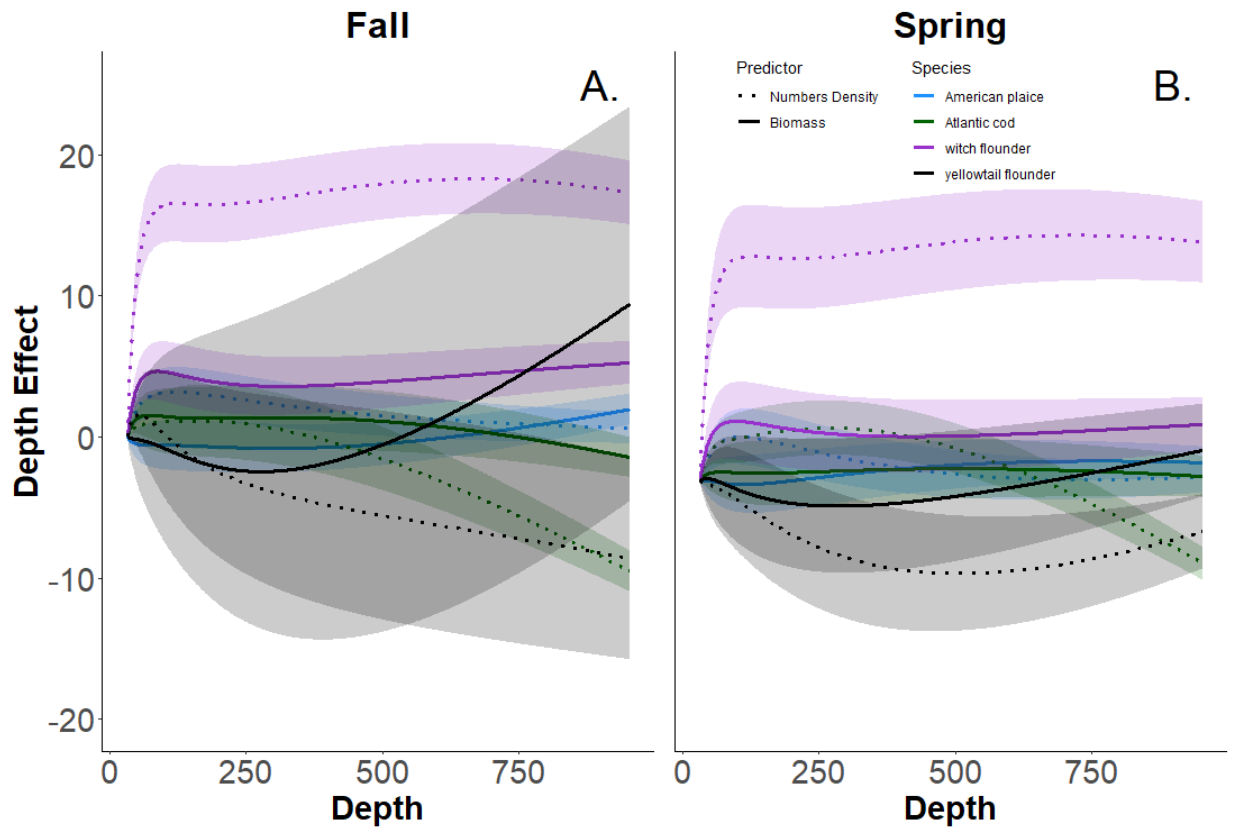
Figure E.14 Performance curves for depth effect on American plaice, Atlantic cod, witch flounder and yellowtail flounder for (A) Fall and (B) Spring in NAFO Div. 3LNO for 1984-2018 for the first (numbers density) and second (biomass) linear predictors of the VAST model.
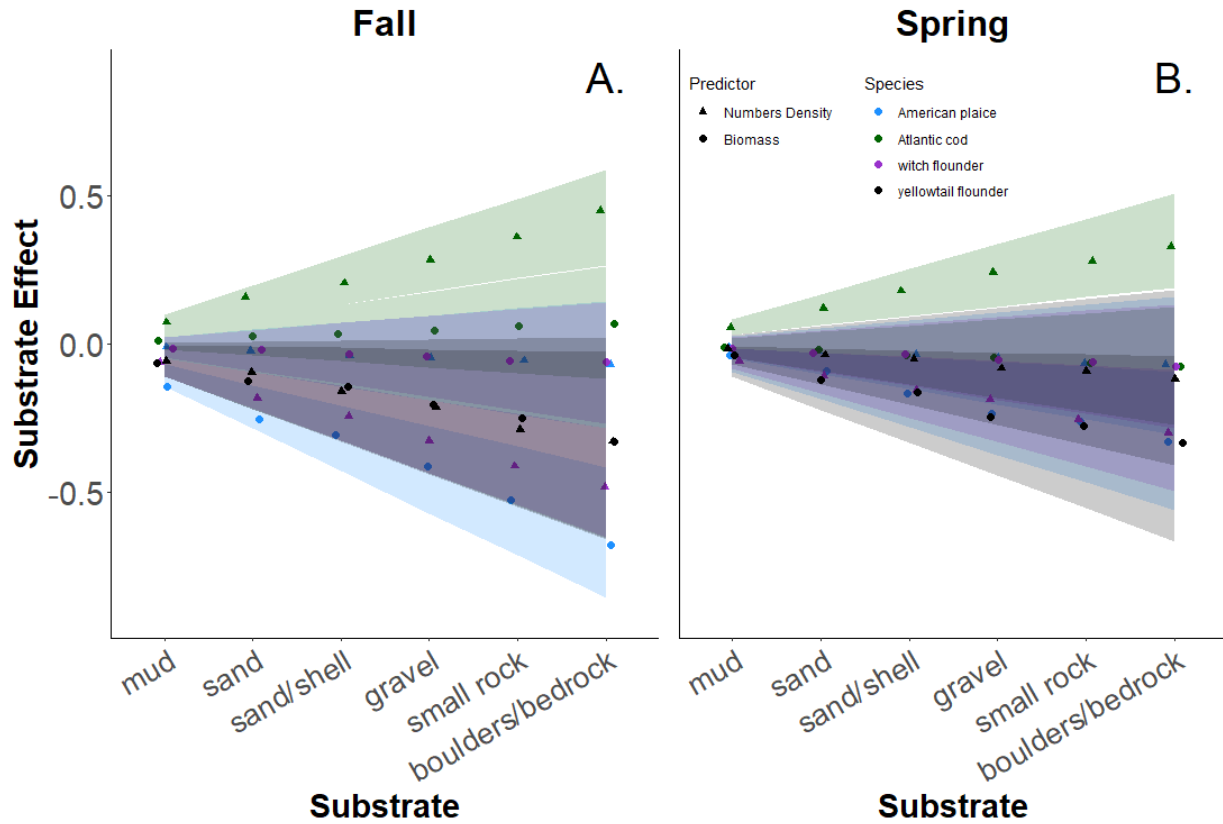
Figure E.15 Performance curves for substrate effect on American plaice, Atlantic cod, witch flounder and yellowtail flounder for (A) Fall and (B) Spring in NAFO Div. 3LNO for 1984-2018 for the first (numbers density) and second (biomass) linear predictors of the VAST model.